MODERATE CHRONIC ETHANOL CONSUMPTION PROVOKES PULMONARY ARTERIAL HYPERTENSION IN MALE RATS

By

Mary Katherine Donovan

May 2024

Director of Dissertation: Dr. Abdel A. Abdel-Rahman

Department of Pharmacology and Toxicology, Brody School of Medicine, East Carolina University

ABSTRACT

Significant attention is dedicated to studying ethanol and the effect it elicits on left-side heart function and systemic blood pressure, ignoring its cardiopulmonary impact, specifically in relation to pulmonary arterial hypertension (PAH). Using male Sprague-Dawley (SD) rats, this study was designed to address this concern in three phases: 1) Analyzing the cardiopulmonary effects of chronic ethanol consumption; 2) Assessing PAH induction via vascular endothelial growth factor (VEGF) receptor inhibition by SU5415 (SU) injection; 3) Evaluating chronic ethanol consumption and its effect in PAH induced by VEGF receptor blockade. Designed to elucidate ethanol's hemodynamic, structural, and molecular effects on cardiopulmonary health in healthy and diseased rats, the overarching hypothesis of this preclinical study was that chronic ethanol consumption predisposes and exacerbates PAH pathophysiology through upregulation of the endothelin-/tumor necrosis factor-a/interleukin-6 (ET-1/TNF-a/IL-6) vasoconstricting/pro-inflammatory signaling axis and subsequent downregulation of cardioprotective bone

morphogenetic protein receptor 2 (BMPR2). Our research demonstrates ethanol alone causes cardiopulmonary remodeling, inflammation, and cardioprotective receptor modulation similar to that of the PAH-inducing injection (SU). Additional observations found that ethanol consumption exacerbates the PAH pathology in male rats with SU-induced PAH, causing increased right ventricle (RV) and left ventricle (LV) hypertrophy, elevated mean pulmonary arterial pressure (mPAP) and mean arterial pressure (MAP), and significant RV fibrosis. Collectively, these results support our hypothesis that chronic ethanol consumption is a cardiopulmonary insult, predisposing and exacerbating PAH pathophysiology.

MODERATE CHRONIC ETHANOL CONSUMPTION PROVOKES PULMONARY ARTERIAL HYPERTENSION IN MALE RATS

A Dissertation

Presented to the Faculty of the Department of Pharmacology & Toxicology

Brody School of Medicine at East Carolina University

In Partial Fulfillment of the Requirements for the Degree

Doctor of Philosophy in Pharmacology and Toxicology

By

Mary Katherine Donovan

May 2024

Director of Dissertation: Abdel A. Abdel-Rahman, Ph.D.

Dissertation Committee Members:

Lisandra E. de Castro Brás, Ph.D.

Jacques Robidoux, Ph.D.

Srinivas Sriramula, Ph.D.

David A. Tulis, Ph.D.

DEDICATIONS

I dedicate this piece of work to my grandmother, Mary Lepore.

Thank you for helping make my dreams possible.

ACKNOWLEDGEMENTS

Accomplishing this dream would not have been possible without my supportive and loving family and friends. Thank you for understanding my academic goals and being there every step of the way.

I would like to acknowledge my parents, David and Linda, for their unconditional support and love throughout my academic career. Mom, thank you for your determination and wisdom, as your advice and motivation is unprecedented. Dad, thank you for your level-headedness and comforting words filled with advice and encouragement. You both have worked so hard to help me not only achieve my goals, but make me into the woman I am today, and for that I am exponentially grateful.

To my older brother and best friend, David IV, thank you for always being there to encourage and support me through all my challenges. I have always looked up to you. Through the use of humor and compassion, you always tell me to keep going and push me to do the best that I can.

I would like to thank my maternal grandparents, Michael and Mary Lepore. While my grandfather no longer is here with us, he instilled the goal of "following your dreams" when I was a child, creating the foundation for this academic achievement. To my grandmother, "Mary Number One," our special connection knows no bounds. Thank you for teaching me to stay "humble, strong, and remember where you came from," qualities that have helped me immensely and I promise to hold onto throughout my career. An additional thank you to my godmother, Linda DeSimone "BeeBop." Thank you for all your help, laughter, and support through this journey.

To my paternal grandparents, David II and Nancy Donovan, thank you. Pop, your academic and military journey has been an inspiration, showing me that with hard work and motivation I can achieve anything. Nan, you have been here for me throughout this whole journey. Our long phone calls filled with laughter and your continuous support has helped immensely.

This dissertation would not be possible without the assistance of my lab members. Special thanks to Hongyan Lin, Minah Zhang, Dr. Fanrong Yao, and Dr. Anees Ahmed for helping me learn the lab skills I needed to make this dissertation possible. An additional thank you to Collin Brinkley for your laughter, support, and friendship throughout this program.

Our department of Pharmacology and Toxicology is special because of the staff and faculty. Throughout my time in the program, I was surrounded by constant support and genuine compassion for learning and teaching, which helped tremendously. I am thankful for the friendships I have made, especially that of Robin Alligood and Jackie Masterson. Your constant support combined with laughter and understanding is greatly appreciated and I look forward to a lasting friendship.

Thank you to all of my committee members: Dr. Srinivas Sriramula, Dr. Lisandra E. de Castro Brás, Dr. Jacques Robidoux, and Dr. David A. Tulis. Your openness, approachability, and encouragement has been extremely helpful. Your guidance is valued, and I am very grateful.

To Dr. Abdel-Rahman, thank you for willingness to give me the intellectual freedom to explore my scientific curiosity, a gift that is uncommon in most labs. I have learned so much from you, scientifically and personally, all of which has made me a better scientist and person than when I first started. I appreciate your willingness to always listen to my ideas and encouraging me "march to the beat of my own drum," making for a positive dissertation experience. Your patience and kindness, combined with your expectation of academic excellence helped me achieve my

academic goals. Encouraging me to formulate, execute, and troubleshoot my own projects under your guidance has gained me scientific independence, a rare characteristic of fresh PhD awardees. I look forward to sharing a life-long friendship.

This dissertation took a team to accomplish. Thank you all for your effort in helping this dream become a reality. Oh, and another thanks to my cats: Sunshine, Mr. Darcy, and Arnie P (R.I.P.). Thanks for putting up with me.

TABLE OF CONTENTS

LIST OF TABLES

LIST OF FIGURES

LIST OF ABBREVIATIONS AND SYMBOLS

BMPR2	Bone Morphogenetic Protein Receptor 2
CMC	Carboxymethylcellulose
EC	Endothelial Cell
EtOH	Ethanol
ETA	Endothelin A Receptor
ETB	Endothelin B Receptor
ET-1	Endothelin-1
IL-6	Interleukin-6
LV	Left Ventricle
LVID; d	Left Ventricular Internal Diameter During Diastole
MAP	Mean Arterial Pressure
MAPK	Mitogen activated protein kinase
mPAP	Mean Pulmonary Arterial Pressure
NF-KB	Nuclear Factor Kappa B
OVX	Ovariectomy
PA	Pulmonary Artery
PAH	Pulmonary Arterial Hypertension
PAAT/PET	Pulmonary Artery Acceleration Time/Pulmonary Artery Ejection Time
PH	Pulmonary Hypertension
PASMC	Pulmonary Artery Smooth Muscle Cell
PV	Pulmonary Vasculature

PVR	Pulmonary Vascular Resistance
RV	Right Ventricle
RVID; d	Right Ventricular Internal Diameter During Diastole
RVSP	Right Ventricle Systolic Pressure
SD	Sprague-Dawley
SU	SU5416
TNF-a	Tumor Necrosis Factor Alpha
VEGF	Vascular Endothelial Growth Factor

CHAPTER ONE: GENERAL INTRODUCTION

1.1 Scientific Premise

Pulmonary arterial hypertension (PAH), a progressive disease characterized by pulmonary arteriole remodeling, increased pulmonary vascular (PV) resistance, and elevated blood pressure within the lungs[1], leads to hypertrophy of the right ventricle (RV) and progressive RV failure[2]. As a rare cardiopulmonary disorder with a complex and multifactorial pathophysiology, PAH causes premature death amongst patients[3]. While PAH is incurable, healthy lifestyle changes can be made to increase quality of life and reduce PAH symptoms[4]. The most recent ethanol research indicates no cardiovascular benefit to ethanol consumption, citing all amounts of alcohol intake increase cardiovascular risk[5]; however, this study is isolated to left-sided heart diseases, ignoring ethanol's elicited cardiopulmonary impact. To address this concern, this preclinical research is designed to increase our understanding of the mechanisms through which chronic ethanol consumption enables or exacerbates PAH development. A recent brief ethanol study showed ethanol-induced RV hypertrophy, increased cardiomyocyte size, and decreased intrapulmonary artery diameter[6], but lacked the mechanism by which ethanol causes these consequences, particularly within the context of PAH molecular signaling.

To address this concern, this preclinical research will evaluate the effect of chronic ethanol consumption on cardiopulmonary structure/hemodynamics in healthy male rats and male rats genetically sensitive to PAH development through vascular endothelial growth factor (VEGF) receptor inhibition[7]. Specifically, this study will give attention to the potent vasoconstrictor and inflammation-inducing protein endothelin-1 (ET-1)[8] and its endothelin A (ETA) and endothelin B

(ETB) receptor expression[9]. Furthermore, this research will provide insight on how ethanol influences cytokine expression, specifically tumor necrosis factor-a (TNF-a) and interleukin-6 (IL-6), whose upregulation can induce experimental PAH[10]. Additional attention to ethanol's influence on the cytostatic pulmonary protective protein, bone morphogenetic receptor 2 (BMPR2), will be addressed in this study, as novel therapies aim to restore the signaling axis in patients who develop PAH due to loss of BMPR2 expression/signaling[11]. Determining the impact of ethanol consumption on cardiopulmonary health and PAH therapeutic targets will contribute knowledge to the understudied PAH research network and provide understanding of how environmental exposure (ethanol consumption) contributes to disease predisposition and progression.

1.2 Ethanol

Cardiovascular research involving ethanol consumption has a paradoxical history, evoking beneficial and detrimental effects[12]; however, the recent ethanol intake recommendations have changed, citing zero cardiovascular benefit to ethanol consumption at acute or chronic levels[13]. Left-side of the heart and blood pressure research involving ethanol consumption is abundant, [14] [15]; however, the effect of ethanol consumption on RV structure/function is limited. Acute ethanol exposure in pigs via intravenous administration documented PAH induction, with significant elevations in mean pulmonary artery pressure (mPAP), PV resistance (PVR), pulmonary vasoconstriction, and subsequent RV dysfunction [16]. Chronic ethanol exposure (5.2% ethanol solution; 4-weeks) in Wistar rats showed ethanol mediated increases in RV pressure, RV hypertrophy, and narrowing of intrapulmonary arteries [6]. Pre-clinical research supports ethanol as a cardiopulmonary modulator; however, the potential of ethanol to alter PAH therapeutic molecular targets has not been determined. Interestingly, ethanol consumption causes

upregulation of PAH inflammatory mediators within the plasma: ET-1[17,18], IL-6[19], and TNF-a[18], all of which are all highly indicated in experimental and clinical PAH. Realizing the potential of ethanol to induce cardiopulmonary remodeling and inflammation, studies are needed to determine the consequences of ethanol consumption on the development/exacerbation of PAH.

1.3 Vascular Endothelial Growth Factor (VEGF) Receptor Inhibition

Within a healthy lung, VEGF is abundantly expressed, helping to maintain lung structure by eliciting pro-survival and antiapoptotic effects on endothelial cells (EC). Both clinical and experimental PAH are characterized by VEGF upregulation, sometimes due to hypoxic exposure and/or genetic factors[20]. It was originally hypothesized by other investigators that VEGF receptor inhibition using SU5416 (SU) would resolve PAH in rats exposed to chronic hypoxia[21]. Instead, these researchers observed the opposite, with SU-treated rats developing severe PAH. The severe PAH was attributed to SU increasing EC apoptosis, generating conditions that favor apoptosis-resistance with high growth potential and eventual EC hyperproliferation[21].

Importantly, injection of SU generates pulmonary arterial changes similar to those observed clinically, unlike other experimental injections[22]. VEGF expression is regulated via numerous factors, including hypoxia, cytokines, and growth factors[23]. When VEGF is inhibited using SU, alterations in the pulmonary vasculature occur, causing EC death. Subsequent stimulation of EC proliferation causes the precapillary arterial lumen to become obliterated with proliferating endothelial cells, a characteristic of severe PAH. Importantly, increased apoptosis of endothelial cells by VEGF receptor blockade causes the loss of survival signaling and apoptosis-resistant cells form within the vasculature, cells with a high growth potential. The formation of plexiform-type lesions similar to human pathophysiology make the SU model favored, as other popular models,

like the monocrotaline model, do not form obstructive lesions within the pulmonary arteries. Therefore, this study is designed to evaluate the effect of SU-induced PAH on integral molecular signaling related to PAH development/therapies. Additionally, this study will determine if ethanol-diet causes SU-induced PAH to worsen.

1.4 Role of Endothelin-1 (ET-1) in PAH

Endothelin-1 (ET-1) is a potent vasoconstricting pro-inflammatory peptide highly indicated in both PAH pathophysiology and therapeutics. Clinically, patients with PAH have elevated serum and lung ET-1 expression[24]. Interestingly, plasma ET-1 expression is upregulated due to ethanol consumption[25] and enhances ET-1 induced vasoconstriction[8]. Under healthy physiological conditions, pulmonary vascular tone is optimally maintained via the balancing of the vasoconstrictor ET-1 and the vasodilating actions of nitic oxide and prostacyclin; during PAH an imbalance induces vasculopathy[26]. ET-1 mediates vasoconstriction via ETA and ETB receptors on vascular smooth muscle cells; however, the ETB receptor present on endothelial cells stimulates vasodilation via NO release. Loss of ETB signaling, and its restoration is central to PAH therapy [27]. Selective ETA receptor antagonism is used as a PAH pharmacological approach to decrease ETA signaling and retain the vasodilating effect mediated by the ETB receptor [27]. Interestingly, ethanol-evoked tissue dependent changes in ET-1 receptor expression profile have been documented, reducing ETB receptor expression within the corpus cavernosum of rats chronically exposed to ethanol [28,29]. Additionally, PAH pathophysiology involves an upregulated inflammatory response. [30] ET-1 mediates intrapulmonary artery inflammation by inducing IL-6 release from human vascular smooth muscle cells via activation of nuclear factor kappa B (NF-KB).[31] Therefore, with ET-1 having a pivotal role in the capacity of ethanol to augment the ET-1

signaling axis combined with its pro-inflammatory properties, it is integral to study the influence of ethanol to better understand the potential ramifications/contraindications to pathophysiology and therapeutic targets. The proposed study will test the hypothesis that ethanol increases ET-1 expression and alters ET-1 receptor signaling, thus predisposing/exacerbating PAH in male rats.

1.5 Role of Interleukin-6 (IL-6) in PAH

Patients with PAH have elevated serum and lung IL-6 [32]. It is important to note that increased IL-6 levels impact patient prognoses, with high concentrations correlating with poorer RV function, quality of life, and decreased patient survival [10]. Experimental research shows overexpression of lung specific IL-6 alone (without hypoxic exposure) in mice leads to spontaneous PAH development, with pulmonary vascular remodeling via the promotion of apoptosis resistant conditions within the pulmonary artery [32]. Additionally, experimental IL-6 blockade ameliorates pulmonary hypertension via inhibiting IL-6 mediated M2 macrophage polarization within the lung[33]. IL-6 expression can be influenced by environmental exposures including ethanol consumption, which is indicated to increase plasma IL-6 levels[34]. Finally, ET-1 promotes IL-6 release [35]. Therefore, with environmental and molecular factors, like ethanol and ET-1 causing IL-6 induction, the proposed studies investigated the function of the IL-6 inflammatory axis and its relation to ethanol-predisposed/exacerbated PAH.

1.6 Tumor Necrosis Factor-α (TNF-α)

Another inflammatory cytokine highly indicated in PAH pathophysiology is TNF-α, with PAH patients exhibiting elevated serum TNF-α levels, and experimental models showing TNF-α

suppressing vasodilating PGI2 mRNA and increasing vascular reactivity[30]. Additionally, TNF-α is indicated to stimulate IL-6 release from vascular smooth muscle cells [36]. TNF-α release is increased with chronic ethanol consumption [37]. Research indicates that TNF-α induces IL-6 synthesis and stimulates inflammation via recruitment of p65 to the IL-6 promoter [36]. Chronic ethanol consumption is indicated to cause organ damage via increased release of TNF-α[38], but it remains unclear if ethanol mediates TNF-α increases within the lung and RV in the context of PAH.

1.7 Bone Morphogenetic Receptor Type 2 (BMPR2) and PAH

Loss of BMPR2 signaling is central to novel PAH research and therapies, with deficiencies found in 70% of patients with hereditary and 20% with idiopathic PAH [39]. BMPR2 is an important target for PAH therapeutics because of the receptor's protective role on the pulmonary vasculature due to anti-proliferative signaling[40]; therefore, research on factors that downregulate BMPR2 are needed to better understand the development of PAH pathophysiology. A multitude of biochemical markers are associated with BMPR2 downregulation in both experimental and clinical PAH[11], including ET-1, TNF-α, and IL-6; molecules elevated due to ethanol. ET-1 downregulates BMPR2 signaling, leading to elevated anti-BMP gremlin-1 expression, causing increased p38 mitogen activated protein kinase (MAPK), resulting in pulmonary artery smooth muscle cell (PASMC) proliferation [41]. Additionally, TNF-α causes a reduction in BMPR2 transcription and mediates BMPR2 cleavage by sheddases, causing PASMC proliferation[42]. Finally, IL-6 is indicated to cause BMPR2 deficiency via negative feedback by activation of STAT3 and the release of miR17-5 and miR20 to bind the 5´UTR of BMPR2 mRNA. This causes degradation of BMPR2 [43], thus investigation on how BMPR2 expression can be augmented due to ethanol consumption is

instrumental to understand ethanol's contribution to PAH pathophysiology. Therefore, our results will provide insight on how an ethanol-diet augments lung BMRP2 expression, which could be detrimental to cardiopulmonary health.

1.8 Innovation

These novel studies are designed to understand how ethanol consumption influences cardiopulmonary disease, sensitivity to PAH development, and the influence of an ethanol diet on pre-existing PAH. This longitudinal study was designed to document time-based PAH development via echocardiographic analysis, with additional postmortem molecular and histological analysis. The findings of this study have determined the influence of an ethanol diet on PAH related molecular signaling, thus advancing our understanding of the cardiopulmonary contraindications of ethanol consumption in relation to PAH therapeutic targets.

1.9 Aims of the Study

Specific Aim 1: Test the hypothesis that chronic ethanol consumption provokes PAH in male rats.

Rationale: Ethanol consumption is indicated to elicit detrimental cardiovascular effects[13]. Importantly, the majority of ethanol research has focused on left-side of the heart disease, limiting our understanding of its right-side of heart effects. A recent comparison study indicates the RV as more sensitive to ethanol-elicited cardiomyocyte hypertrophy[6]; however, time-based progression of RV hemodynamic changes and the effect of ethanol on integral PAH mediators have not been determined. Patients with PAH have vasoconstriction of pulmonary arterioles, mediated by ET-1, which is upregulated in patient plasma[9]. Ethanol upregulates ET-1 plasma expression and disrupts the ET-1 signaling axis by enhancing contraction in the carotid artery via altered receptor

expression[8] . Noteworthy, ethanol upregulates the ET-1 induced protein IL-6[31,34] , a pro-inflammatory protein whose overexpression induces experimental PAH[44] and is upregulated in PAH patients[45]. The literature shows that IL-6 expression is induced by ET-1[31], as well as the pro-inflammatory TNF-a [46,47], a protein known to govern PAH development[42] . Collectively, it important to understand the influence of ethanol consumption on these PAH pro-inflammatory mediators, known to modulate BMPR2 expression/signaling[11,42,43], a protein of novel therapeutic importance[11] . To address the hypothesis that chronic ethanol consumption provokes PAH in male rats, this study addressed the following questions:

1. Will chronic ethanol consumption cause alterations in cardiopulmonary echocardiographic parameters used in PAH diagnostics?
2. What is the effect of ethanol on mean arterial pressure and/or cardiac contractility?
3. Does ethanol cause intrapulmonary artery remodeling and subsequent RV hypertrophy?
4. Does ethanol upregulate the vasoconstricting/pro-inflammatory ET-1 axis within the lung and RV, causing alterations in ETA and ETB receptor expression within the lung?
5. Is the pro-inflammatory ET-1-TNFα-IL-6 axis upregulated by ethanol consumption, influencing BMPR2 expression in the lung?

Specific Aim 2: Test the hypothesis that male Sprague-Dawley (SD) rats (CD strain) from Charles River Laboratories (Raleigh, North Carolina) are sensitive to a single injection (20 mg/kg) of the VEGF receptor inhibitor SU5416 (SU) and develop PAH without hypoxic exposure.

Rationale: An early issue faced in this study was the lack of access to whole body experimental hypoxia chambers, making the utilization of the Sugen + Hypoxia *in vivo* model of PAH unattainable at our current institution. Importantly, studies have documented strain-dependent sensitivity to the SU injection, ranging from unresponsive (does not cause PAH) to hyperresponsive (developing severe PAH)[2,7]. Specifically, Charles River Laboratory male SD rats of different geographic locations have been observed to develop PAH after a single injection of SU, without hypoxic exposure[2,7]. Therefore, this preclinical study sought to determine if SD rats from Charles River Laboratories (Raleigh, North Carolina) developed PAH after a single injection of SU, without hypoxia, as documented in the literature. Furthermore, the mechanism by which rats sensitive to SU develop PAH remains unclear. These studies addressed the following questions to understand the development of PAH in SD rats:

1. Does SU cause RV hypertrophy and change cardiopulmonary hemodynamics?
2. Does SU upregulate the inflammatory peptide ET-1 and modulate ETA and ETB receptor expression in the lungs?
3. Will SU cause an upregulation of the ET-1-TNF-a-IL-6 pro-inflammatory axis in the RV and lungs?
4. How is the expression of BMPR2 affected due the SU injection?

Specific Aim 3: Does ethanol diet cause an exacerbation in the PAH disease profile caused by VEGF receptor blockade in rats sensitive to PAH induction?

Rationale: Clinically, the development of PAH can be multifactorial, with patients developing PAH due to drugs, toxins, and/or genetic factors [48]. Currently there is an unmet need to

understand how environmental exposures, such as ethanol consumption, can impact the disease profile of PAH. These exploratory studies will elucidate how ethanol consumption impacts healthy and diseased rats and contribute to our understanding of how diet impacts cardiopulmonary health. The following questions will be answered to address this aim:

1. Will an ethanol diet and VEGF receptor inhibition compromise cardiopulmonary hemodynamic function and increased RV hypertrophy?
2. Does the SU-injection + ethanol diet cause an exacerbation in ET-1 expression and its downstream induction of the pro-inflammatory cytokines TNF-a and IL-6?
3. Will there be a change in ET-1 and BMPR2 receptor expression within the lungs of SU-injection + EtOH-diet rats.

CHAPTER TWO: MATERIALS AND METHODS

2.1 Animals

Male 6-week-old (200-250g) CD strain Sprague-Dawley rats (Charles River, Raleigh, North Carolina) were individually housed in standard plastic cages at the animal facility at East Carolina University. During the one-week acclimation period, rats were allowed free access to water and chow until the beginning of the protein liquid diet administration. A 12-h light/dark cycle and a room temperature of 23 ± 1 °C was maintained for the duration of the experiment. This study was approved by the East Carolina University Institutional Animal Care and Use Committee and was consistent with the Guide for the Care and Use of Laboratory Animals as governed by the U.S. National Institutes of Health (2023).

2.2 Ethanol-Feeding Regimen

Upon arrival, rats were given free access to water and standard chow diet for one week. Rats were weighed, matched for body weight, and divided into two groups (n=7-8 per group). A one- week acclimation period was allowed by adding 2.5% (w/v) ethanol to balanced liquid protein diet (Alcohol rodent liquid diet, LD 102A, TestDiet). The control rats were pair-fed with isocaloric control diet (Rodent liquid diet, 102, TestDiet). Thereafter, ethanol concentration was increased to 5% (w/v), water was removed, and pair-feeding continued for 8-weeks. Liquid diets were prepared fresh daily (contents detailed in Table 1) and tail blood was drawn on weeks 3, 6 and 8 to determine blood ethanol levels. Weekly EchoMRI™ and transthoracic echocardiography were conducted. After 8-weeks at 5% ethanol, rats underwent femoral artery catheterization followed by euthanasia and tissue collection.

2.3 Induction of Pulmonary Arterial Hypertension using SU5416

Rats were given free access to water and standard chow diet. After a one-week acclimation period, rats were matched for body weight, divided into two groups (n=8-9 per group), baseline echocardiography and EchoMRI was conducted, liquid-protein diet was administered, and a one-week acclimation period was given. SU5416 (Cayman Chemical, #13342) was suspended in 0.05% vehicle CMC (0.05% carboxymethycellulose sodium, 0.9% sodium chloride, 0.4% Tween 80, 0.9% benzyl alcohol in deionized water) and rats were administered a single subcutaneous injection of SU (20 mg/kg) suspended in 0.05% CMC or vehicle control 0.05% CMC[7,49]. Eight-weeks post-injection, rats underwent femoral artery catheterization followed by euthanasia and tissue collection. Male rats were exclusively used in this study to reduce variability. A general experimental timeline schematic is provided for each study aim (Fig(s) 3.1, 4.1, & 5.1).

2.4 Transthoracic Echocardiography

Transthoracic echocardiography was conducted using the VisualSonics Vevo3100 ultrasound system under isoflurane (2%) anesthesia. Rat chest hair was removed using Veet® hair removal cream, and the heart rate was titrated to approximately 300/min. Echocardiography data analysis was conducted using VivoLab 5.5.0 Software.

2.5 Assessment of Pulmonary Hemodynamics

Pulmonary artery (PA) visualization was obtained in the modified left parasternal-long axis view in B-mode. Color Doppler was used to identify the location to assess the PA, then using Pulsed-waved Doppler (PW-Doppler), the PW-doppler sample area was set and measured in the

area of optimal flow. Pulmonary artery acceleration time (PAAT) and pulmonary artery ejection time (PET) were measured. PAAT was adjusted by PET to account for heart rate variability [50].

2.6 Evaluation of Right Ventricle Structure

A left modified parasternal long-axis view [51] was used to obtain a clear view of the RV, aortic valve, intraventricular septum (IVS), and LV in B-mode. Using M-mode, the sample volume line was placed between the shadow of two contiguous vertebrae. Images obtained from this orientation were used to calculate the RV internal diameter during diastole (RVID; d) and the LV internal diameter during diastole (LVID; d) [52].

2.7 Determination of Left Ventricle Mass

Left ventricle (LV) mass was analyzed using weekly echocardiography for the duration of the experiment. A clear view of the LV was visualized in short-axis orientation using B-mode and a reference image was taken. Next, the cursor was put over the LV in M-mode to obtain a clear view the LV walls (anterior and posterior). Measurements of the LV anterior and posterior walls during diastole and systole were recorded with additional measurement of the left ventricle internal diameter during diastole and systole. All measurements were recorded for 5 cycles and the instances were averaged.

2.8 Measurement of Mean Arterial Pressure

Rats were anesthetized by intraperitoneal injection (0.1 mL/100g) of ketamine (90 mg/mL) and xylazine (10 mg/kg). An incision was made in the inner thigh to expose the femoral artery. Using a 25-gauge needle a small arteriotomy was made in the artery and a catheter was guided into

the femoral artery. The catheter's position within the artery was verified visually. Blood pressure was recorded, and analyzed using LabChart software (v.7, AD Instruments, Colorado Spring, CO) as in our previous studies [53,54].

2.9 Determination of Plasma Ethanol Concentration

Plasma ethanol (EtOH) concentration was determined using the method established in the lab previously published studies [55]. Using a microplate reader (Tecan Group Ltd., Männedorf, Schweiz), absorbance was detected at 340 nm and using a standard calibration curve, ethanol concentration was calculated as in our previous studies [54,56]

2.10 Body Composition Analysis

Whole body composition analyzer, EchoMRI™ (Echo Medical Systems, Houston, Texas), was used weekly to monitor body composition. Rats were inserted into analysis tube and then into EchoMRI™ machine for body composition analysis. Lean muscle and fat mass values were corrected by the respective body weight of each rat throughout the experiment.

2.11 Enzyme-linked Immunoassay (ELISA)

Lung and RV tissues were homogenized in PBS and ELISA was used to determine the levels of ET-1, IL-6, and TNF-α (R&D Systems #DET100, #R6000B, #RTA00,) according to manufacturer's instructions.

2.12 Western Blot

Lung tissue was homogenized in lysis buffer with a protease inhibitor cocktail. Samples were centrifuged for 15 min at 12,000 g, supernatant was collected, and 20 μg of protein was loaded into each well to be separated via 2-14% bis-tris gel electrophoresis. Gels were then transferred onto nitrocellulose membranes, blocked with 2.5% non-fat dry milk for 2 hours, and incubated with the following: BMPR2 monoclonal antibody (Invitrogen #MA5-15827, 1:1,000 dilution), ETA (Invitrogen PA3-065, 1:1,000 dilution), ETB (Invitrogen PA3-066, 1:1,000 dilution) receptors, β-actin (Abcam #ab115777, 1:20,000 dilution), or GAPDH (Invitrogen #MA1-16757), and were incubated at 4°C for 24 hours. Membranes were washed in PBST and incubated with IRDye680-conjugated goat anti-mouse (1:15,000) and IRDye800-conjugated goat anti-rabbit (1:15,000) from LICOR Biosciences for one hour. Membranes were washed using PBST, and proteins were observed using Odyssey M. Imager (LI-COR) and analyzed using LI-COR ImageStudio 5.2 software.

2.13 Histology

Lung and RV samples were fixed in 4% paraformaldehyde, in O.T.C., cut to 4 μm thickness at -24℃ using a cryostat, and mounted onto positively charged slides (Fisher Scientific). H&E staining was conducted, and slides were imaged (Keyence microscope). Lung intrapulmonary arteries were imaged at 200X magnification (15 arteries per sample) and medial layer % thickness was quantified as (% wall thickness = [(medial thickness × 2)/ (external diameter)] × 100), [57,58]. RV cross-sectional area (CSA, 400X) was calculated using random images of RV cardiomyocytes (8 random images per sample, 20 cardiomyocytes per image, 480 cardiomyocytes per group). Masson's trichrome staining was conducted, and slides were imaged (Keyence microscope) at

100x and 200x. Percent fibrotic area, intrapulmonary artery thickness, and CSA were calculated using ImageJ software (NIH).

Table 1.1: Liquid Diet Formulation.

Diet Type	Water (mL)	Powder Diet (g)	Maltodextrin (g)	Ethanol (mL)
Control	771	229g: LD102	0	0
EtOH (2.5%)	792.7	139g: LD102A	40	28.3
EtOH (5%)	810.1	139g: LD102A	0	50.9

CHAPTER THREE: LUNG AND RIGHT VENTRICLE INFLAMMATION AND REMODELING PREDISPOSE ETHANOL-INDUCED PULMONARY ARTERIAL HYPERTENSION

3.1 Abstract

Current research on ethanol-induced cardiovascular anomalies has focused on left ventricular (LV) function and blood pressure. Therefore, the aim of this study was to determine if ethanol induced alterations in the right ventricle (RV) and pulmonary artery (PA) structure and function lead to pulmonary arterial hypertension (PAH). Two groups of male Sprague-Dawley rats received balanced liquid diet containing 5% ethanol (w/v) or pair-fed isocaloric liquid diet for 8-weeks. Weekly echocardiography was conducted to evaluate cardiopulmonary function and lung, RV tissues were collected for *ex vivo* histological and molecular studies. The ethanol-treated rats exhibited: (1) Elevated mean pulmonary arterial pressure (mPAP) and decreased pulmonary artery acceleration time/ejection time (PAAT/PET); (2) Pulmonary vascular remodeling comprising intrapulmonary artery medial layer thickening; (3) RV hypertrophy along with increased RV/LV+Septum, RV diameter, RV cardiomyocyte cross-sectional area, and LV mass/body weight ratio. These responses were associated with (A) increased lung and RV pro-inflammatory markers, endothelin-1 (ET-1), TNF-α and IL-6 levels; (B) higher ET-1, ETA/ETB receptor ratio and downregulation of the cytoprotective protein, bone morphogenetic protein receptor 2 (BMPR2) in the lungs. These findings suggest that moderate ethanol-induced cardiopulmonary changes underlie progression to PAH via upregulated proinflammatory ET1-TNFα-IL6 pathway and suppressed anti-inflammatory BMPR2.

3.2 Introduction

Previous translational studies have focused on the effect of ethanol on left ventricle (LV) structure and function as well as vasculature [14]. However, there has been significantly less focus on the right ventricle (RV) or pulmonary artery hemodynamics. It is noteworthy that there are differences in the LV and RV responses to pathological stressors [59]. RV function and cardiopulmonary hemodynamics are important to heart health, with changes contributing to a multitude of cardiac diseases, including pulmonary arterial hypertension (PAH) [60]. Research dedicated to understanding factors that influence cardiopulmonary health is increasingly important, as prevalence of pulmonary hypertension has increased [61]. Notably, increased pulmonary vascular (PV) remodeling and resistance, which lead to RV hypertrophy and failure, are major hallmarks of pulmonary arterial hypertension (PAH) [62]. Therefore, with habitual alcohol consumption being associated with increased risk of cardiovascular disease development [5], studies are needed to elucidate the effects of chronic ethanol consumption on RV and pulmonary arterial function and structure, with attention to mechanisms leading to cardiopulmonary dysfunction.

The recapitulation of the clinical manifestations of PAH discussed above [48,63] has been modeled in rats [64], offering validated PAH models for preclinical research. Earlier findings showed that acute ethanol administration elevated mean pulmonary artery pressure (mPAP) and was associated with RV dysfunction in pigs [16]. A more recent study showed chronic ethanol induced RV pressure, RV hypertrophy, and narrowing of intrapulmonary arteries in rats [6]. However, it is possible that the use of a 4-week ethanol (5% in drinking water) model hindered the progression to PAH phenotype in this recent study. Importantly, studies that demonstrated evidence of LV injury and dysfunction utilized an 8-week ethanol (5% in balanced liquid diet) model[65]**.** Therefore,

this study utilized, for the first time, the 8-week model to investigate the long-term effects of ethanol on cardiopulmonary function and structure.

In particular, PAH patients exhibit upregulated plasma and lung tissue endothelin-1 (ET-1) [9]which enhances pulmonary artery tone via activation of vascular smooth muscle ETA and ETB receptors [27]. Additionally, ethanol administration influences the ET-1 axis via increasing plasma ET-1 levels[25]and inducing tissue dependent changes in ET-1 receptor expression [28]. However, studies on lung tissue and RV ET-1 levels or ETA/ETB receptor expression following long-term moderate ethanol consumption have not been conducted.

PAH research supports the role of inflammation in pulmonary vasculopathy [66], particularly upregulations of plasma ET-1 [67], and serum TNF-α and IL-6 [68]. Importantly, elevations in circulating IL-6 or its signaling in smooth muscles of remodeled vessels of human and experimental PAH are associated with decreased RV function, quality of life, and survival amongst PAH patients [10,69]. While ethanol increases TNF-α and IL-6 in other tissues[18,19], it remains unknown if long-term ethanol consumption causes their increase in the RV and lung, leading to PAH.

Growing evidence supports anti-proliferative role for bone morphogenic protein receptor 2 (BMPR2) because its expression/signaling is downregulated in pulmonary artery smooth muscle cells due to increases in local ET-1[70], lung and circulating IL-6 [71], and vascular TNF-α levels [72]. Loss of BMPR2 signaling due to downregulation or low levels of its activator, bone morphogenic protein (BMP), causes pulmonary artery smooth muscle cell proliferation [11]. However, the possibility of reduced lung BMPR2 expression as a mechanism for chronic ethanol induced adverse PA pathology has not been investigated.

The present study had two aims. First, to determine whether long-term moderate ethanol consumption alters the RV and PA structure and function leading to PAH in rats. Second, to assess the hypothesis the observed effects are caused, at least partly, via ethanol-induced upregulation of the pro-inflammatory ET-1-TNF-α -IL-6 axis and/or downregulation in its counterbalancing BMPR2 in the lung.

3.3 Protocols and Experimental Groups

A general experimental timeline of this preclinical study is provided in figure 3.1. Male 6-weeks old (200-250g) Sprague-Dawley CD rats (Charles River, Raleigh, North Carolina) were individually housed in standard plastic cages at the animal facility at East Carolina University. A 12-h light/dark cycle and a room temperature of 23 ± 1°C was maintained for the duration of the experiment. This study was conducted and approved by the East Carolina University Institutional Animal Care and Use Committee and were consistent with the Guide for the Care and Use of Laboratory Animals as governed by the U.S. National Institutes of Health (2023). Upon arrival, rats were given free access to water and a standard chow diet for one week. Rats were weighed, matched for body weight, and divided into two groups (n=7-8 per group). Animals were individually housed to monitor liquid diet intake and facilitate pair-feeding. A one-week acclimation period was allowed by adding 2.5% (w/v) ethanol to balanced liquid protein diet (Alcohol rodent liquid diet, LD 102A, TestDiet). The control rats were pair-fed with isocaloric control diet (Rodent liquid diet, 102, TestDiet). Thereafter, ethanol concentration was increased to 5% (w/v), and pair-feeding continued for 8-weeks. Liquid diets were prepared fresh daily and tail blood was drawn on weeks 3, 6 and 8 to determine blood ethanol levels. Weekly EchoMRI™

and transthoracic echocardiography were conducted. After 8-weeks at 5% ethanol, rats underwent femoral artery catheterization followed by euthanasia and tissue collection.

3.4 Data Analysis and Statistics

Values are presented as mean ± SEM. Time-course data was analyzed by Two-Way ANOVA with repeated measures followed by multiple comparisons testing to determine the effect of ethanol over the entire 8-week treatment period and at different time points, compared with control diet. Other group data was analyzed for difference between control and ethanol-fed rats by unpaired two-tailed *t*-test. All statistical analyses were conducted using Prism 9.5.1 (GraphPad software Inc., La Jolla, CA) with $P < 0.05$ considered significant.

3.5 Results

3.5.1 Ethanol-induced RV Hypertrophy with no change in body weight or composition.

Ethanol-fed rats exhibited blood ethanol concentration of 39.8 $\pm$ 1.9 mg/dL (Fig. 3.2 A) along with higher ($P<0.01$) RV/BW (Fig. 3.2 B) and RV/LV+Septum (Fig. 3.2 C) ratios, compared with control. Time-course studies revealed similar progressive increase in body weight (Fig. 3.2 D) and fat composition/body weight ratio (Fig. 3.2 E) while lean mass/body weight ratio (Fig. 3.2 F) progressively decreased in ethanol-fed and in isocaloric diet fed control rats.

3.5.2 Ethanol increased right ventricle afterload.

Transthoracic echocardiography measurements revealed significant ($P<0.05$) reductions in pulmonary artery acceleration time (PAAT) in ethanol fed, compared with control, rats over the entire 8-week period (Fig. 3.3 A). The overall PAAT reduction was more evident when the

normalized PAAT/PET ratios (Fig. 3.3 B) were compared over the 8-week treatment period, which also showed lower ($P<0.01$) ratios in ethanol-treated rats at weeks 6 ($P<0.05$) and 8. These findings show chronic ethanol-fed rats exhibited an overall increase in RV afterload.

3.5.3 Ethanol-induced elevation in pulmonary artery pressure and right ventricular remodeling.

Assessment of RV structure was obtained in the modified parasternal-long axis orientation where the RV, interventricular septum, and LV are all together. Time-course M-mode of RV internal diameter during diastole (RVID; d) to the LV internal diameter during diastole (LVID; d) ratio (RVID; d/ LVID; d) was higher ($P<0.01$) in ethanol-fed rats (Fig. 3.3 C). Additional time-course echocardiographic analysis showed that ethanol-fed rats exhibited significantly ($P<0.05$) higher mean pulmonary artery pressure (mPAP; Fig. 3.3 D) compared to control. Ethanol-fed rats exhibited overall significantly ($P<0.001$) higher LV mass/body weight ratio (Fig. 3.3 E) during the 8-week treatment period.

3.5.4 Ethanol-induced pulmonary vascular remodeling and cardiomyocyte hypertrophy.

Ethanol-fed rats exhibited pulmonary vascular remodeling and RV hypertrophy, two hallmark phenotypes of PAH. H&E staining of the intrapulmonary arteries revealed greater ($P<0.001$) medial layer thickness in ethanol-fed rats reflecting pulmonary vascular remodeling (Fig. 3.4 A & B). Further H&E staining showed ethanol-induced RV cardiomyocyte hypertrophy based on the greater ($P< 0.05$) RV cross sectional area, compared to control values (Fig. 3. 4 C & D).

3.5.5 Ethanol Induces a RV and Lung Pro-Inflammatory Environment.

Quantification of pro-inflammatory mediators involved in experimental PAH showed higher ($P < 0.05$) levels of endothelin-1 (ET-1), IL-6 and TNF-α in the lung (Fig. 3.5 A, C, E) and right ventricle (Fig. 3. 5 B, D, F) of ethanol-fed, compared with control rats. These data showed an ethanol-evoked pro-inflammatory environment in the lungs and RV, supporting PAH pulmonary and cardiac phenotypes.

3.5.6 Ethanol increases the ETA/ETB receptor ratio and suppresses BMPR2 in the lung.

Western blot analysis showed minimal alteration in endothelin-1 type A (ETA) receptor (Fig. 3.6 A) and substantial reduction ($P < 0.01$) in ETB receptor (Fig. 3.6 B) in the lungs of ethanol fed, compared with control rats. These results reflect an increased lung ETA/ETB receptor ratio in ethanol-fed rats. Further, the lungs of the ethanol-fed rats exhibited reduced ($P<0.05$) levels of the anti-inflammatory protein BMPR2, compared to control rats (Fig. 3.6 C).

3.5.7 Ethanol-induced elevation in mean arterial pressure.

MAP, recorded via femoral artery catheterization, was higher ($P<0.01$) in the ethanol fed rats (Fig. 3.6 D). However, there were no differences in derivative pressure over time (+dp/dt and -dp/dt) (Fig. 3.6 E & F) between groups.

3.6 Discussion

This study contributes new knowledge on the adverse cardiopulmonary effects of moderate (5% (w/v) chronic (8-weeks) ethanol consumption in male rats. The most important findings of the present study include ethanol induced: (1) elevations in mean pulmonary artery pressure and

RV afterload; (2) RV hypertrophy and intrapulmonary remodeling as evidenced by higher cardiomyocyte cross sectional area and increased pulmonary artery medial layer thickness; (3) higher lung and RV endothelin-1, IL-6 and TNF-α; (4) lower lung endothelin-1 receptor B (ETB) and BMRP2 expression. Collectively, the present findings are the first to demonstrate ethanol-induced adverse cardiopulmonary structural and functional effects along with possible mechanisms for the progression toward a pulmonary arterial hypertension phenotype in male rats.

Previous preclinical cardiopulmonary studies on ethanol had limitations in duration and administration of ethanol exposure, which include conducting acute studies in pigs[16] and a relatively short (4-week) exposure to 5% ethanol (in drinking water) in rats[6] . Here, we used a well-accepted 5% ethanol regimen in a balanced liquid diet with pair-fed controls and extended the exposure duration to 8- weeks[65]. Further, we studied, for the first time, the effect of this ethanol regimen in a Sprague-Dawley CD sub-strain, with documented sensitivity to PAH induction [7]. The adopted regimen resulted in blood ethanol concentration of approx. 40 mg/dL (Figure 3.2 A), consistent with moderate ethanol consumption [73]. Noteworthy, the observed effects were ethanol mediated without any reduction in body weight (Figure 1D) contrary to the reduction produced by the same ethanol regimen in the Sprague-Dawley (SD) sub-strain rats in our previous study[65], suggesting sub-strain specific effects of ethanol.

The ethanol-induced RV hypertrophy, which is expressed as higher RV/body weight ratio and Fulton index (RV/LV+ Septum) (Figure 3.2 B, C), likely resulted from increased RV afterload, a hallmark cardiac phenotype of PAH [74]. As discussed earlier, elevated RV afterload is supported by ethanol-induced: (1) progressive reductions in both PAAT and PAAT/PET (Figure 3.3 A,B), which are inversely related to RVSP derived from right ventricle catheterization [50,75], and (2) elevation in mPAP (Figure 3.3 D). Our echocardiographic findings of ethanol-induced progressive

increases in RV chamber size (Figure 3.3 C) likely reflect adaptive response to RV pressure overload, which ultimately leads to RV dilation and PAH phenotype [76,77].

The present study demonstrated ethanol-induced increases in LV mass/body weight ratio (Figure 3.3 E) and MAP (Figure 3.6 D) denoting LV hypertrophy and elevated LV afterload. The higher MAP in ethanol-fed rats is consistent with a recent comprehensive epidemiological study that linked ethanol consumption to higher blood pressure [15]. Notably, ethanol had no effect on LV contractility indices (Figure 3.6 E & F). It is likely that longer exposure to ethanol might be required to cause LV dysfunction. While studies on the effects of longer exposure period to ethanol are warranted, combining the ethanol regimen and the PAH sensitive rat strain used in the present study uncovered the first evidence of ethanol-induced RV and PAH phenotypes in the absence of LV dysfunction.

To determine if structural changes contributed to increased RV afterload, we conducted histological analysis of intrapulmonary artery medial layer wall thickness and RV cardiomyocyte cross sectional area (CSA). The findings showed reduced intrapulmonary artery diameter (Figure 3.4 A & B) and increased RV cardiomyocyte CSA (Figure 3.4 C & D) in ethanol-fed rats. Similar findings were observed in ethanol-fed rats [6] with no evidence of PAH phenotype likely due to the shorter (4-week) exposure to ethanol. Therefore, these findings suggest that the RV and intrapulmonary artery structural changes predispose to the progression toward PAH phenotype following extended ethanol consumption (Fig. 3.4 A & B) possibly via thickened pulmonary arteries following vascular smooth muscle proliferation [78].

We hypothesized that upregulation of ET-1 and its receptors ETA/ETB ratio contribute to the ethanol-induced PA and RV remodeling for the following reasons. First, serum and lung ET-1 levels are higher in PAH patients [9,24]. Consistent with these findings, ethanol increased lung and

RV ET-1 level (Figure 3.5 A & B) and in reported studies [8], and enhanced ET-1-induced vascular contraction [25,28]. It is noteworthy that ET-1 mediates opposing vascular effects dependent on its receptor subtype location because activation of vascular smooth muscle ETA and ETB receptors causes vasoconstriction [26] while activation of endothelial cell ETB receptors mediates vasodilation [79]. Therefore, a higher ETA/ETB receptor ratio indicates a shift in ET-1 effects towards vasoconstriction. The latter constitutes the basis for using ETA selective antagonists as PAH therapeutics [27]. Our findings demonstrate, for the first-time, ethanol- increased lung ETA/ETB receptor ratio (Figure 3. 6 A & B), which contributes to the ethanol-induced PA pathological changes (Figure 3.3 A,B,D & 3.4 A,B). These findings also raise a concern about ethanol use by PAH patients, particularly when ETA receptor antagonists are used as therapeutics. This is particularly important because little is known about potential ethanol interactions with ETA receptor antagonist therapy in PAH patients. Future studies are needed to address this health-related issue.

ET-1 increases pro-inflammatory cytokine production, particularly IL-6 [35], which is implicated in clinical and experimental PAH [32]. The elevations in RV and lung IL-6 (Figure 3.5 C & D) likely play a pivotal role in ethanol induced PAH because: (1) overexpression of lung specific IL-6 leads to PAH development in mice [32]; (2) Lung IL-6 is elevated in PAH patients and experimental models of PAH [30], and correlates with RV dysfunction and poorer patient survival [10]; (3) Ethanol-induced increases in lung and RV TNF-α (Figure 3.5 E, F) stimulates the release of IL-6 from vascular smooth muscle cells [36]. Collectively, these findings support a role for the upregulated ET-1-TNF-α-IL-6 axis in ethanol-induced PAH phenotype in our study. It is also likely that downregulation in anti-inflammatory molecules contributed to the observed effects in ethanol-fed rats.

Recent evidence supports BMPR2 downregulation as a novel PAH trigger in 70% of patients with hereditary, and 20% with idiopathic, PAH [39]. Notably, BMPR2 protects the pulmonary vasculature due to its anti-proliferative signaling [40]. The contribution of the downregulation of lung BMPR2 (Figure 3.6 C) to the ethanol-induced RV and PA detrimental effects gains credence from the following findings. First, ET-1, which is increased by ethanol (Figure 3.5 A, B), downregulates BMPR2 signaling resulting in pulmonary artery smooth muscle cell proliferation [41]. Second, TNF-α, which is increased by ethanol (Figure 3.5 E, F), reduces BMPR2 transcription and enhances its cleavage [42]. Third, IL-6 promotes BMPR2 deficiency via a negative feedback loop [43]. Therefore, the novel downregulation of lung BMPR2 contributes to ethanol-induced PAH pathophysiology.

This work is a contribution to the understudied area of ethanol effects on RV and PA pathophysiology. However, this work should be interpreted within the boundaries of its limitations. This study establishes ethanol as a cardiopulmonary insult, but its limitations warrant recognition. Echocardiography is a non-invasive diagnostic and surveillance tool for PAH, but the absence of invasive RVSP measurement is a limitation that needs to be addressed in future studies. Future research needs to determine if ethanol effects on the pulmonary artery and RV hypertrophy are permanent, or reversible once ethanol consumption ceases. This study supports ethanol as a cardiopulmonary insult in male rats; however, future research in female rats is needed to determine if these effects of ethanol are influenced by animal sex. This is important because: (1) ethanol-induced LV cardiac dysfunction is exaggerated in sex/estrogen dependent manner [80], and (2) women more commonly develop PAH, but have a higher survival rate than men [81].

In summary, this study advances current knowledge on moderate ethanol induced cardiopulmonary remodeling and dysfunction. Specifically, the shift towards RV and PA

pathologies is initiated, at least partly, by ethanol-induced imbalance between the increased proinflammatory (ET-1, TNF-α and IL-6) and the downregulated counterbalance BMPR2 arms in the RV and PA. The present findings yield new insight into the adverse effect of ethanol on cardiopulmonary health, providing a foundation for future studies.

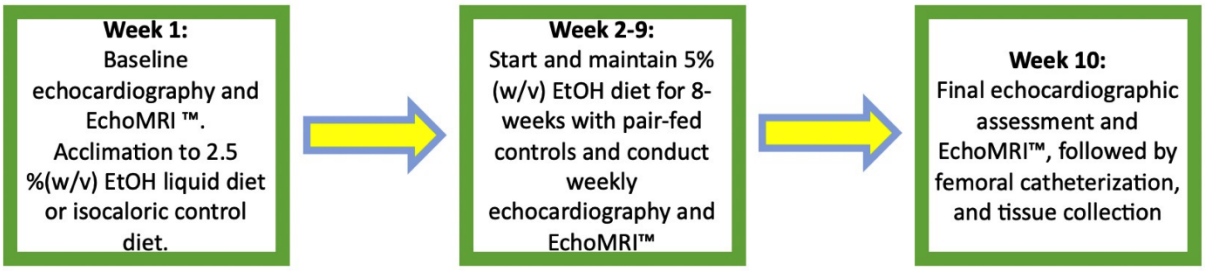
Week 1:
Baseline echocardiography and EchoMRI ™.
Acclimation to 2.5 %(w/v) EtOH liquid diet or isocaloric control diet.
Week 2-9:
Start and maintain 5% (w/v) EtOH diet for 8-weeks with pair-fed controls and conduct weekly echocardiography and EchoMRI™
Week 10:
Final echocardiographic assessment and EchoMRI™, followed by femoral catheterization, and tissue collection

Figure 3.1: Aim One Experimental timeline. A timeline outlining experimental procedures, including feeding regimen, ethanol concentration, echocardiographic measurements, EchoMRI ™**,** femoral catheterization, and tissue collection of male Sprague-Dawley (CD stain) rats.

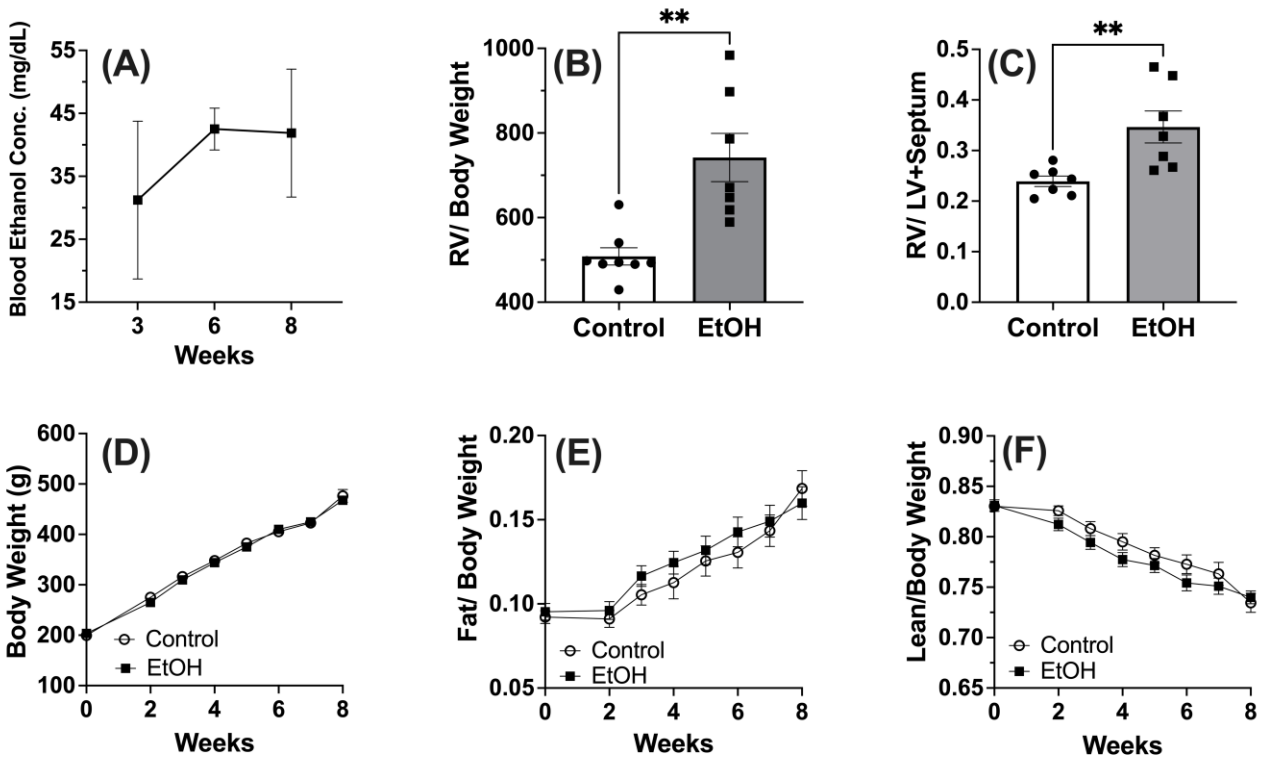
(A)
Blood Ethanol Conc. (mg/dL)
55
45
35
25
15
3
6
8
Weeks
(B)
**
RV/ Body Weight
1000
800
600
400
Control
EtOH
(C)
**
RV/ LV+Septum
0.5
0.4
0.3
0.2
0.1
0.0
Control
EtOH
(D)
Body Weight (g)
600
500
400
300
200
100
0
2
4
6
8
Weeks
Control
EtOH
(E)
Fat/ Body Weight
0.20
0.15
0.10
0.05
0
2
4
6
8
Weeks
Control
EtOH
(F)
Lean/Body Weight
0.90
0.85
0.80
0.75
0.70
0.65
0
2
4
6
8
Weeks
Control
EtOH

Figure 3.2: **Moderate chronic ethanol consumption causes right ventricular hypertrophy with no alteration in body weight or composition.** Blood ethanol concentration **(A)**, Higher right ventricle (RV) weight to body weight (BW) ratio **(B)** and Fulton index (RV/ LV+Septum) **(C)** indicated RV hypertrophy in ethanol-fed rats. Time-course of body weight **(D)**, and EchoMRI™ analysis of body fat content/body weight **(E)**, and lean mass/body weight **(F)** of ethanol (5%)-fed and control rats. Data presented as means ± SEM (n=7-8 in each group); $^{**}P < 0.01$, compared to control group.

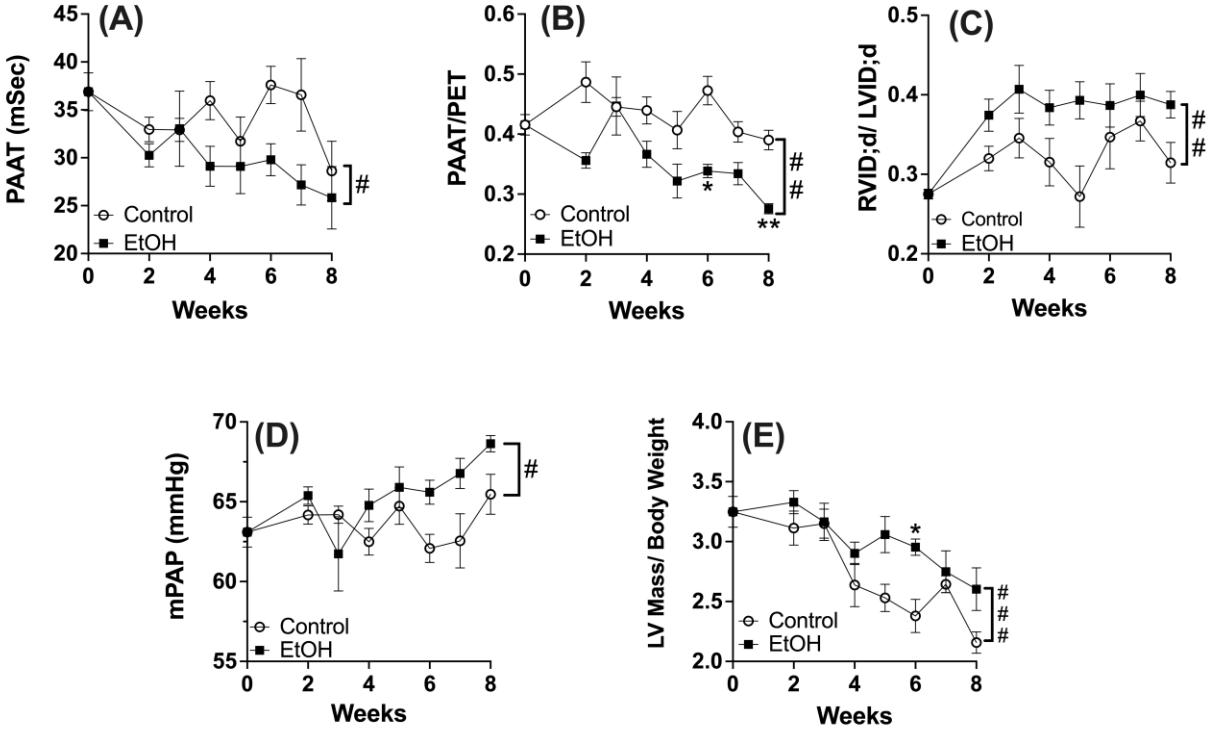
(A)
PAAT (mSec)
Weeks
Control
EtOH
#
(B)
PAAT/PET
Weeks
Control
EtOH
*
**
#
#
(C)
RVID;d/ LVID;d
Weeks
Control
EtOH
#
#
(D)
mPAP (mmHg)
Weeks
Control
EtOH
#
(E)
LV Mass/ Body Weight
Weeks
Control
EtOH
*
#
#
#

Figure 3.3: Ethanol Increases pulmonary vascular resistance and RV diameter along with LV hypertrophy. Echocardiographic pulsed-wave Doppler mode analysis of PAAT **(A),** PAAT/PET ratio **(B)**, RVID; d/ LVID; d **(C),** mPAP **(D)**, and LV mass/BW. Values are reported as means ± SEM (n= 7 per group). Time-course data analyzed by two-way ANOVA with repeated measures followed by Bonferroni multiple comparisons testing. $^{\#}P<0.05$, $^{\#\#}P<0.01$, $^{\#\#\#}P<0.001$ vs control pair-fed rats, $^{*}P<0.05$, $^{**}P < 0.01$ vs. corresponding weekly value.

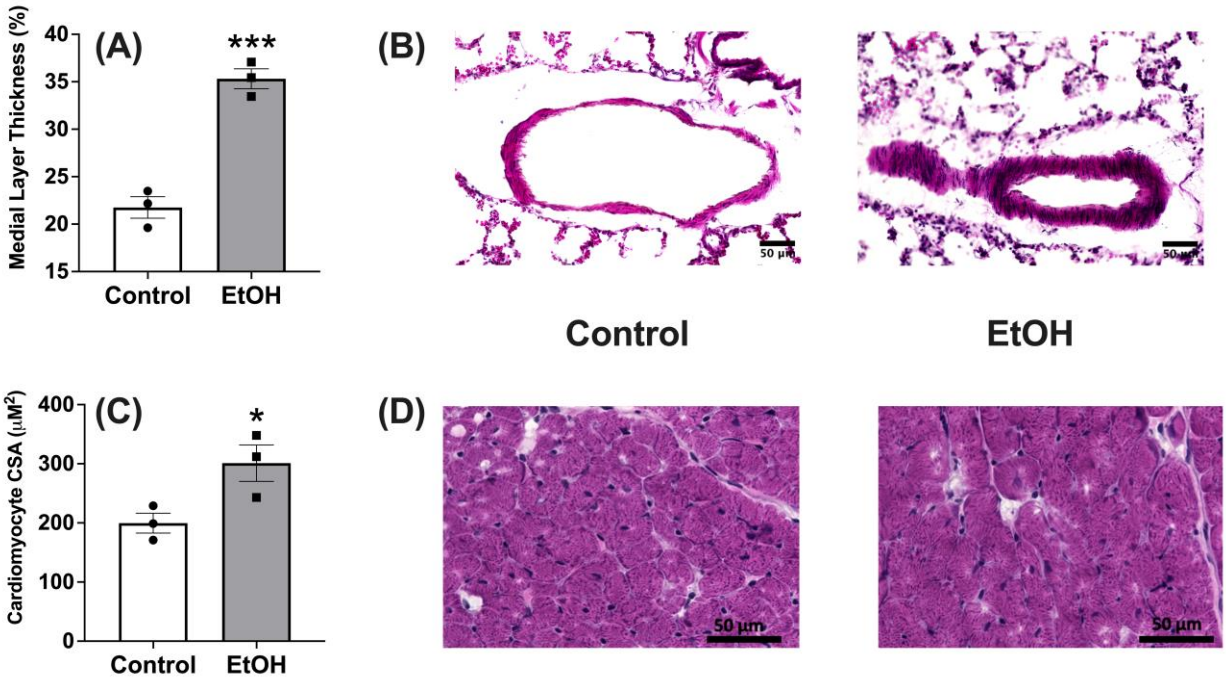
(A)
Medial Layer Thickness (%)
40
35
30
25
20
15
***
Control
EtOH
(B)
50 µm
50 µm
Control
EtOH
(C)
Cardiomyocyte CSA (µM²)
400
300
200
100
0
*
Control
EtOH
(D)
50 µm
50 µm

Figure 3.4: Ethanol causes pulmonary arteriole thickening and RV cardiomyocyte hypertrophy. Quantification of medial layer thickness of H&E-stained intrapulmonary arteries (**A)**. Values reported as mean ± SEM, compared to control group. H&E staining illustrating effect of chronic ethanol consumption on intrapulmonary remodeling (**B**). Cross-sectional area (CSA) quantification of RV cardiomyocytes (**C**) and representative images of H&E-stained RV cardiomyocytes (**D**). Values are reported as mean ± SEM (n=3), $^{*}P < 0.05$, $^{***}P < 0.001$ compared to control group.

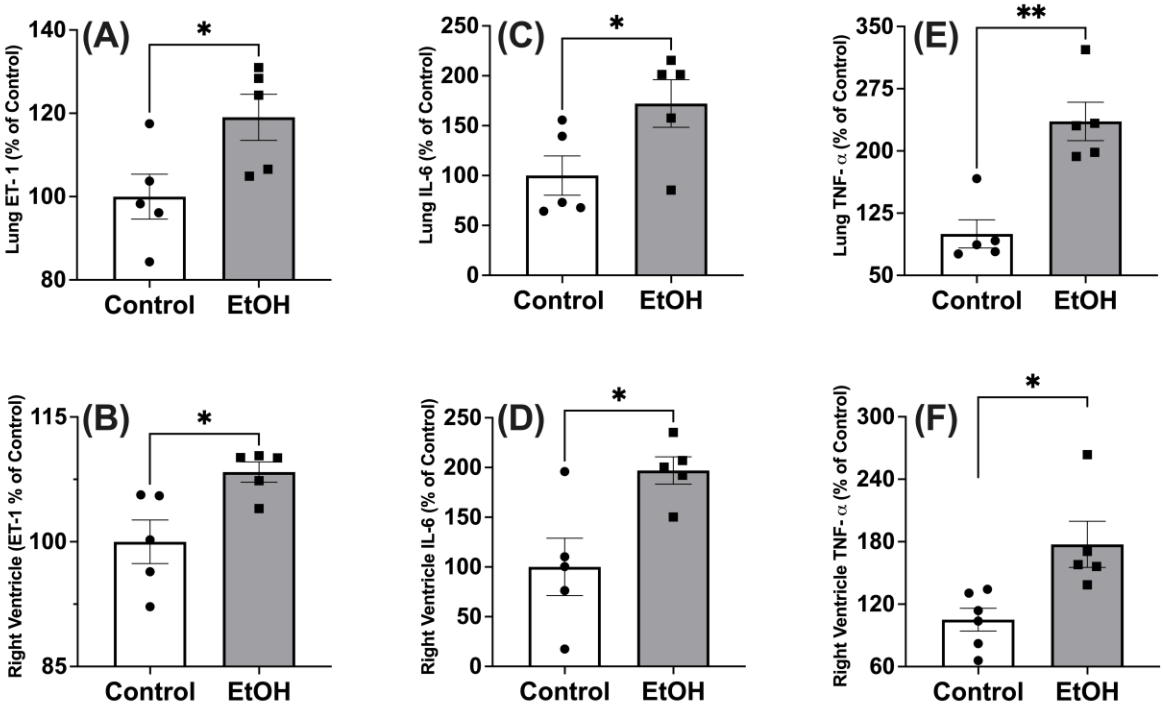
(A)
Lung ET-1 (% of Control)
140
120
100
80
*
Control
EtOH
(C)
Lung IL-6 (% of Control)
250
200
150
100
50
0
*
Control
EtOH
(E)
Lung TNF-α (% of Control)
350
275
200
125
50
**
Control
EtOH
(B)
Right Ventricle (ET-1 % of Control)
115
100
85
*
Control
EtOH
(D)
Right Ventricle IL-6 (% of Control)
250
200
150
100
50
0
*
Control
EtOH
(F)
Right Ventricle TNF-α (% of Control)
300
240
180
120
60
*
Control
EtOH

Figure 3.5: Ethanol-evoked upregulation of lung and RV key pro-inflammatory mediators of PAH. ET-1 (**A & B**), IL-6 (**C & D**) , and TNF-α (**E & F**) levels in lung and RV tissues of ethanol-fed, compared with isocaloric liquid diet fed (control), rats. Values are means ± SEM (n=5-6 in each group), $^{*}P < 0.05$, $^{**}P < 0.01$, compared to control group.

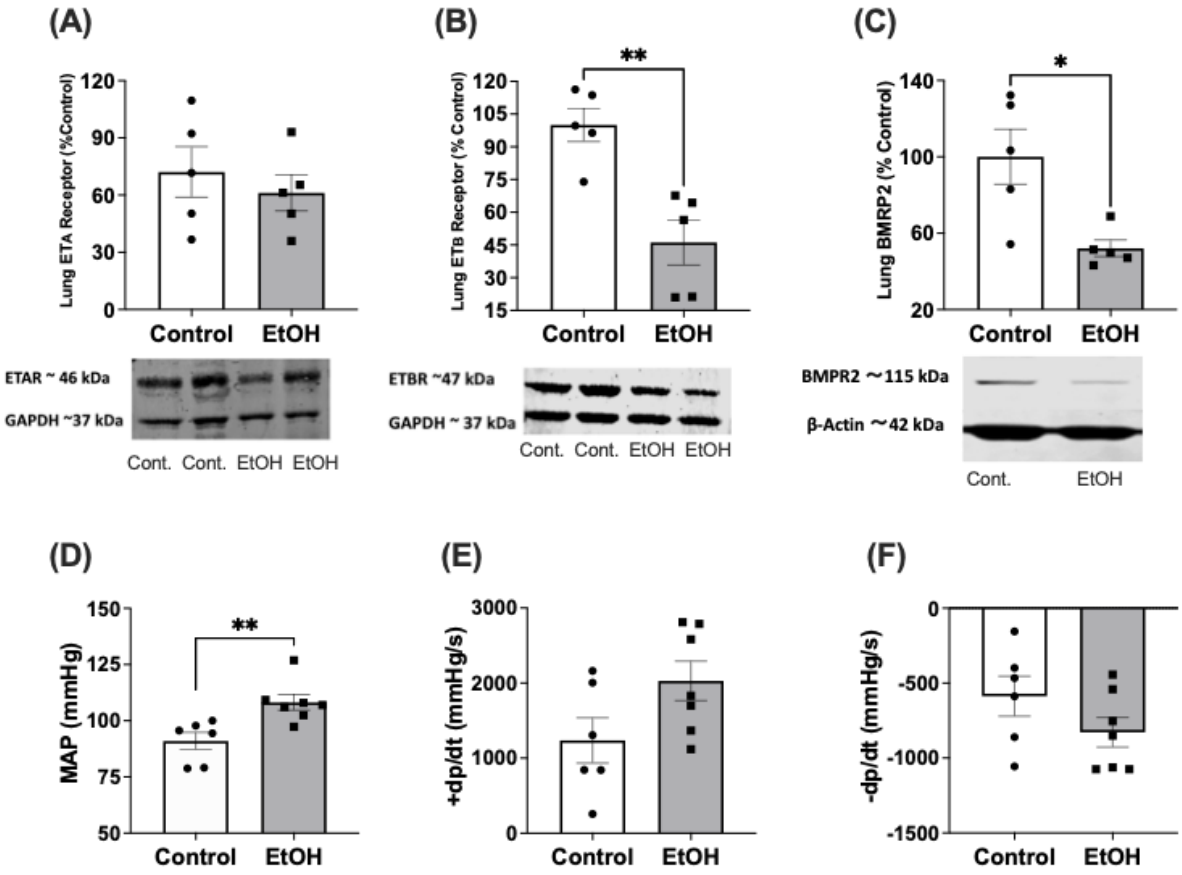
(A)
Lung ETA Receptor (%Control)
120
90
60
30
0
Control
EtOH
ETAR ~ 46 kDa
GAPDH ~37 kDa
Cont. Cont. EtOH EtOH
(B)
**
Lung ETB Receptor (% Control)
120
105
90
75
60
45
30
15
Control
EtOH
ETBR ~47 kDa
GAPDH ~ 37 kDa
Cont. Cont. EtOH EtOH
(C)
*
Lung BMRP2 (% Control)
140
100
60
20
Control
EtOH
BMPR2 ~115 kDa
β-Actin ~42 kDa
Cont.
EtOH
(D)
**
MAP (mmHg)
150
125
100
75
50
Control
EtOH
(E)
+dp/dt (mmHg/s)
3000
2000
1000
0
Control
EtOH
(F)
-dp/dt (mmHg/s)
0
-500
-1000
-1500
Control
EtOH

Figure 3.6: Ethanol affects lung receptor expression, mean arterial pressure (MAP), and contractility. Lung endothelin A receptor (ETA; **A**), endothelin B receptor (ETB; **B**) and bone morphogenetic protein receptor 2 (BMPR2, **C**) levels in ethanol-fed, compared with isocaloric liquid diet fed (control), rats. Mean arterial pressure (MAP; **D)** and dp/dt **(E, F)** generated via femoral artery catheterization. Data presented as means ± SEM (n=5-6 rats per group). Values presented as means ± SEM, $^{*}P < 0.05$, $^{**}P < 0.01$ compared to control group.

CHAPTER FOUR: Investigating the Sensitivity of Sprague-Dawley Rats to the Vascular Endothelial Cell Growth Factor Receptor (SU5416) Inhibitor and the Development of Pulmonary Arterial Hypertension

4.1 Abstract

Pulmonary arterial hypertension (PAH) is a progressive vasculopathy characterized by elevated pulmonary arterial pressure, hypertrophy of the right ventricle (RV), and eventual right-heart failure. Animal models of PAH pathophysiology are complex, with the Sugen + Hypoxia model being favored (subcutaneous injection of a vascular endothelial growth factor receptor inhibitor (SU5416 (SU)) followed by a 3-week exposure to chronic hypoxia to produce sustained PAH without recovery. Unfortunately, limited access to hypoxic chambers causes decreased accessibility to the model, negatively impacting progress in PAH research. Studying rat strain responses to SU can contribute to the development of an affordable PAH model and increase PAH research accessibility forgoing the current necessary hypoxic exposure. Previous studies have found certain strains of Sprague-Dawley (SD) rats from Charles River Laboratories of different geographic locations have heightened sensitivity to the SU injection, developing PAH without hypoxic exposure[2,7]. Therefore, the goal of this study was to evaluate the cardiopulmonary hemodynamic response of SD rats from Charles River Laboratories (Raleigh, North Carolina) to the SU injection and understand its influence on clinical and experimental PAH mediators. Interestingly, SU injected rats exhibited: 1) Elevated RV and LV afterload; 2) Significant cardiac hypertrophy and RV dilation; 3) Cardiac fibrosis; 4) Upregulation of the lung and RV pro-inflammatory endothelin-1 (ET-1), TNF-α and IL-6 signaling; 5) higher ET-1, ETA/ETB receptor ratio and downregulation of the cardioprotective protein, bone morphogenetic protein receptor 2

(BMPR2), in the lungs. Therefore, SD rats of Charles River Laboratories (Raleigh, North Carolina) are sensitive to PAH induction via a single injection of SU causing an upregulation of the proinflammatory ET1/TNFα/IL6 pathway and suppressed anti-inflammatory BMPR2.

4.2 Introduction

Pulmonary arterial hypertension (PAH) is a progressive cardiopulmonary disease characterized by elevated blood pressure within the lungs, leading to right ventricular hypertrophy and failure. The pathophysiology and development of the disease is poorly understood [82], likely due to limitations in the capacity of animal models to replicate human PAH[83]. Currently, the preclinical gold standard rat model known as the Sugen + Hypoxia model [84], produces PAH via injection of the vascular endothelial growth factor (VEGF) receptor inhibitor SU5416 (SU, 20 mg/kg), followed by a 3-week exposure to chronic hypoxia (10% O_2). While this model provides the best representation of clinical PAH, institutional access to hypoxic chambers is limited, causing decreased model accessibility.

Notably, differences in sensitivity to SU amongst rat strains has been reported, ranging from unresponsiveness to the development of severe PAH, without hypoxic exposure. Evidence suggests that rat colonies from different origins have a range of sensitivity to SU injection (Charles River Laboratories in Wilmington, MA and Montreal, QC, Canada [2,7]); however, it remains unknown if Sprague-Dawley CD stain rats from Charles River in Raleigh, North Carolina develop PAH after a single SU injection, without hypoxic exposure. Research investigating the responsiveness of rat strains to the SU injection could expand access to a clinically relevant PAH model, without the need for hypoxic exposure, an environment unattainable for many academic institutions.

The clinical PAH vasculopathy involves the upregulation of inflammatory mediators, ET-1, tumor necrosis factor alpha (TNF-a) and IL-6, with SU facilitating their induction[85–87] . ET-1 is a potent pro-inflammatory vasoconstrictor that can regulate pulmonary artery tone via activation of ETA and ETB receptors on vascular smooth muscle cells[9]. *In vitro* treatment of human lung

microvascular endothelial cells with SU resulted in ET-1 upregulation [87]. Therefore, studying if SU-sensitive rats develop PAH due to an upregulation ET-1 and an alteration in the ET-1 signaling axis warrants attention.

The PAH pathophysiology involves the upregulation of influential inflammatory markers, including ET-1 [88], TNF-α [18], and its downstream IL-6 [19 36] . It remains unclear if SU-sensitive rats develop PAH due to an enhancement in pro-inflammatory signaling within the lungs and RV.

PAH therapeutic research has investigated the protective role of the bone morphogenetic protein receptor type 2 (BMPR2), with loss of BMPR2 signaling causing pulmonary smooth muscle proliferation. BMPR2 expression is modulated by inflammation, with increased ET-1, TNF-a, and IL-6 contributing to BMRP2 deficiency [11], with the role of inflammation mediated BMPR2 deficiency in rats sensitive to SU remaining elusive.

The presented study had the following aims: First, determine whether the Sprague-Dawley CD colony at Charles River Laboratories in Raleigh, North Carolina develop PAH pathophysiology after a single injection of SU. Second, test the hypothesis that VEGF inhibition causes upregulation of ET-1/TNFα/IL-6 axis and/or downregulation of BMPR2.

4.3 Protocols and Experimental Groups

Male Sprague-Dawley rats (6-weeks; 200-250g) from Charles River Laboratories (Raleigh, North Carolina) were individually housed in standard plastic cages at the animal facility at East Carolina University, maintaining a 12-h light/dark cycle and a room temperature of 23 ± 1 °C for the duration of the experiment. This study was approved by the East Carolina University Institutional Animal Care and Use Committee and was consistent with the Guide for the Care and Use of Laboratory Animals as governed by the U.S. National Institutes of Health (2023).

Rats were given free access to water and standard chow diet. After a one-week acclimation period, rats were matched for body weight, divided into two groups (n=8-9 per group), baseline echocardiography and EchoMRI was conducted, liquid-protein diet was administered, and a one-week acclimation period was given. SU5416 (Cayman Chemical, #13342) was suspended in 0.05% vehicle CMC (0.05% carboxymethycellulose sodium, 0.9% sodium chloride, 0.4% Tween 80, 0.9% benzyl alcohol in deionized water) and rats were administered a single subcutaneous injection of SU (20 mg/kg) suspended in 0.5% CMC or vehicle control 0.5% CMC. For the duration of the experiment, liquid diets were prepared and administered fresh daily, and echocardiography and EchoMRI^{TM} were conducted weekly. Eight-weeks post-injection, rats underwent femoral artery catheterization followed by euthanasia and tissue collection. A general experimental timeline schematic is provided (Figure 4.1).

4.4 Data Analysis and Statistics

Values are presented as mean ± SEM. Time-course data was analyzed by Two-Way ANOVA with repeated measures followed by multiple comparisons testing to determine the effect of ethanol over the entire 8-week treatment period and at different time points, compared with control. Other group data was analyzed for difference between control and SU rats by unpaired two-tailed *t*-test. All statistical analyses were conducted using Prism 9.5.1 (GraphPad software Inc., La Jolla, CA) with $P < 0.05$ considered significant.

4.5 Results

4.5.1 *SU induced right ventricular hypertrophy in male SD rats after a single subcutaneous injection (20mg/ kg).*

SU-injected male rats exhibited increased RV/ LV + Septum ratio (Fig. 4.2A) and RV/Body Weight ratio (Fig. 4.2 B) 8-weeks post injection compared to control, indicative of RV hypertrophy.

4.5.2 *Liquid protein diet caused no change in body composition.*

Time-course of body weight (Fig. 4.2 C) and fat composition/body weight (Fig. 4.2) showed progressive increases while lean muscle/body weight (Fig. 4.2 E) progressively decreased during the course of the study. Diet and injection had no significant effects on body weight or body composition during the course of the study (Fig. 4.2 C-E).

4.5.3 *Echocardiographic changes in cardiac structure due to VEGF receptor inhibition.*

Representative transthoracic echocardiographic short-axis images of control (Fig. 4.3 A) and SU injected (Fig. 4.3 B) hearts 8-weeks post injection with showing RV dilation and septal shift in SU treated rats. Further m-Mode imaging of control and SU rats (Fig. 4.4 A) supports SU mediated RV dilation, exhibiting increased RV internal diameter compared to control. Time-course quantification of RVID; d/ LVID; d ratio (Fig 4.4 B) showed significant time-course increases in RV diameter.

4.5.4 *SU injection increased RV afterload.*

Echocardiographic pulsed-wave doppler example images of the pulmonary artery show significant changes in waveform (Fig. 4.5A) due to the SU injection (doppler images at 8-weeks post

injection). Time-course analysis of mPAP (Fig. 4.5 B) showed an overall significantly increased mPAP in rats treated with SU compared to control, with significant increases at weeks 6 and 7 post-injection. Analysis of pulmonary artery acceleration time (PAAT, Fig. 4.5 B, C) showed a significant decrease in time to peak velocity. The PAAT/PET ratio (Fig. 4.6 E, F) was significantly reduced due to the SU injection. These results reflect SU-induced increases in RV afterload. Representative histological images showed healthy intrapulmonary arteries within the lungs of control rats (Fig. 4.6 A); however, rats treated with SU showed the formation of plexiform lesions within the lung (Fig, 4.6 B).

4.5.5 *VEGF Receptor Inhibition Induces a Lung and RV Pro-Inflammatory Environment.*

Quantification of pro-inflammatory mediators involved in experimental and clinical PAH showed SU induced elevation in lung endothelin-1 (ET-1, Fig. 4.7A) compared to control, with no significant change in RV ET-1 (Fig. 4.7B). Tumor necrosis factor-alpha (TNF-α) was increased in both lung and RV (Fig. 4.7 C&D) compared to control. Further increases in lung and RV interleukin-6 (IL-6; Fig. 4.7 E, F) were observed in SU injected rats compared to control. These data showed a pro-inflammatory environment in the lungs and RV of SU injected rats, which exhibited pulmonary and cardiac phenotypes related to PAH.

4.5.6 *VEGF receptor inhibition induces cardiac fibrosis within the right ventricle 8-weeks post injection.*

Quantification of cardiac fibrosis (Fig. 4.8 A) of Masson's Trichrome stained RV tissue showed SU injected rats having significantly higher percent fibrotic area compared to control rats 8-weeks post injection. Representative microscopic imaging of RV cardiac fibrosis (Fig. 4.8 B) shows SU

treated rats having increased collagen (blue stain) compared to control, indicative of cardiac fibrosis, a consequence of PAH.

4.5.7 *SU injection causes modification to lung receptors important in PAH therapeutics.*

Western blot analysis of both endothelin A (ETA) and endothelin B (ETB) receptors showed no significant change in ETA receptor expression (Fig. 4.9 A) but a significant downregulation in ETB receptor expression (Fig. 4.9 B). Additional analysis of the anti-inflammatory/anti-angiogenic lung bone morphogenetic protein receptor 2 (BMPR2) exhibited significant downregulation in rats injected with SU compared to vehicle control (Fig. 4.9 C).

4.5.8 *VEGF receptor inhibition causes significant change to arterial pressure and contractility.*

Final mean arterial pressure (MAP; Fig. 4.10 C) obtained via femoral artery catheterization was elevated in rats injected with SU compared to control. Time-based echocardiographic analysis of the LV showed increased LV mass/body weight ratio (Fig. 4.10 A) compared to control. Analysis of -dp/dt and +dp/dt (Fig. 4.10 C &D) via final femoral artery catheterization showed a significant decrease in -dp/dt in SU injected rats compared to control, and no alteration in +dp/dt. These results are consistent with SU-induced LV hypertrophy and decreased cardiac relaxation during diastole.

4.6 Discussion

The SU injection (20mg/kg) in combination with chronic hypoxia is the favored method to induce PAH in rats, inducing sustainable PAH without recovery upon return to normoxia[89]. Strain sensitivity of SD male rats to VEGF receptor inhibition and incidence of PAH development

without hypoxia has been reported in previous studies[2,7]. The present study demonstrates the capacity of a single SU injection to produce PAH characteristics and alter influential PAH mediators in male SD rats (CD stain) from Charles River Laboratories (Raleigh, North Carolina).

Analysis of RV/LV + Septum and RV/body weight ratios (Figure 4.2 A & B) determined significant SU-induced RV hypertrophy, consistent with previous studies[2,7]. The RV hypertrophy observed in this study is likely due to increased RV afterload, a classic phenotype of PAH[74]. This is supported by our longitudinal pulsed-wave doppler assessment of the pulmonary artery, detailing significant SU-mediated reductions in PAAT and PAAT/PET (Figure 4.5 C & D), an echocardiographic measurement that inversely correlates with RV systolic pressure (RVSP) obtained from RV catheterization [75,90]. Additional echocardiographic assessment found a significant increase in mPAP (Figure 4.5 B) in SU-injected rats, a key diagnostic of PAH [91].

Chronic pressure overload due to PAH induces change in the RV extracellular matrix, resulting in collagen deposition in the form of fibrosis [92]. Masson's trichrome staining (Figure 4.8 A & B) of the RV showed collagen deposition with significant increase in percent fibrotic area SU-injected rats compared to control. Importantly, elevations in RV afterload can induce RV structure change, specifically RV dilation [77]. Echocardiographic assessment of RV chamber size in M-mode showed (Figure 4.3 A) increased chamber size 8-weeks post injection with SU compared to control. Additional time-based assessment RVID; d/ LVID; d ratio (Figure 4.3 B) showed a progressive and significant increase in RV diameter due to the SU injection, suggesting RV dilation.

It is important to address the observation that effects of VEGF receptor inhibition were not isolated to the RV and pulmonary artery. Assessment of LV mass/body weight (Figure 10A) determined LV hypertrophy in SU-injected rats. Notably, an SU-induced change in cardiac

contractility derived from femoral artery catheterization showed a significant decrease in -dp/dt and unchanged +dp/dt (Figure 4.10 C & D), indicative of compromised cardiac relaxation during diastole, a characteristic significantly altered in hypertrophy [93]. Additionally, there was a marked increase in MAP (Figure 4.10 B) derived from direct assessment of blood pressure in SU-injected rats was recorded, indicating hypertension, the most common source of LV hypertrophy [94]. These results support that VEGF receptor inhibition increases LV afterload, resulting in LV hypertrophy, and a subsequent alteration in LV relaxation during diastole.

It is important to note the pair-fed liquid-based protein diet and the injection (vehicle or SU) did not result in reduction in body weight, fat, or lean muscle (Figure 4.3), supporting the cardiac hypertrophy and blood pressure changes were due to SU and not the diet.

This study hypothesized that VEGF receptor inhibition will cause an upregulation of endothelin-1 (ET-1) and change its receptor ratio (ETA/ETB), contributing to SU-induced pulmonary and RV remodeling. This study showed significant elevation lung ET-1 and unchanged RV ET-1 (Figure 4.7 A, B) concentrations in rats treated with SU, consistent with upregulated lung ET-1 in PAH patients [95]. ET-1 is a dynamic protein, mediating opposing vascular effects dependent on activation of receptor subtypes and their location. Activation of the ETA and ETB receptors on vascular smooth muscle cells induces vasoconstriction[26], while activation of ETB receptors located on endothelial cells causes vasodilation[79]. This study displayed an increase in lung ETA/ETB receptor ratio in SU-injected rats (Figure 4.9 A & B), indicating a shift toward ET-1 mediated vasoconstriction. This study demonstrates VEGF receptor inhibition causes ET-1 upregulation and an increased lung ETA/ETB receptor ratio, which could contribute to the pathological hemodynamic changes in the pulmonary artery. These findings indicate that SU

sensitivity in SD rats from Charles River Laboratories could be attributed to a shift in the ET-1 signaling axis within the lungs.

ET-1 influences cytokine production, increasing production the pro-inflammatory mediator IL-6 [10], a highly influential molecule in clinical and experimental PAH, with elevations associated with increased RV dysfunction and poor patient outcome [10]. Additionally, clinical, and experimental PAH have upregulated TNF-a [30], a known stimulator of IL-6 release from vascular smooth muscle cells [36]. This study showed SU-induced elevations in lung and RV IL-6 and TNF-a (Figure 4.7 C-F). Collectively, these results support the SU-evoked upregulation of the ET-1/TNF-α/IL-6 axis contributes PAH development.

BMPR2, a member of the TGF-b family and novel target in PAH therapeutics, it known to be downregulated in PAH patients[96]. Its role in anti-proliferative signaling protects the pulmonary vasculature from the occlusion seen in PAH patients[40]. This study showed SU-mediated downregulation of lung BMPR2 levels (Figure 4.9, C), which possibly contributes to pulmonary artery alterations and change in RV structure. ET-1, found to be upregulated in this study, downregulates BMPR2 signaling, leading to pulmonary artery smooth muscle cell proliferation[41]. Previous studies report TNF-a as a reducer of BMPR2 transcription and enhancer of its cleavage[97]; therefore, SU-induced TNF-a upregulation could contribute to the downregulation of BMPR2 in this study. Finally, BMPR2 is repressed through an IL-6-STAT-3 pathway[43]. Therefore, lung BMPR2 expression could be downregulated via SU-enhancement of a pro-inflammatory ET-1/TNF-a/IL-6 pathway, leading to a promotion of PAH pathophysiology in SD male rats from Charles River Laboratories (Raleigh, North Carolina).

This work is a contribution to PAH research in an effort to advance our understanding on strain sensitivity to VEGF receptor inhibition amongst rat colonies of different locations. This

work should be interpreted within the area of its inherent limitations. This study establishes the SU injection as an inducer of PAH in SD rats, but it is uncertain if the experimental timeline was increased if the disease would progress or recovery would occur. This experiment was conducted using a small cohort of male SD rats. Future experiments should use increased sample size with the addition of female rats to better assess overall sensitivity to PAH induction using SU without hypoxia. Additionally, while echocardiography is a highly utilized non-invasive diagnostic and longitudinal study tool for PAH, this study lacks direct measurement of RVSP, a limitation to be addressed in future studies. Finally, the molecular analysis conducted in this study was done using tissue homogenates, thus additional cell type specific research (i.e., pulmonary endothelial cells) would increase specificity of the results.

In summary, this study adds to our current knowledge on SU-induced PAH. While further research is needed, it could contribute to eventual development of an SU-sensitive strain that develops severe PAH, similar to the Sugen + Hypoxia model, thus increasing animal model accessibility to institutions without hypoxic chambers, and eventual increase in PAH research.

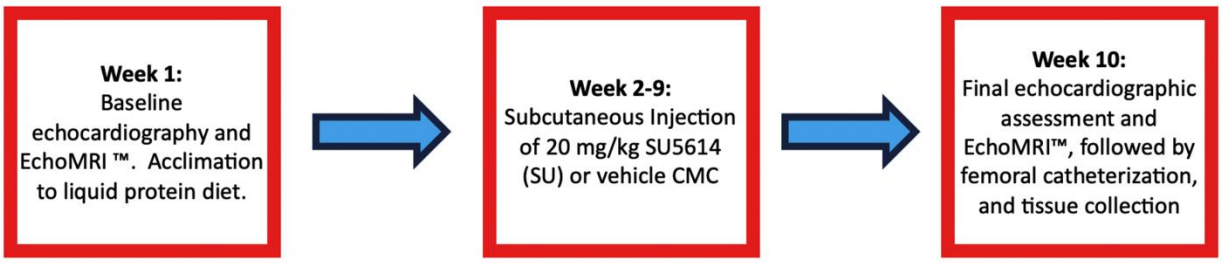
Week 1:
Baseline echocardiography and EchoMRI ™. Acclimation to liquid protein diet.
Week 2-9:
Subcutaneous Injection of 20 mg/kg SU5614 (SU) or vehicle CMC
Week 10:
Final echocardiographic assessment and EchoMRI™, followed by femoral catheterization, and tissue collection

Figure 4.1: Aim Two Experimental Timeline. A synopsis of the experimental diet regimen, injection of SU or vehicle control, echocardiographic and EchoMRI™ schedule, femoral catheterization, and final tissue collection in control and SU groups.

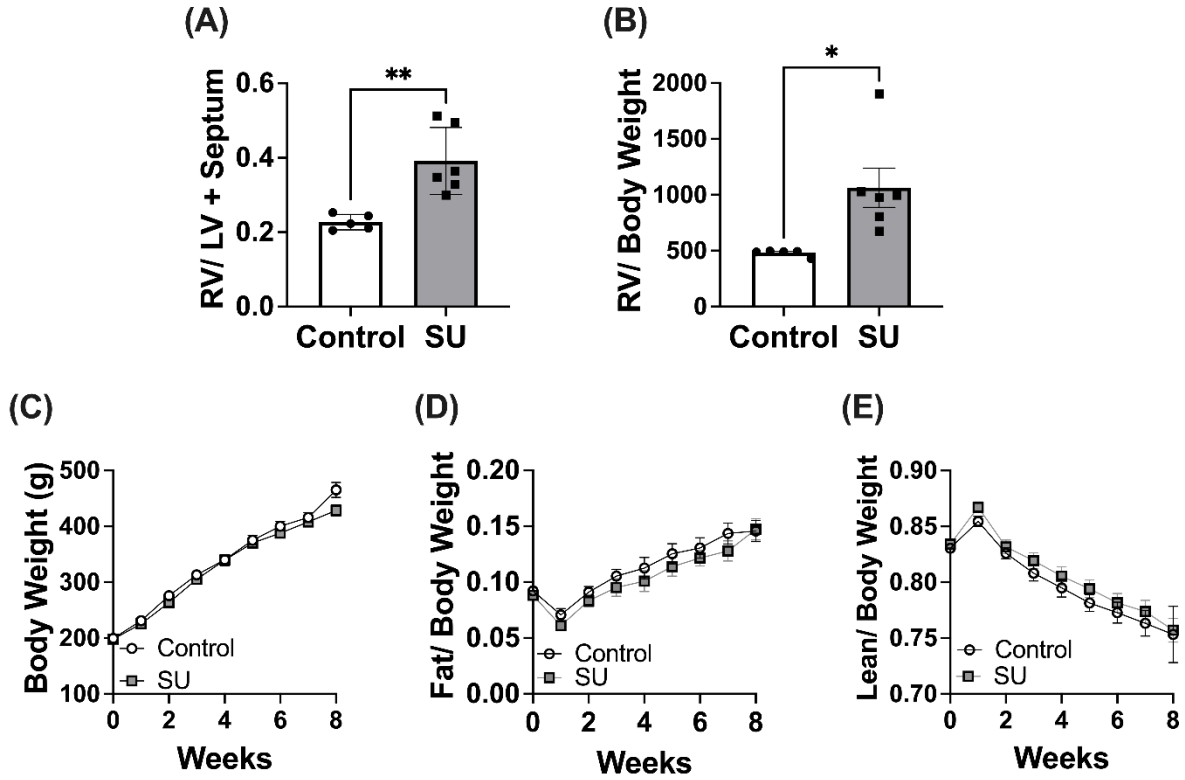
(A)
RV/ LV + Septum
0.6
0.4
0.2
0.0
**
Control
SU
(B)
RV/ Body Weight
2000
1500
1000
500
0
*
Control
SU
(C)
Body Weight (g)
500
400
300
200
100
Control
SU
0
2
4
6
8
Weeks
(D)
Fat/ Body Weight
0.20
0.15
0.10
0.05
0.00
Control
SU
0
2
4
6
8
Weeks
(E)
Lean/ Body Weight
0.90
0.85
0.80
0.75
0.70
Control
SU
0
2
4
6
8
Weeks

Figure 4.2: **VEGF receptor inhibition via SU5416 injection causes right ventricular hypertrophy in CD strain Sprague-Dawley male rats.** Higher Fulton index (RV/ LV+Septum) **(A)** and right ventricle (RV) weight to body weight ratio **(B)** were observed, indicating RV hypertrophy in SU treated rats compared to control. Time-course of body weight **(D)**, and EchoMRI™ analysis of body fat content/body weight **(E)**, and lean mass/body weight **(F)** of SU-treated and control rats. Data are presented as mean ± SEM (n=6-9 in each group); $^{*}P < 0.05$, $^{**}P < 0.01$, compared to control group.

(A)

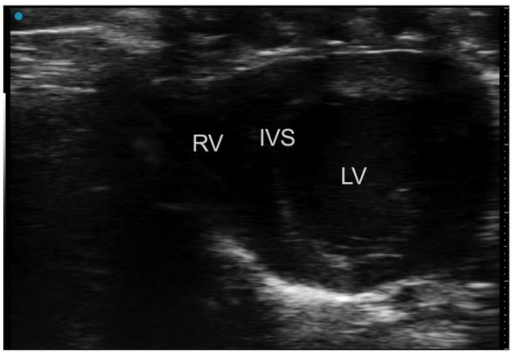

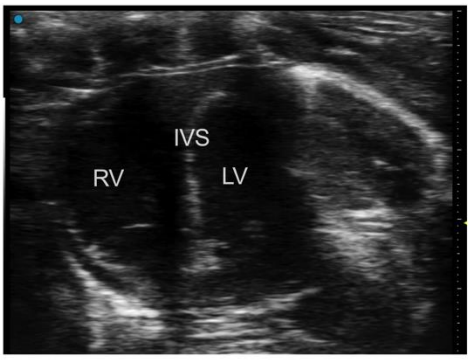

Control

Su

(B)

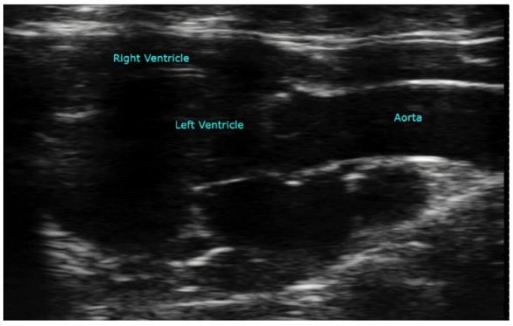

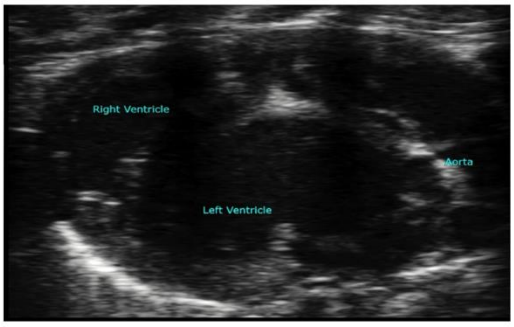

Figure 4.3: **Representative echocardiographic images of control and SU treated rats.** Short-axis **(A)** and long-axis **(B)** transthoracic echocardiography showing control and SU rats showing right ventricle (RV), left ventricle (LV), and intraventricular septum (IVS) alterations 8-weeks post-injection.

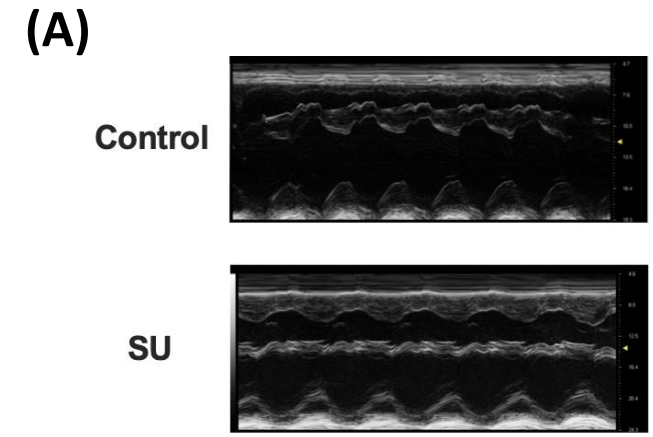
(A)
Control
SU

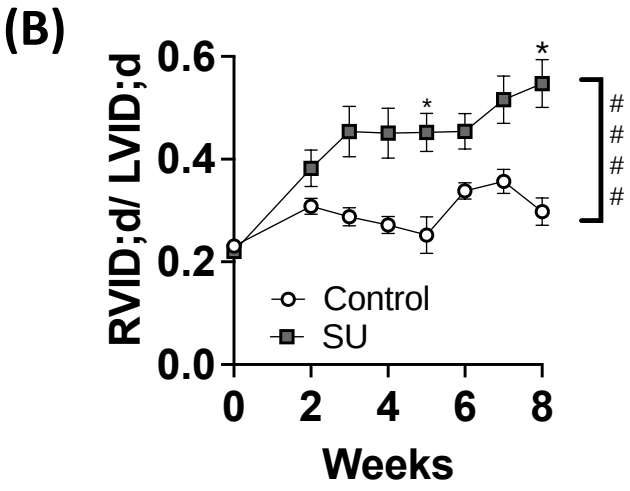
(B)
RVID;d/ LVID;d
0.6
0.4
0.2
0.0
0
2
4
6
8
Weeks
Control
SU
*
*
#
#
#
#

Figure 4.4: VEGF receptor inhibition evokes right ventricle dilation. (A) Example echocardiographic images showing RV and LV diameter in control and SU injected rats 8-weeks post injection. Time-course echocardiographic RVID; d/LVID (**B)** showing increased RV diameter in SU injected rats. Time-course data analyzed by two-way ANOVA with repeated measures followed by Bonferroni multiple comparisons testing. $^{\#}P<0.05$, $^{\#\#}P<0.01$, $^{\#\#\#}P<0.001$ vs control pair-fed rats, $^{*}P<0.05$, $^{**}P<0.01$ vs. corresponding weekly value.

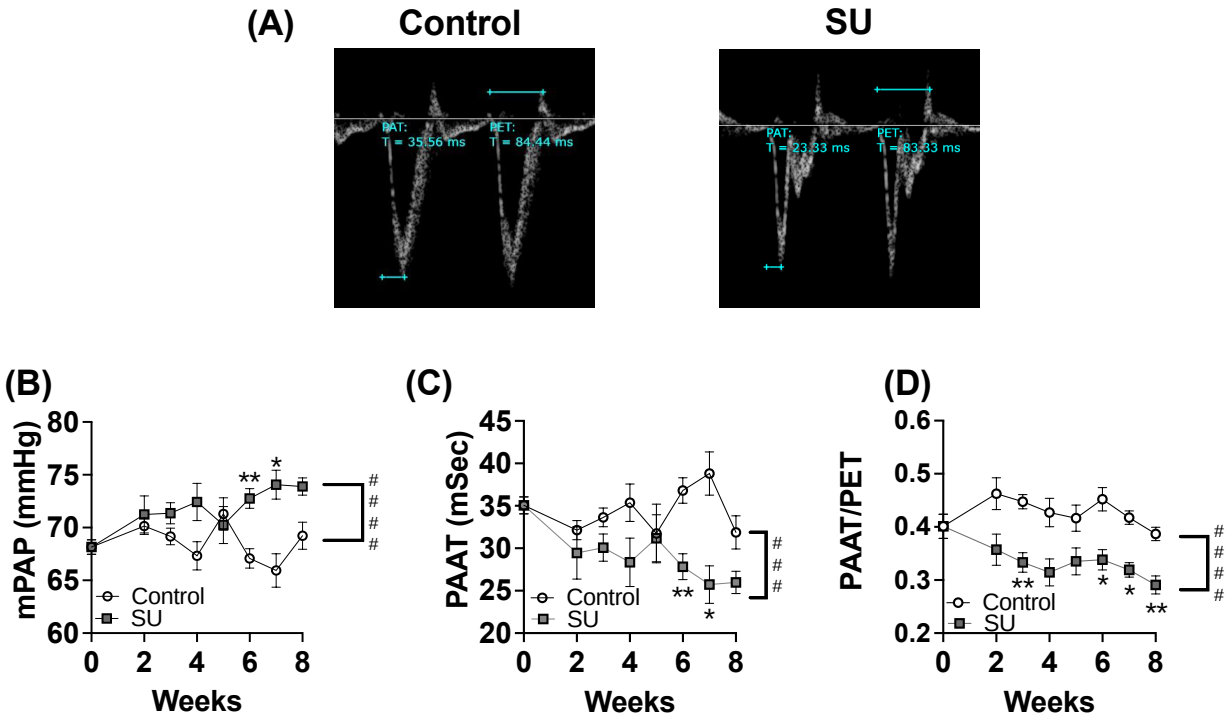
(A)
Control
SU
PAT:
T = 35.56 ms
PET:
T = 84.44 ms
PAT:
T = 23.33 ms
PET:
T = 93.33 ms
(B)
mPAP (mmHg)
Control
SU
Weeks
(C)
PAAT (mSec)
Control
SU
Weeks
(D)
PAAT/PET
Control
SU
Weeks

Figure 4.5: Time-course echocardiographic analysis of the pulmonary artery. Representative pulsed-wave doppler images **(A)** of control and SU pulmonary artery 8-weeks post-injection. Time course analysis of mPAP **(B),** PAAT **(C)** PAAT/PET ratio **(D)**. Values are reported as means ± SEM (n= 8-9 per group). Data analyzed by two-way ANOVA with repeated measures followed by Bonferroni multiple comparisons testing. $^{\#}P<0.05$, $^{\#\#}P<0.01$, $^{\#\#\#\#}P<0.0001$ vs control rats, $^{*}P<0.05$, $^{**}P<0.01$ vs. corresponding weekly value.

(A)

Control

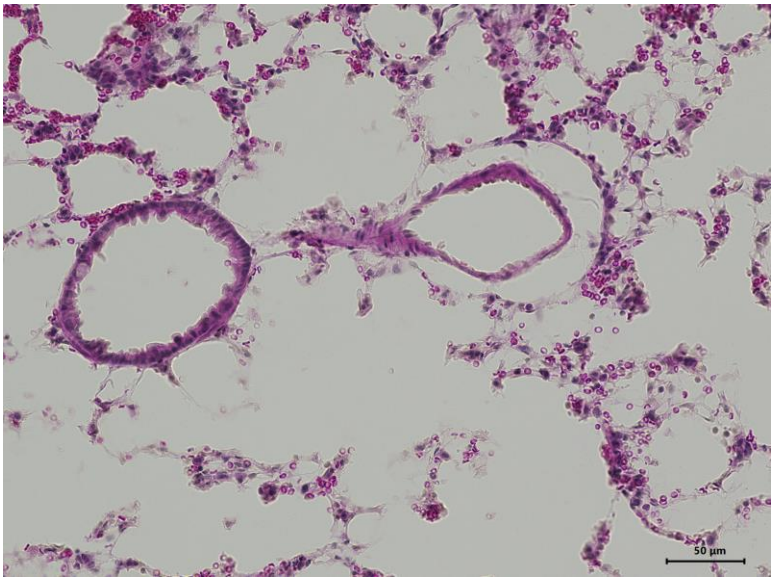

(B)

SU

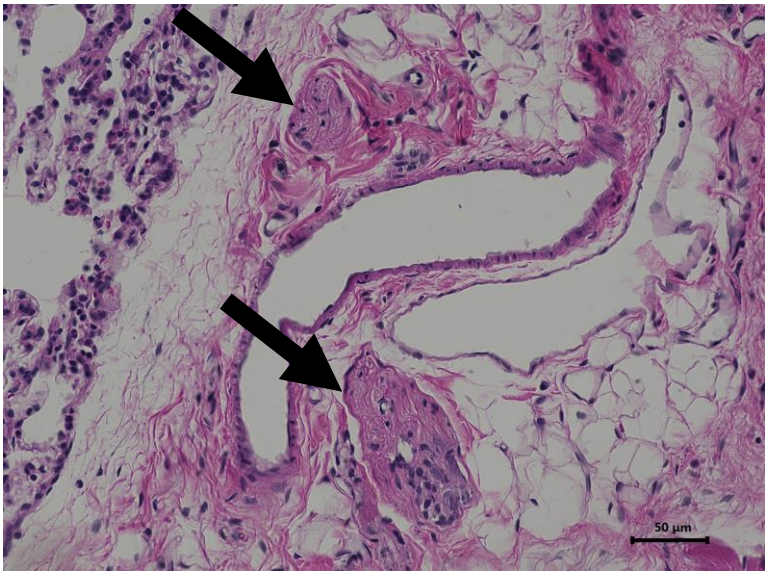

Figure 4.6: VEGF inhibition induced plexiform lesions within the lung. H & E staining of lung tissue showed healthy intrapulmonary arteries in control rats and the presence of plexiform lesions in SU-injected rats **(B)**.

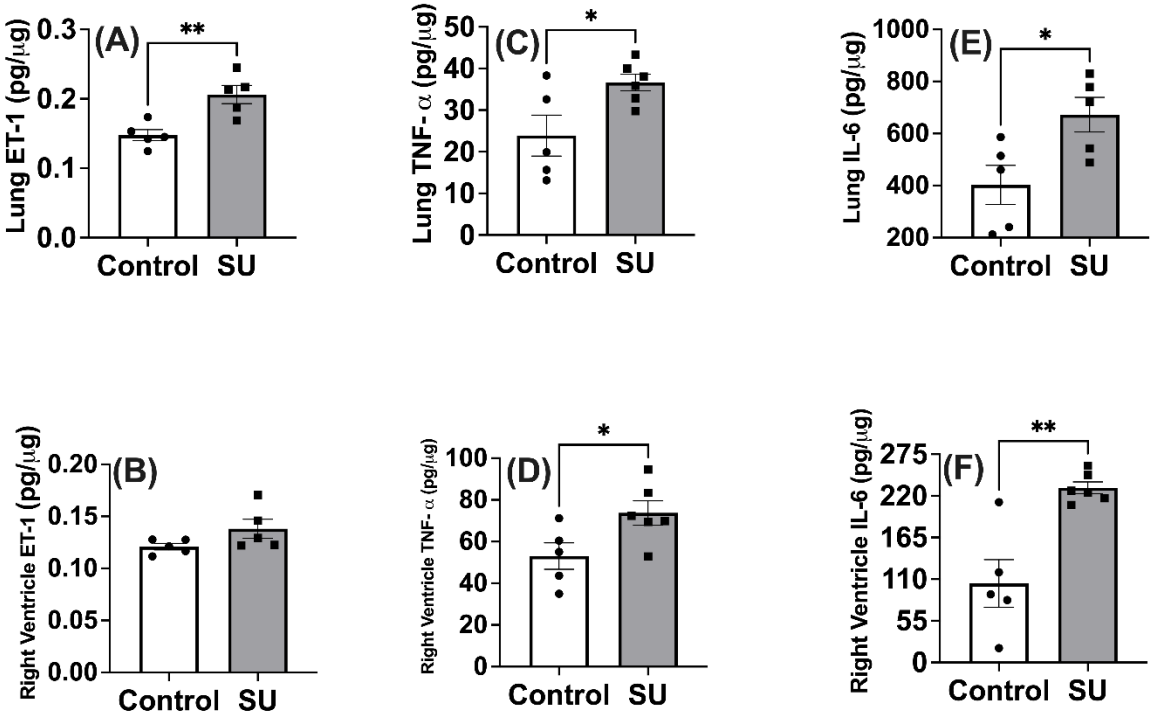
(A)
**
Lung ET-1 (pg/μg)
0.3
0.2
0.1
0.0
Control
SU
(C)
*
Lung TNF- α (pg/μg)
50
40
30
20
10
0
Control
SU
(E)
*
Lung IL-6 (pg/μg)
1000
800
600
400
200
Control
SU
(B)
Right Ventricle ET-1 (pg/μg)
0.20
0.15
0.10
0.05
0.00
Control
SU
(D)
*
Right Ventricle TNF- α (pg/μg)
100
80
60
40
20
0
Control
SU
(F)
**
Right Ventricle IL-6 (pg/μg)
275
220
165
110
55
0
Control
SU

Figure 4.7: Upregulation of key pro-inflammatory markers of PAH pathophysiology within the lungs and RV due to VEGF receptor inhibition. ELISA quantification of ET-1 (**A, B**), IL-6 (**C, D**) , and TNF-α (**E, F**) in lung and RV tissue from differing experimental groups. Values reported in mean ± SEM (n=5-6 in each group), $^{*}P < 0.05$, $^{**}P < 0.01$, compared to control group.

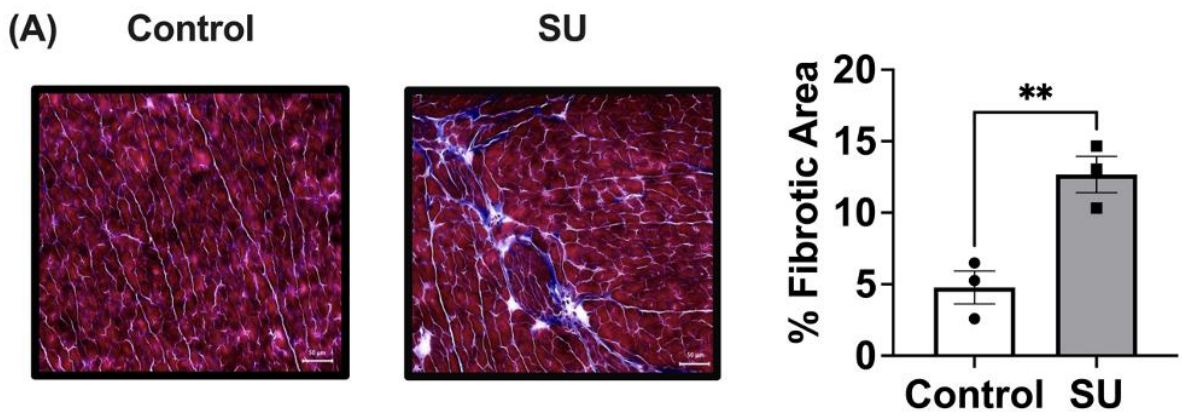
(A)
Control
SU
% Fibrotic Area
20
15
10
5
0
**
Control
SU

Figure 4.8: Trichrome staining of the right ventricle showed fibrosis due to VEGF receptor inhibition. Quantification of fibrotic area in Masson's Trichrome-stained RV (**A**) with representative images (**B**) illustrating increased SU- induced fibrosis compared to control. Values are reported as mean ± SEM (n=3), $^{**}P < 0.01$, compared to control group.

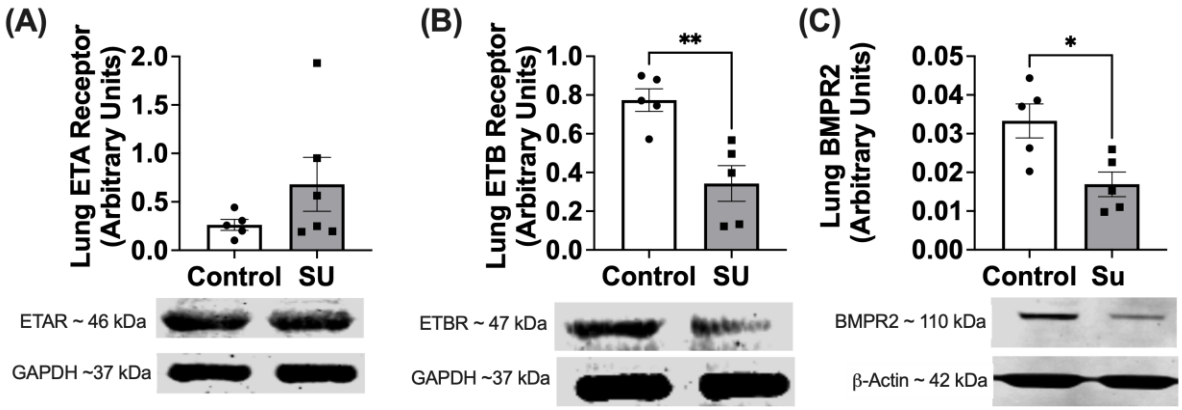
(A)
Lung ETA Receptor (Arbitrary Units)
2.0
1.5
1.0
0.5
0.0
Control
SU
ETAR ~ 46 kDa
GAPDH ~37 kDa
(B)
Lung ETB Receptor (Arbitrary Units)
**
1.0
0.8
0.6
0.4
0.2
0.0
Control
SU
ETBR ~ 47 kDa
GAPDH ~37 kDa
(C)
Lung BMPR2 (Arbitrary Units)
*
0.05
0.04
0.03
0.02
0.01
0.00
Control
Su
BMPR2 ~ 110 kDa
β-Actin ~ 42 kDa

Figure 4.9: Determination of SU elicited effect on lung receptor expression. Western blot analysis of lung endothelin A receptor (ETA, **A**), endothelin B receptor (ETB, **B**) and bone morphogenetic protein receptor 2 (BMPR2, **C**). Data are presented as mean ± SEM (n=5-6 rats per group). Values presented as means ± SEM, $^{*}P < 0.05$, $^{**}P < 0.01$ compared to control group.

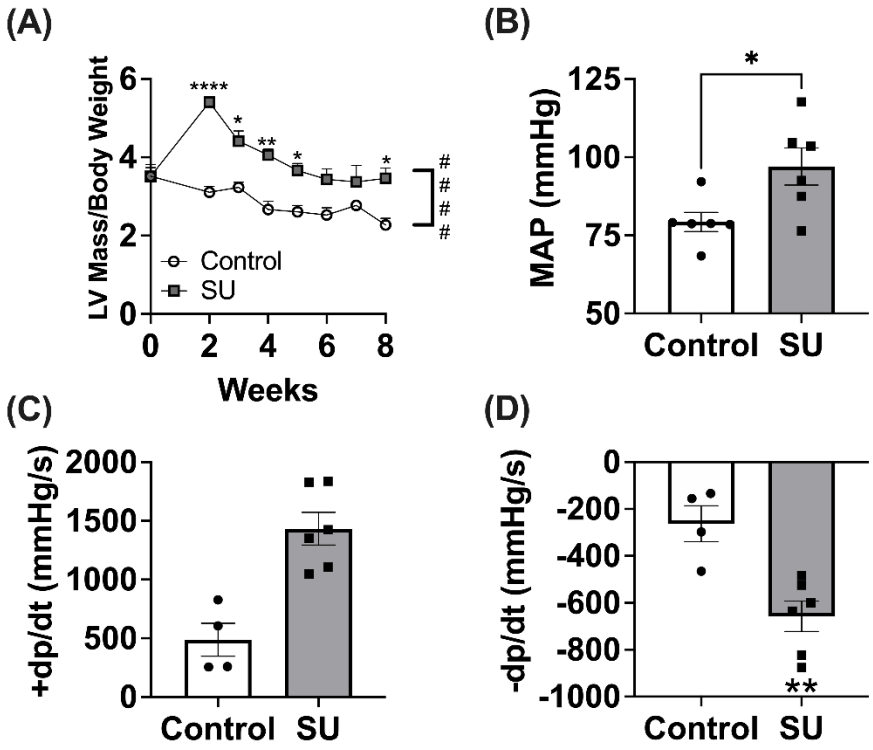
(A)
LV Mass/Body Weight
6
4
2
0
****
*
**
*
*
#
#
#
#
Control
SU
0
2
4
6
8
Weeks
(B)
MAP (mmHg)
125
100
75
50
*
Control
SU
(C)
+dp/dt (mmHg/s)
2000
1500
1000
500
0
Control
SU
(D)
-dp/dt (mmHg/s)
0
-200
-400
-600
-800
-1000
**
Control
SU

Figure 4.10: VEGF receptor inhibition causes LV hypertrophy and elevated arterial pressure. Time-course echocardiographic analysis of LV mass/Body Weight was significantly increased due to SU treatment (A). Mean arterial pressure (MAP; **B)** and dp/dt **(C, D)** generated via femoral artery catheterization. Data presented as means ± SEM (n=5-6 rats per group). Values presented as means ± SEM, $^{*}P < 0.05$, $^{**}P < 0.01$ compared to control group. Time-course data analyzed by two-way ANOVA with repeated measures followed by Bonferroni multiple comparisons testing. $^{\#}P<0.05$, $^{\#\#}P<0.01$, $^{\#\#\#}P<0.001$ vs control pair-fed rats, $^{*}P < 0.05$, $^{**}P < 0.01$ vs. corresponding weekly value.

CHAPTER FIVE: MODERATE CHRONIC ETHANOL CONSUMPTION ENHANCES SU5416 INDUCED PULMONARY ARTERIAL HYPERTENSION IN MALE RATS

5.1 Abstract

Our previous study determined that moderate ethanol consumption is a cardiopulmonary insult that predisposes pulmonary arterial hypertension (PAH) development. Furthermore, the same CD-strain of Sprague-Dawley (SD) rats displayed sensitivity to developing PAH after single injection of the VEGF receptor inhibitor SU5416 (SU). This preclinical study involved the co-administration of single administration of the VEGF receptor inhibitor SU and 8-week exposure to chronic moderate ethanol consumption (5% w/v). Four groups of male Sprague-Dawley rats were divided into the following groups: 1) Vehicle + pair-fed isocaloric liquid diet; 2) Vehicle + balanced liquid diet containing 5% ethanol (w/v); 3) SU injection + pair-fed isocaloric liquid diet; 4) SU injection + balanced liquid diet containing 5% ethanol (w/v). Weekly echocardiography was conducted to assess cardiopulmonary function, followed by tissue collection for *ex vivo* histological and molecular testing. Rats exposed to ethanol-diet plus VEGF receptor blockade exhibited: (1) Elevated RV afterload (2) Cardiac hypertrophy; (3) higher ET-1, lung ETA/ETB ratio, and downregulation of cardioprotective bone morphogenetic receptor protein 2 (BMPR2). These observations reveal that chronic ethanol exposure causes cardiopulmonary insult and contributes to the exacerbation SU-induced PAH pathophysiology.

5.2 Introduction

Pulmonary arterial hypertension (PAH) is paradoxical disease brought on via genetic predisposition or environmental factors, usually in multifactorial combination[98]. The VEGF receptor inhibitor, SU5416 (SU), accompanied by a 3-week exposure to chronic hypoxia is one of the best animal (or experimental) models of PAH [89], inducing angioobliterative lesions similar to plexiform lesions observed clinically, a characteristic not reflected in other popular PAH experimental models[99]. Recent studies observed hypersensitivity to the SU injection, developing PAH after single administration of SU, without hypoxic exposure in male SD rats [2,7]. Notably, our recent study (chapter four) confirmed the presence of SU-hypersensitivity (single administration of 20 mg/kg injection) in SD rats from Charles River Laboratories, Raleigh, NC, inducing PAH characteristics in absence of hypoxia. This research combines the findings of moderate ethanol consumption inducing PAH predisposition[100] (chapter three) with the observed hypersensitivity of SU-mediated PAH induction (chapter four) in SD rats to follow a "second-hit hypothesis" of PAH exacerbation.

The experimental PAH "second-hit hypothesis" theorizes at risk individuals (usually genetic) develop PAH through exposure certain drugs/toxins, thus contributing to the development of the disease. Therefore, this preclinical study follows "two-hit" exposure: 1) SD rats hyperresponsive to VEGF receptor blockade using SU; 2) 8-week exposure to chronic moderate ethanol consumption. The present study is the first to assess the impact of VEGF receptor blockade in rats chronically administered an ethanol-based diet.

Our previous studies showed ethanol and SU-mediated changes in cardiopulmonary hemodynamics, development of cardiac hypertrophy and fibrosis, upregulated PAH-

inducing/mediating inflammation (ET-1, IL-6, TNF-α) with increased ETA/ETB ratio and downregulated BMPR2 expression. Therefore, the third phase of this research will address the following hypothesis: exposure to chronic ethanol-diet will exacerbate PAH induced by VEGF receptor blockade in rats sensitive to PAH development. To test this hypothesis this study will assess: 1) hemodynamic function and cardiac hypertrophy; 2) pro-inflammatory cytokine expression; 3) alterations to endothelin receptor profile and BMPR2 within the lung. This preclinical research adds to our understanding of how lifestyle choices, like ethanol consumption, combined an inducer of PAH (SU) can influence the pathophysiology of PAH in rats sensitive to PAH development.

5.3 Protocols and Experimental Groups

Six-week-old male SD (CD strain, 200-250g) rats from Charles River (n=7-9 per group) were used in this study. Baseline echocardiography, body weight, and EchoMRI were conducted after one week acclimation period, and repeated weekly throughout the experiment. Next, rats were divided into four treatment groups: 1) Isocaloric control liquid diet with vehicle injection of 0.05% CMC; 2) Ethanol-based (5%) liquid protein diet with vehicle injection of 0.05% CMC; 3) Isocaloric control liquid diet with 20 mg/kg injection of SU; 4) Ethanol-based (5%) liquid protein diet with 20 mg/kg SU injection. Rats were housed individually, and liquid-protein diet administration began, with rats receiving 2.5% ethanol liquid protein diet or an isocaloric pair-fed control diet for one week. After one week at 2.5%, ethanol concentration was increased to 5%, water was removed from the cage, and food was prepared fresh daily. At 8-weeks of 5% ethanol, femoral catheterization to record hemodynamic measurements were conducted, followed by tissue

collection for molecular and histological analyses. A general schematic of the experimental timeline is provided (Figure 5.1).

5.4 Statistical Analysis

Statistical analyses were conducted using GraphPad Prism 9.2 software and data was expressed in mean ± SEM. Analyses of Western blot and ELISA results were conducted using a one-way ANOVA followed by Tukey's multiple comparison post hoc testing. Two-way ANOVA with multiple comparisons post hoc testing was used on change from baseline data.

5.5 Results

5.5.1 VEGF receptor inhibition in combination with ethanol-diet exacerbates right ventricular hypertrophy. The ethanol-feeding regimen tested every other week resulted in a blood ethanol concentration range of 31-49 mg/dL (Fig. 5.2 A), consistent with our previous findings[100], and did not differ between ethanol-consuming groups. Post-euthanasia analysis of RV/LV + Septum (Fig. 5.2 B) ratio was significantly increased in the SU + EtOH group, and RV/body weight (Fig. 5.2 C) ratio was significantly increased in all experimental groups compared to control.

5.5.2 Ethanol-diet with pair-fed controls showed no alteration in body weight and composition.

Time-based analysis (Fig. 5.3 A) showed no difference in body weight between groups. Body composition was not significantly altered for the duration of the experiment, as fat/body weight (Fig. 5.3 B) and lean/body weight (Fig. 5.3 C) were not significantly different from one another.

5.5.3. A combination of ethanol and SU causes increased right ventricular afterload.

Mean pulmonary arterial pressure (mPAP, Fig. 5.4 B) was elevated from baseline in ethanol-drinking vs. control rats and SU+ EtOH diet-rats vs. control rats. Pulsed-wave doppler echocardiographic assessment of the pulmonary artery showed visual (Fig. 5.4 A) wave-form alterations in SU + EtOH vs. control group. Analysis of pulmonary artery acceleration time (PAAT, Fig. 5.4 C) showed significant decreases in EtOH vs. control and SU vs. control, with the most significant decrease in SU + EtOH compared to healthy control rats. Further analysis of PAAT/pulmonary artery ejection time (PAAT/PET) ratio (Fig. 5.4 D) showed significant decreases in both EtOH and SU treated groups compared to control with an additional decrease in the SU+EtOH group compared to control.

5.5.4 Right ventricle dilation was present but not exacerbated.

Representative M- mode echocardiographic images of RVID ;d/ LVID; d at 8-weeks of 5% (w/v) ethanol consumption (Figure 5.5 A) show increased RV internal diameter with a decrease in LV internal diameter. Echocardiographic analysis of RVID; d/ LVID; d ratio (Fig. 5.5 B) showed significant increases in SU vs. control, SU vs. EtOH, and SU + EtOH vs. control groups, indicating the presence of RV dilation, a hallmark of PAH.

5.5.5 EtOH + SU causes significant PAH-related inflammation within the lungs.

ELISA quantification of PAH pro-inflammatory markers within the lungs (Fig. 5.6) showed upregulated ET-1 (Fig. 5.6 A) in the SU + EtOH treated rats compared to control with additional increases in SU + EtOH vs. EtOH-diet rats, suggesting EtOH in combination with SU causes

significant ET-1 upregulation. TNF-a concentration (Fig. 5.6B) was significantly upregulated in EtOH-diet vs control groups. Additionally, SU + EtOH vs. control, SU + EtOH vs EtOH-diet, and SU + EtOH vs. SU were all significantly different, with SU + EtOH rats expressing the highest TNF-a concentration. Additional quantification of lung IL-6 concentration (Fig. 5.6 C) showed a marked increase in SU vs. control, with the most significant upregulation in SU + EtOH vs. control rats.

5.5.6 SU + EtOH combination upregulates right ventricle IL-6 expression.

ELISA quantification of RV ET-1 (Fig. 5.7 A) showed significant upregulation in only the SU vs. control groups. Analysis of RV TNF-a levels (Fig. 5.7 B) showed a marked increase in the EtOH-diet vs. control rats. Further analysis of IL-6 (Fig. 5.7 C) expression showed a significant increase in EtOH-diet vs. control-diet and the most significant increase in SU+ EtOH-diet vs. control-diet rats.

5.5.7 Chronic ethanol consumption in combination with VEGF receptor inhibition exhibits RV fibrosis.

Histological analysis of RV fibrosis using Masson's Trichrome staining (Fig. 5.8 A, B) found significant collagen formation in EtOH and SU +EtOH groups compared to control. Further, results indicated significantly increased fibrosis in the SU + EtOH group compared to EtOH alone and SU + EtOH compared to SU alone. These results support that the combination of ethanol diet and SU injection cause the most significant RV fibrosis in male SD rats.

5.5.8 ETB and BMPR2 expression is decreased, but not additive.

Western blot analyses showed no significant alterations in lung ETA receptor expression (Fig. 5.9 A) but significant decreases in lung ETB receptor expression (Fig. 5.9 B) in all experimental groups compared to control. Additionally, analysis of lung BMPR2 (Fig. 5.10 C) showed a significant downregulation in SU vs. control and SU + EtOH vs. control groups. These results support that ethanol and SU cause ETB and BMPR2 downregulation; however, their combined administration does not exacerbate the effect.

5.5.9 Significantly elevated mean arterial pressure without change in contraction and relaxation.

Mean arterial pressure (MAP) derived from end of experiment femoral artery catheterization (Fig. 5.10 A) revealed significant elevations in MAP the EtOH-group and SU + EtOH group compared to control. Additional recording of +dp/dt and -dp/dt (Fig. 5.10 B, C) showed no alterations amongst experimental groups, with the most sigificant hypertrophy observed in SU + EtOH vs. control rats.

5.6 Discussion

The ethanol-feeding model (5% w/v) used in this study was found to induce PAH characteristics in male SD rats[100] (chapter 3). Our results showed no significant difference in blood ethanol concentration between ethanol-fed rats and rats receiving ethanol and SU injection (Figure 5.2 A), supporting rats in different groups consumed similar amounts of ethanol and the SU injection did not influence blood ethanol concentration. Furthermore, the same strain of rat

was found to be hyperresponsive to the SU-injection, developing PAH without hypoxic exposure (chapter 4), in alignment with previous literature[2,7]. The present study is the first to evaluate the response VEGF receptor blockade in combination with long-term moderate ethanol consumption in a rat strain sensitive to PAH induction[2,7].

Using the ethanol-feeding regimen previously established within the lab[54,55], the experimental blood ethanol concentration in ethanol-drinking rats (vehicle and SU-injected) was approximately 41 mg/dL (Figure 5.2 A), consistent with moderate ethanol-consumption[73] and the resulting blood ethanol concentration quantified in chapter 3[100]. Ethanol diet with VEGF receptor inhibition causes increased RV hypertrophy, evidenced by higher RV/body weight and RV/LV + Septum ratios (Figure 5.2B, C). Importantly, RV hypertrophy is a hallmark compensatory adaptive (retains RV function) or maladaptive (associated with dilation, fibrosis, and RV failure) feature of PAH[101]. Here, we present evidence of potential maladaptive RV hypertrophy in rats exposed to ethanol diet with VEGF receptor inhibition. This study confirmed significant RV dilation in all experimental groups compared to the healthy control group (Figure 5.5 A, B), with increased RVID; d/ LVID; d ratios. The combination of SU and EtOH was significant but not additive; however, histological analysis of RV fibrosis (Figure 5.8), a maladaptive form of RV remodeling associated with PAH[102], revealed ethanol-diet induced fibrosis with exacerbated fibrosis occurring from the addition of VEGF receptor blockade. The fibrotic response in PAH is an adaptation to prevent ventricular dilation, a clinical feature of RV failure[76], a potential explanation of why RV dilation was not exacerbated in the SU + EtOH experimental group.

Myocardial remodeling in the form of hypertrophy, a response to chronic pressure overload[103], was observed in this study via longitudinal assessment of the pulmonary artery. The most significant reductions in both PAAT and PAAT/PET (Figure 5.4 B & C) in rats dually treated

with SU and ethanol-diet. These echocardiographic measurements inversely correlated with right ventricle systolic pressure (RVSP) gained from surgical right ventricle catheterization and are a reliable indirect measurement of RV function[50,75]. Furthermore, echocardiographic analysis of mean pulmonary arterial pressure (mPAP, Figure 5.4 A) showed ethanol-diet alone and SU-injection alone caused significant elevations in mPAP; however, co-administration of SU and ethanol caused the highest mPAP, being significantly higher than rats administered ethanol-diet only (Figure 5.5 A, B). Collectively, the elevation in mPAP reduces the time in which blood flow within the pulmonary artery reaches maximum velocity, causing a decrease in the PAAT/PET ratio. Therefore, a low PAAT/PET is a predictor of PAH, with a decreased ratio correlating with more severe PAH[104]. These results suggest that ethanol-diet accompanied by the SU injection caused an exacerbation in RV afterload and decreased RV function compared to that of ethanol consumption alone.

Noteworthy, the elevated afterload and hypertrophic responses were not isolated to the RV and pulmonary artery. Mean arterial pressure (MAP) derived through end of experiment femoral artery catheterization (Figure 5.10 A) was elevated due to ethanol-diet and ethanol-diet plus SU injection groups compared to control. Additionally, no alteration in contractility (Figure 5.10 B, C), a response observed in pulmonary hypertension induced by aortic stenosis[105]. These results suggest that the combination of ethanol-diet and VEGF receptor inhibition in the PAH sensitive rat strain may lead to development of PAH or pulmonary hypertension due to left-heart disease, a type of pulmonary hypertension of a different classification[106] . Further studies are needed to address this observation.

We hypothesized ethanol consumption in combination with VEGF receptor inhibition would cause additive upregulation of the ET-1/TNF-α/IL-6 pro-inflammatory axis within the lungs

and RV on the basis of results generated from chapters 3 and 4. Consistent with these findings, this study revealed upregulated ET-1 expression in lung (Figure 5.6 A) SU + EtOH vs. control and + EtOH SU vs. SU groups, suggesting lung ET-1 upregulation was additive when ethanol and SU were co-administered. Significant RV ET-1 expression was found to be SU-mediated, with no significant change in other experimental groups (Figure 5.7 A), suggesting ET-1 upregulation and its elicited vasoconstrictive effects are more significant within the lung, rather than the RV. Consistent with the findings of chapter 3, lung TNF-a expression (Figure 5.6 B) was upregulated with ethanol consumption vs. control; however, the most significant upregulation was when the ethanol diet was combined with VEGF receptor inhibition. While lung TNF-α was with co-administration of SU and ethanol, RV TNF-α was only upregulated when ethanol-diet was administered alone (Figure 5.7 B). Furthermore, the most significant increase in IL-6 expression in lung and RV was seen in rats exposed to ethanol-diet with VEGF receptor blockade (Figure 5.6 C & 5. C).

Similar to the results of chapters 3 and 4, ETA expression profile was unchanged (Figure 5.9 A), with significant decreases in ETB expression (Figure 5.9 B) in all experimental groups compared to control, suggesting an increased lung ETA/ETB receptor ratio. While this is significant, co-administration of SU and ethanol did not further increase the ETA/ETB receptor ratio as what was hypothesized.

Further analysis of lung BMPR2 showed significant decreases in rats exposed to SU alone and rats exposed to SU with ethanol-diet compared to control (Figure 5.9 C). While the results were significantly different from control, co-administration of ethanol and SU did not have an exacerbated decrease on lung BMPR2 expression.

In summary, the results of this study demonstrate the effect of how environmental exposure (chronic moderate ethanol consumption) can impact PAH development induced by VEGF inhibition in rats genetically sensitive to PAH development. Specifically, this preclinical study exposed rats of ethanol and SU, a double-hit model exposure, mimicking the multiple exposure characteristics of the human pathology.

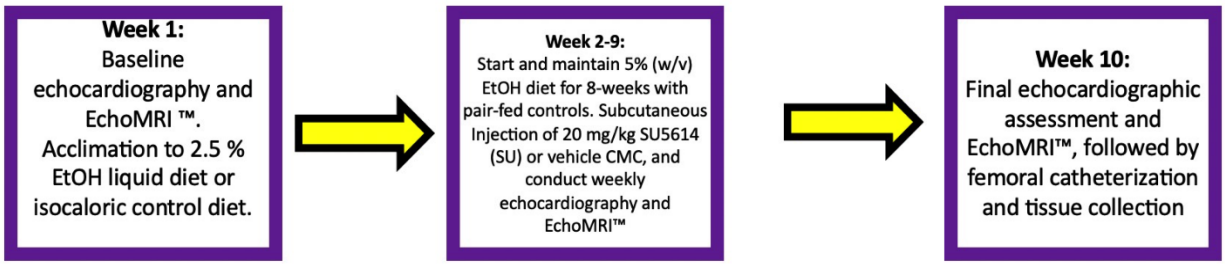
Week 1:
Baseline echocardiography and EchoMRI ™. Acclimation to 2.5 % EtOH liquid diet or isocaloric control diet.
Week 2-9:
Start and maintain 5% (w/v) EtOH diet for 8-weeks with pair-fed controls. Subcutaneous Injection of 20 mg/kg SU5614 (SU) or vehicle CMC, and conduct weekly echocardiography and EchoMRI™
Week 10:
Final echocardiographic assessment and EchoMRI™, followed by femoral catheterization and tissue collection

Figure 5.1: Aim Three Experimental Timeline. Graphical synopsis of experimental procedure including dosage, feeding regimen, echocardiography and EchoMRI schedule, femoral catheterization, and final tissue collection in CD strain male Sprague-Dawley rats.

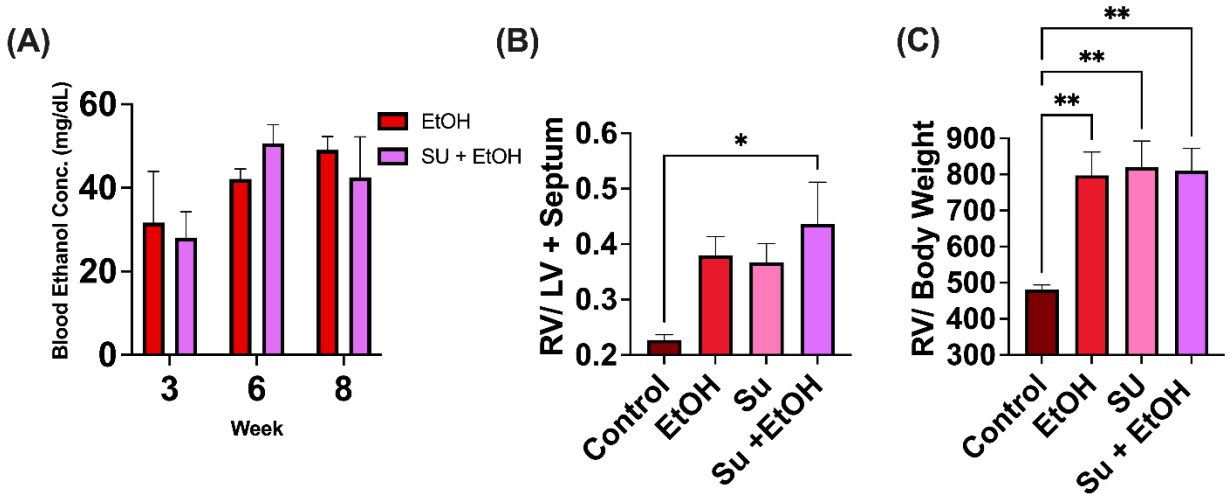
(A)
Blood Ethanol Conc. (mg/dL)
60
40
20
0
3
6
8
Week
EtOH
SU + EtOH
(B)
RV/ LV + Septum
0.6
0.5
0.4
0.3
0.2
*
Control
EtOH
Su
Su +EtOH
(C)
RV/ Body Weight
900
800
700
600
500
400
300
**
**
**
Control
EtOH
SU
Su + EtOH

Figure 5.2: Ethanol-diet in combination with SU injection causes right ventricular hypertrophy. The experiment yielded a range of blood ethanol concentration of 32-51 mg/dL of EtOH and SU + EtOH groups (**A**). Effect of ethanol and/or SU after 8-weeks showed increased RV/LV+ Septum ratio (**B**) and RV/ body weight ratio (**C**). Data are presented as mean ± SEM (n=5-6 in each group). Data were analyzed by one-way ANOVA followed by Tukey's Multiple Comparison Test. $^{*}P < 0.05$, $^{**}P < 0.01$, compared to control group.

(A)

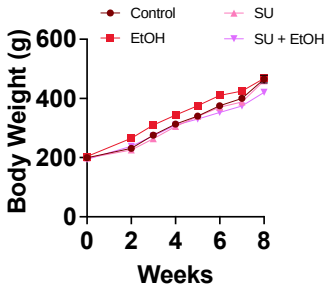
Control
SU
EtOH
SU + EtOH
Body Weight (g)
600
400
200
0
0
2
4
6
8
Weeks

(B)

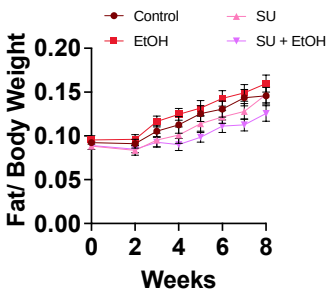
Control
SU
EtOH
SU + EtOH
Fat/ Body Weight
0.20
0.15
0.10
0.05
0.00
0
2
4
6
8
Weeks

(C)

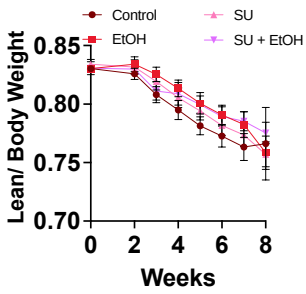
Control
SU
EtOH
SU + EtOH
Lean/ Body Weight
0.85
0.80
0.75
0.70
0
2
4
6
8
Weeks

Figure 5.3 Moderate ethanol consumption or injection causes no significant alteration in body weight and composition. Time-course of body weight **(A)**, EchoMRI analysis of body fat content/body weight **(B)**, and lean muscle/body weight **(C)** of all experimental groups. Data are presented as mean ± SEM (n=5-6 in each group).

(A)

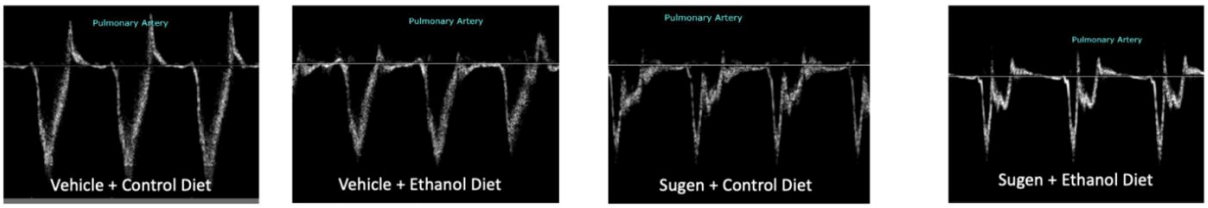
Pulmonary Artery
Vehicle + Control Diet
Pulmonary Artery
Vehicle + Ethanol Diet
Pulmonary Artery
Sugen + Control Diet
Pulmonary Artery
Sugen + Ethanol Diet

(B)

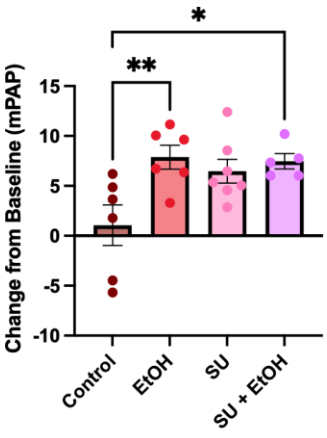
Change from Baseline (mPAP)
15
10
5
0
-5
-10
**
*
Control
EtOH
SU
SU + EtOH

(C)

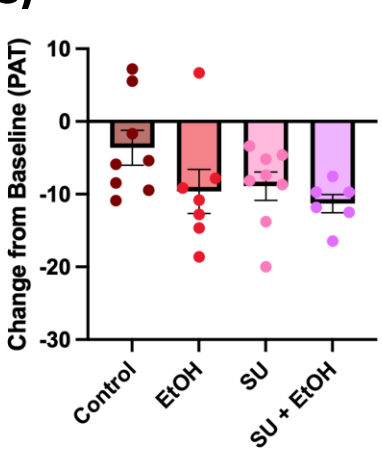
Change from Baseline (PAT)
10
0
-10
-20
-30
Control
EtOH
SU
SU + EtOH

(D)

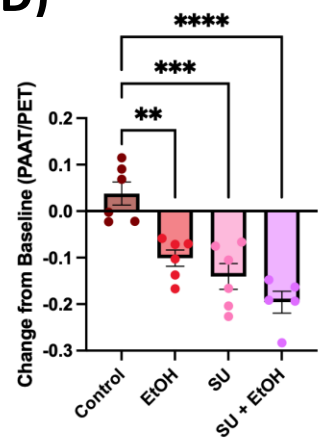
Change from Baseline (PAAT/PET)
0.2
0.1
0.0
-0.1
-0.2
-0.3
**
***
****
Control
EtOH
SU
SU + EtOH

Figure 5.4: Ethanol-diet in combination with VEGF receptor inhibition increases right ventricular afterload. Example echocardiographic pulsed-wave doppler images of the pulmonary artery **(A)** showing changes in PAAT and PET measurements after 8-weeks post injection and ethanol-diet compared to control. Change from baseline analysis of the pulmonary artery showed increased of mPAP **(B)** with decreased PAAT **(C)**, and PAAT/PET ratio **(D)**. Values are reported as means ± SEM (n=5-6 in each group), $^{*}P < 0.05$, $^{**}P < 0.01$, $^{***}P < 0.01$, $^{****}P < 0.0001$ using two-way ANOVA with post hoc multiple comparison testing.

(A)

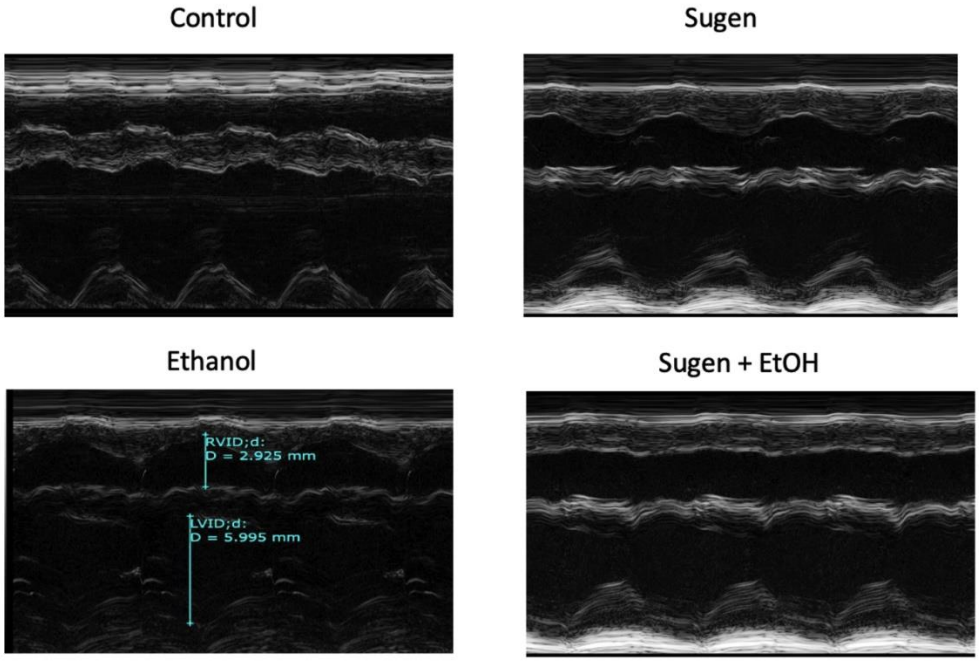
Control
Sugen
Ethanol
Sugen + EtOH
RVID;d:
D = 2.925 mm
LVID;d:
D = 5.995 mm

(B)

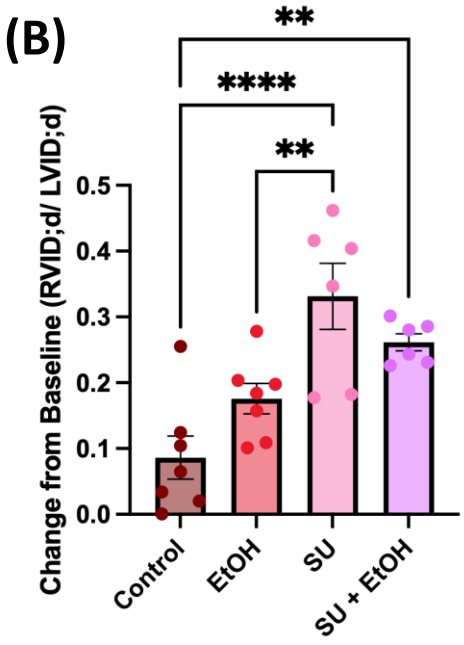
**
****
**
Change from Baseline (RVID;d/ LVID;d)
0.5
0.4
0.3
0.2
0.1
0.0
Control
EtOH
SU
SU + EtOH

Figure 5.5: Right ventricle dilation was significant in rats treated with ethanol-diet, SU, or a combination. Example M-mode echocardiographic images after 8-weeks of ethanol-diet, injection, or combination of control and SU + EtOH groups **(A)** showing RV, intraventricular septum (IVS), and LV chambers. Analysis of right ventricle internal diameter during diastole (RVID ;d/ LVID; d, **(B)**) showed significant RV dilation due to all treatments compared to control. Values are reported as means ± SEM (n=5-7 in each group), $^{*}P < 0.05$, $^{***}P < 0.001$, using two-way ANOVA with post hoc multiple comparison testing.

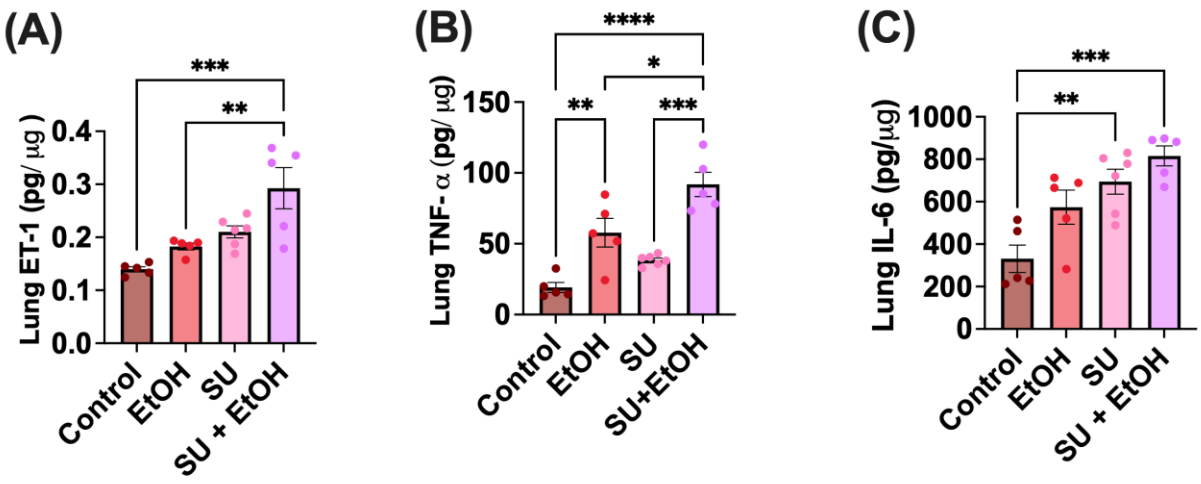
(A)
Lung ET-1 (pg/ µg)
0.0
0.1
0.2
0.3
0.4
***
**
Control
EtOH
SU
SU + EtOH
(B)
Lung TNF- α (pg/ µg)
0
50
100
150
****
*
**
***
Control
EtOH
SU
SU+EtOH
(C)
Lung IL-6 (pg/µg)
0
200
400
600
800
1000
***
**
Control
EtOH
SU
SU + EtOH

Figure 5.6: VEGF receptor inhibition in combination with chronic ethanol consumption increases key PAH pro-inflammatory markers within the lungs. ELISA quantification of lung ET-1 **(A)**, TNF-α **(B)**, and IL-6 **(C)** in the lung of experimental groups. Values are reported as means± SEM (n=5-6 in each group), $^{*}P < 0.05$, $^{**}P < 0.01$, $^{***}P < 0.01$, $^{****}P < 0.0001$ using one-way ANOVA with Tukey's post hoc test.

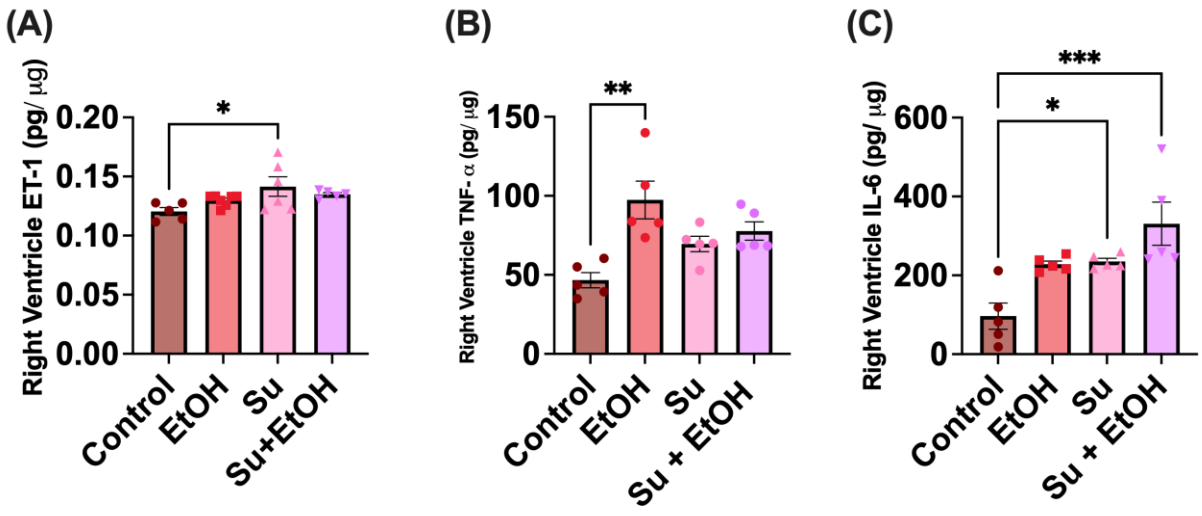
(A)
Right Ventricle ET-1 (pg/ μg)
0.20
0.15
0.10
0.05
0.00
*
Control
EtOH
Su
Su+EtOH
(B)
Right Ventricle TNF- α (pg/ μg)
150
100
50
0
**
Control
EtOH
Su
Su + EtOH
(C)
Right Ventricle IL-6 (pg/ μg)
600
400
200
0
***
*
Control
EtOH
Su
Su + EtOH

Figure 5.7: Upregulation of key pro-inflammatory markers associated with PAH within the right ventricle. ELISA quantification of right ventricle ET-1 **(A)**, TNF-α **(B)**, and TNF-α **(C)** from differing experimental groups. Values reported in means ± SEM (n=5-6 in each group), $^{*}P < 0.05$, $^{**}P < 0.01$, $^{***}P < 0.001$ using one-way ANOVA with Tukey's post hoc test.

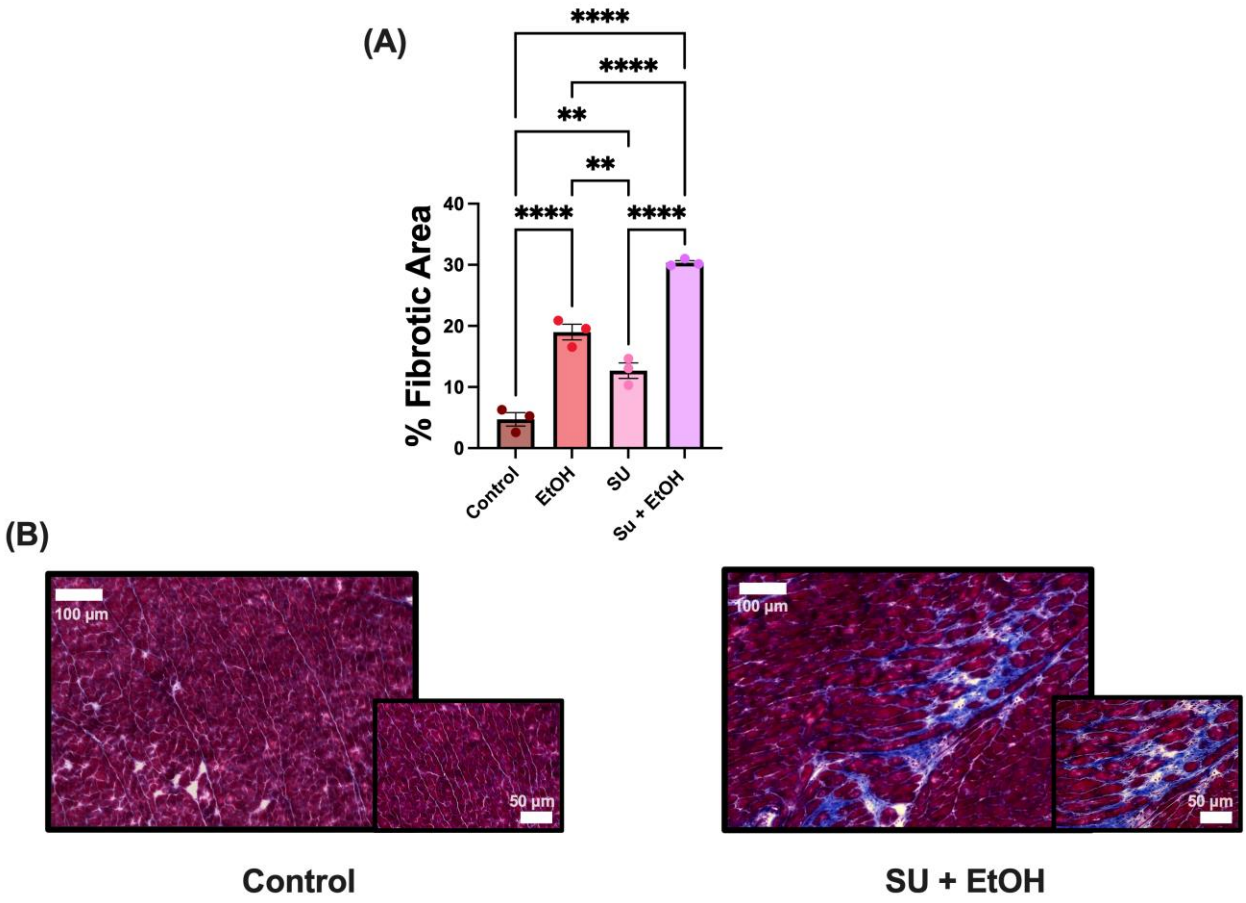
(A)
****
****
**
**
****
****
% Fibrotic Area
40
30
20
10
0
Control
EtOH
SU
Su + EtOH
(B)
100 µm
50 µm
100 µm
50 µm
Control
SU + EtOH

Figure 5.8: Ethanol-diet in combination with VEGF receptor inhibition causes right ventricular fibrosis. Quantification 200X magnification of fibrotic area in Masson's Trichrome-stained right ventricle **(A)** and representative images (100X and 200X magnification) **(B)** illustrating control and the combined effect of VEGF receptor inhibition and chronic ethanol consumption on the right ventricle. Values are reported as mean ± SEM (n=5), $^{*}P<0.05$, $^{**}P<0.01$, $^{****}P<0.0001$ using one-way ANOVA with Tukey's post hoc test.

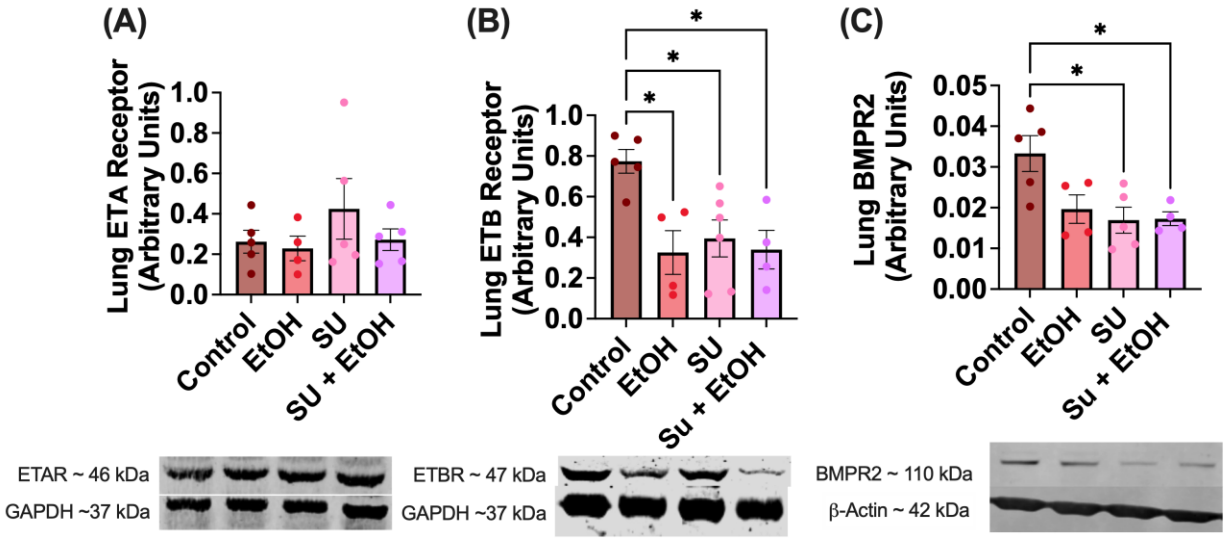
(A)
Lung ETA Receptor (Arbitrary Units)
1.0
0.8
0.6
0.4
0.2
0.0
Control
EtOH
SU
SU + EtOH
(B)
Lung ETB Receptor (Arbitrary Units)
1.0
0.8
0.6
0.4
0.2
0.0
*
*
*
Control
EtOH
SU
Su + EtOH
(C)
Lung BMPR2 (Arbitrary Units)
0.05
0.04
0.03
0.02
0.01
0.00
*
*
Control
EtOH
SU
Su + EtOH
ETAR ~ 46 kDa
GAPDH ~37 kDa
ETBR ~ 47 kDa
GAPDH ~37 kDa
BMPR2 ~ 110 kDa
β-Actin ~ 42 kDa

Figure 5.9: Ethanol-diet in combination with VEGF receptor inhibition augments ET-1 receptor expression and BMPR2. Western blot analyses of lung endothelin A receptor (ETA, **A**), endothelin B receptor (ETB, **B**) and bone morphogenetic protein receptor 2 (BMPR2, **C**). Data are presented as mean ± SEM (n=5-6 rats per group). $^{*}P < 0.05$ using one-way ANOVA with Tukey's post hoc test.

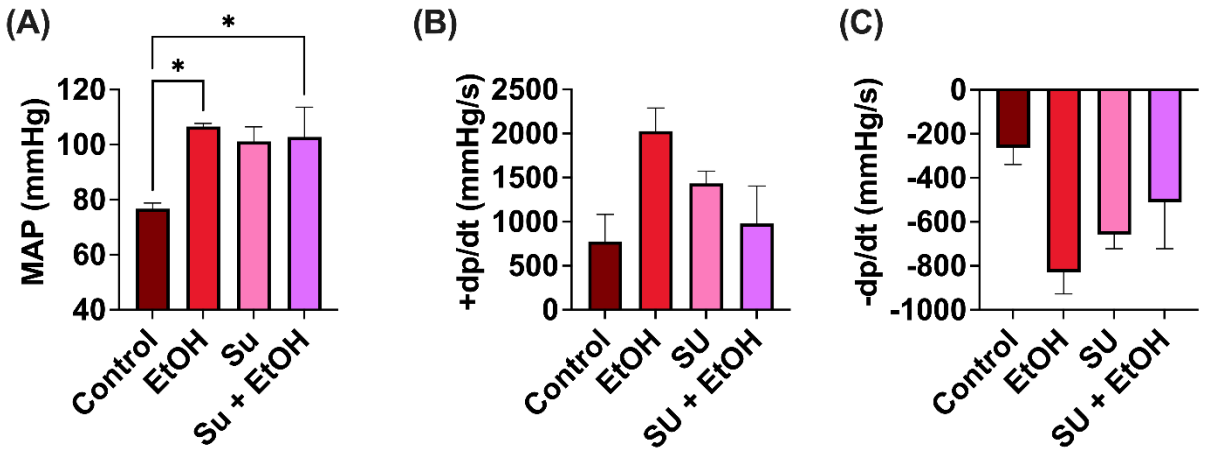
(A)
MAP (mmHg)
120
100
80
60
40
*
*
Control
EtOH
Su
Su + EtOH
(B)
+dp/dt (mmHg/s)
2500
2000
1500
1000
500
0
Control
EtOH
SU
SU + EtOH
(C)
-dp/dt (mmHg/s)
0
-200
-400
-600
-800
-1000
Control
EtOH
SU
SU + EtOH

Figure 5.10: Ethanol in combination with SU causes elevated mean arterial pressure with unchanged contractility. Mean arterial pressure **(A)**, +dp/dt **(B)**, and -dp/dt **(C)** derived from end of experiment femoral artery catheterization. Data are presented as mean ± SEM (n=5-6 rats per group). $^{*}P < 0.05$ using one-way ANOVA with Tukey's post hoc test.

CHAPTER SIX: GENERAL DISCUSSION

6.1 Chapter Three Summary

The first phase of this preclinical study sought examine the cardiopulmonary effects chronic ethanol consumption, an underrepresented area of ethanol-based cardiovascular research. Using the ethanol-feeding model previously published within our lab [65], this research provided novel data, supporting the role of ethanol in provoking PAH, providing time-course echocardiographic data and hemodynamic changes, along with RV and lung physiological remodeling induced by ethanol exposure. Additional molecular analyses established significant inflammation indicated to disrupt vascularly protective pulmonary receptors.

The ethanol-diet (5% w/v) used in this study produces clinically relevant cardiopulmonary remodeling associated with PAH. Similar to other ethanol research[6], this study replicated ethanol-induced RV hypertrophy, increased cardiomyocyte size, and decreased intrapulmonary artery diameter [6]. Collectively, these results provided evidence that chronic moderate ethanol consumption negatively affects cardiopulmonary structure.

Pathological cardiac hypertrophy is a physiological response to increased afterload[107]. The results of this research showed marked increases in mPAP and MAP, citing ethanol as a hemodynamic modulator, consistent with other findings[108]. Elevation in RV afterload is associated with compromised RV function, an observation recorded in this study through time-course decreases in PAAT/PET. Decreased PAAT/PET ratio suggests RV dysfunction [75,104], likely due to the observed ethanol-induced elevations RV afterload.

The molecular targets analyzed in this study were chosen due to their physiological importance in PAH development and therapy. This study hypothesized that an upregulation of ET-

1 and the ETA/ETB receptor ratio within the lungs partially contributes to the ethanol-evoked remodeling within the intrapulmonary arteries and RV. Upregulation of lung and RV ET-1 due to ethanol is critical, as patients with PAH have elevated ET-1[9]. Therefore, exposures such as ethanol consumption that increased ET-1 levels could be contraindicated in PAH patients, as the ET-1 signaling axis being important in therapeutics[109]. The results of this study show upregulated lung ETA/ETB receptor ratio, a result that cannot be overlooked, as since selective endothelin receptor blockers aim to preserve ETB receptor vasodilating signaling and block the vasoconstricting signaling of the ETA receptor[110]. Therefore, ethanol consumption interrupts balanced ET-1 receptor signaling within the lung in favor of vasoconstriction.

Upregulated pro-inflammatory cytokine production was observed within the RV and lungs of ethanol-fed rats. Interestingly, IL-6 overexpression in experimental research can induce PAH[32], whose signaling is important in PAH pathogenesis [33]. Additionally, this study found TNF-a upregulation, a protein linked to IL-6 upregulation[46] and PAH development[36]. It is essential to recognize the role of inflammatory cytokines to contribute to BMPR2 deficiency. IL-6 and TNF-a both contribute to downregulated BMPR2 expression[11,39], an observation in patients with hereditary and idiopathic PAH[111].

Collectively, this study shows ethanol-evoked increases in vasoconstrictive/pro-inflammatory signaling contributing to BMPR2 downregulation, likely contributing to the observed structural and functional cardiopulmonary changes in this study. Therefore, these findings provide novel insight on the contraindications of chronic moderate ethanol consumption to cardiopulmonary health, supporting an ethanol-evoked PAH environment within the RV and lungs of male rats. A graphical abstract of the mechanism in which ethanol promotes PAH is provided in figure 6.1.

6.2 Chapter Four Summary

The overarching goal of this research was to evaluate the impact of ethanol consumption not only in healthy rats, but in rats with PAH. With no access to hypoxic chambers for the Sugen + Hypoxia rat model, alternative options to induce PAH were investigated. Specifically, male SD rats (CD strain) from Charles River Laboratories were used as they had been cited to be sensitive to PAH development (Charles River Laboratory SD rats of different locations) after a single injection[2,7]. Therefore, this second research phase focused on physiological, hemodynamic, and molecular responses of rats to a single injection (20mg/kg) of the VEGF receptor inhibitor SU.

It is important to note that this study observed genetic susceptibility to PAH development using the SU injection alone, without hypoxic exposure. The results of this study provided an acceptable alternative to the Sugen + Hypoxia rat model, gaining us access to a PAH model in the absence of chronic hypoxia to further study ethanol consumption's effect on PAH (chapter 5).

The 20mg/kg single dose of SU caused cardiac remodeling in the form of hypertrophy. Post-euthanasia analysis showed significant RV hypertrophy, while time-course echocardiographic analysis of LV mass documented LV hypertrophy. The observed cardiac hypertrophy is likely due to increased cardiac afterload, supported by increases in mPAP and MAP, with afterload associated with the development of cardiac hypertrophy[107]. These results suggest the cardiovascular effects of VEGF receptor blockade are not isolated to right-side of heart and the pulmonary vasculature but elicit additional effects on the left-side and systemic vasculature.

Further RV remodeling was observed in this study in the form of RV dilation and fibrosis, both adaptive responses to ventricular pressure overload associated with PAH[92,102]. Increased afterload and decreased RV function was observed through echocardiographic analysis of PAAT

and PAAT/PET. Significant decreases in these measurements inversely correlate with increased RVSP[75], the gold-standard of PAH diagnostics[112].

Studies involving SD rats and SU attribute their hypersensitivity to SU-mediated PAH development to increased expression of apoptosis inducing lung caspase-3[7], without attention to key PAH modulators: ET-1 (ET-1 receptor profile), TNF-a, IL-6, and BMPR2. Similar to results of the ethanol study (chapter 3), a single injection of SU caused significant upregulated lung ET-1, TNF-a, and IL-6. Additionally, RV TNF-a and IL-6 increased significantly, but ET-1 was not significant. Therefore, SU-induced inflammation/vasoconstriction is most significant in the lung compared to the RV. Therefore, with inflammation known to augment ET-1 receptors and BMPR2[48], a higher ETA /ETB receptor ratio and downregulation of BMPR2 was determined. These results support SU-induced PAH can be attributed to upregulated inflammatory signaling and augmentation of integral receptors involved in PAH development and therapeutics.

6.3 Chapter Five Summary

The third aim of this study was developed due to the results of chapters three and four. Considering the heterogenous nature of PAH, we sought to understand how an environmental exposure (ethanol consumption) impacts PAH pathophysiology within a PAH rat model. The results of this study were an effort to observe how lifestyle choices can impact PAH pathophysiology.

Central to PAH is the development of RV hypertrophy and remodeling, usually due to increased RV afterload as a result of intrapulmonary artery thickening[63]. This study found significant RV remodeling in the form of hypertrophy, fibrosis, and dilation.

The results of this study found significant upregulation of the ET-1/TNF-a/IL-6 inflammatory axis within the lung and RV; however, the effect was not completely additive when ethanol-diet and SU were combined. Within the lung, the only additive effect observed was in TNF-a expression, with significant upregulation in the SU + EtOH group vs. EtOH alone and SU alone. Additional analysis of RV inflammatory markers showed no exacerbation in the ET-1- TNF-a-IL-6 pro-inflammatory axis. However, significant lung inflammation was observed, suggesting the inflammatory effects associated with PAH development are mostly pulmonary mediated.

Collectively, these results show moderate ethanol consumption can exacerbate certain inflammatory PAH markers that are linked to BMPR2 downregulation. For clinical relevance, this study identifies ethanol consumption as a potential risk factor for PAH and supports ethanol abstinence in PAH patients.

6.4 Conclusions

These preclinical studies provide insight on cardiopulmonary consequences of ethanol consumption in healthy rats and rats with PAH induced by VEGF receptor blockade. While more studies are needed to understand the mechanisms of ethanol-mediated PAH predisposition, SU-induced PAH development, and their combined effect, this study was able to provide evidence of the following: 1) Ethanol and SU elicit cardiac hypertrophy in response to increased RV afterload in healthy and diseased rats; 2) Ethanol facilitates intrapulmonary artery remodeling and elevations in mean arterial pressure (pulmonary and systemic); 3) Ethanol provokes and exacerbates PAH through upregulated inflammation and downregulation of receptors protective to cardiopulmonary health. This research project provides a foundation and future for ethanol-related

PAH research, as it highlights the importance on how exposure can facilitate and exacerbate cardiopulmonary disease.

6.5 Overall Limitations

This work is a contribution to the understudied effect of ethanol, SU, and their combination on RV and PA pathophysiology. This study establishes ethanol and VEGF receptor blockade as cardiopulmonary insults; however, this work should be interpreted within the boundaries of its inherent limitations. Echocardiography is a non-invasive diagnostic and surveillance tool for PAH[75,104,113], but the absence of invasive RVSP measurement (the gold-standard diagnostic tool for PAH) obtained via RV catheterization[114] is a limitation that needs to be addressed in future studies. Future research needs to determine if ethanol and SU effects on the pulmonary artery and RV hypertrophy are permanent, or reversible once ethanol consumption ceases. Additionally, research determining the effects of ethanol, SU, and their combination elicit similar or juxtaposing effects in females is needed. While these studies have limitations, they generate a foundation for future ethanol-based PAH research.

6.6 Future Directions

This study supports ethanol, SU, and their combination as potent cardiopulmonary and hemodynamic modulators with the novelty of these preclinical studies providing a foundation for future research.

As addressed in our limitations, these studies lacked the representation of female rats, but produced pilot data for a more robust study. Female representation in PAH research is essential, as the global female/male PAH ratio is 1.6:1; however, a greater ratio is documented in younger patients (18–65-year-old), with a ratio of 2.3:1[115]. The ratio equalizes between the sexes at age 65. These sex differences in PAH are represented by a concept known as the "estrogen paradox." This paradox has two major points: 1) Females are more susceptible to PAH development but have better survival and response to treatment than males; 2) Experimental animal models show protective and detrimental effects of estrogen on the pulmonary vasculature[115]. Estrogen elicits cardiopulmonary effects that related to PAH via estrogen receptor alpha having pro-proliferative actions associated with decreased BMPR2 expression[81]. Furthermore, estrogen receptor beta facilitates antifibrotic, anti-inflammatory, and vasodilatory actions within the RV and lungs[81]. Therefore, the addition of female rats to future alcohol/PAH investigation is essential. To address this concern, the study will utilize protocols previously established in the lab which include: 1) the ethanol-feeding regimen of 5% (w/v)[56]; and 2) ovariectomy and estradiol (E2) replacement[116] to better isolate the physiological impact of estradiol on cardiovascular health. It is noteworthy to address this strain of rat has sex-dependent differences in responsiveness to the SU injection, with 72% of males compared to 27% of females exhibiting severe PAH development likely due to estrogen elicited protection[117]. However, previous lab studies show ethanol promotes E2 dependent myocardial toxicity through its counterbalancing receptors[55] . Therefore, ethanol could potentially generate a toxicological estrogen environment and increase female responsiveness to SU-induced PAH. Future studies will aid in addressing sex differences in the cardiopulmonary effects of ethanol, SU, and their combination, with the additional isolation of the potential effects of estrogen.

The SD male rats from Charles River Laboratories were selected because of their documented sensitivity to SU induced PAH (without hypoxic exposure). Researching strain sensitivity to SU provides opportunity, as PAH research is limited at institutions, as many lack hypoxic chambers. Studying rat-strain dependent responses to VEGF receptor blockade could facilitate the development of rats genetically prone to PAH development, therefore generating a PAH rat model that increases accessibility to PAH research by bypassing hypoxic exposure.

Another aspect to consider is the RV and LV response to stress overload is not the same, likely due to their biological, structural, and functional differences[118]. Therefore, the data generated from this, and future studies could be used to generate an ethanol-based RV and LV study comparison study to elucidate if a particular ventricle is more or less susceptible to ethanol-induced toxicity.

The novel preclinical data presented provides a foundation for future PAH research. Future studies encompassing sex-differences, susceptibility to PAH induction, attention to ventricular differences will further elucidate the complex pathophysiology of PAH.

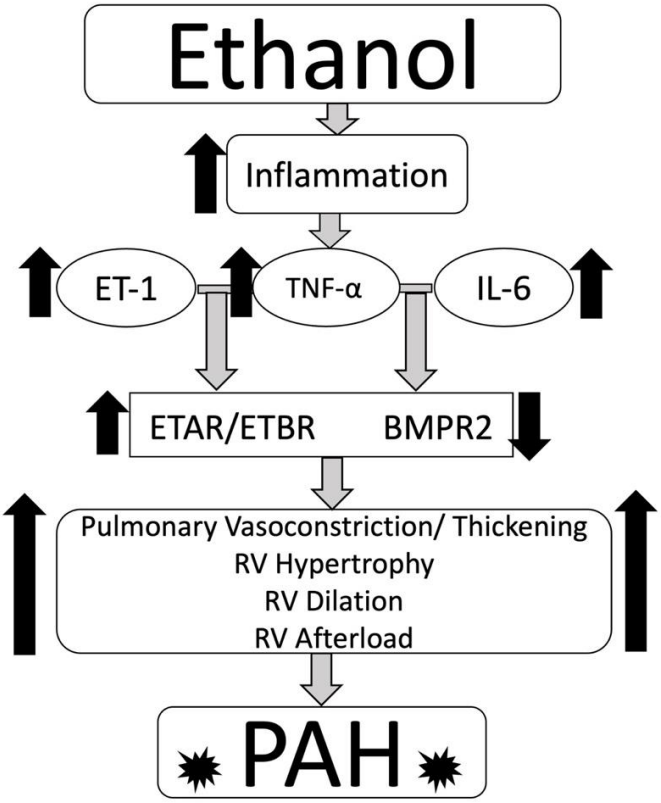
Ethanol
Inflammation
ET-1
TNF-α
IL-6
ETAR/ETBR
BMPR2
Pulmonary Vasoconstriction/ Thickening
RV Hypertrophy
RV Dilation
RV Afterload
PAH

Figure 6.1: Summary of the cardiopulmonary effects of moderate ethanol consumption. Chronic moderate ethanol consumption causes cardiopulmonary remodeling in the form of thickened intrapulmonary arteries, RV hypertrophy, RV dilation, and elevated RV afterload. The observed response to ethanol is due to, at least partially, the upregulation of inflammatory PAH mediators, specifically the ET-1-TNF-α-IL6 pathway. Ethanol further disrupts the ET-1 axis, causing elevated ETA/ETB receptor ratio (promoting vasoconstriction) and downregulation of cytoprotective BMPR2.

REFERENCES

1. Thibault HB, Kurtz B, Raher MJ, Shaik RS, Waxman A, Derumeaux G, Halpern EF, Bloch KD, Scherrer-Crosbie M. Noninvasive Assessment of Murine Pulmonary Arterial Pressure. *Circulation: Cardiovascular Imaging*. 2010;3(2):157–163.

2. Christou H, Hudalla H, Michael Z, Filatava EJ, Li J, Zhu M, Possomato-Vieira JS, Dias-Junior C, Kourembanas S, Khalil RA. Impaired Pulmonary Arterial Vasoconstriction and Nitric Oxide-Mediated Relaxation Underlie Severe Pulmonary Hypertension in the Sugen-Hypoxia Rat Model. *The Journal of pharmacology and experimental therapeutics*. 2018;364(2):258–274.

3. Anon. Pulmonary arterial hypertension: updates in epidemiology and evaluation of patients. *The American Journal of Managed Care*. 2021;27(Suppl 3):S35–S41.

4. Vinke P, Jansen SM, Witkamp RF, van Norren K. Increasing quality of life in pulmonary arterial hypertension: is there a role for nutrition? *Heart Failure Reviews*. 2018;23(5):711–722.

5. Biddinger KJ, Emdin CA, Haas ME, Wang M, Hindy G, Ellinor PT, Kathiresan S, Khera A V., Aragam KG. Association of Habitual Alcohol Intake With Risk of Cardiovascular Disease. *JAMA Network Open*. 2022;5(3):e223849.

6. Silva AF, Sousa-Nunes F, Faria-Costa G, Rodrigues I, Guimarães JT, Leite-Moreira A, Henriques-Coelho T, Negrão R, Moreira-Gonçalves D. Effects of chronic moderate alcohol consumption on right ventricle and pulmonary remodelling. *Experimental Physiology*. 2021;106(6):1359–1372.

7. Jiang B, Deng Y, Suen C, Taha M, Chaudhary KR, Courtman DW, Stewart DJ. Marked Strain-Specific Differences in the SU5416 Rat Model of Severe Pulmonary Arterial Hypertension. *American Journal of Respiratory Cell and Molecular Biology*. 2016;54(4):461–468.

8. Tirapelli CR, Casolari DA, Montezano AC, Yogi A, Tostes RC, Legros E, D'Orléans-Juste P, Lanchote VL, Uyemura SA, de Oliveira AM. Ethanol Consumption Enhances Endothelin-1-Induced Contraction in the Isolated Rat Carotid. *Journal of Pharmacology and Experimental Therapeutics*. 2006;318(2):819–827.

9. Chester AH, Yacoub MH. The role of endothelin-1 in pulmonary arterial hypertension.

10. Pullamsetti SS, Seeger W, Savai R. Classical IL-6 signaling: a promising therapeutic target for pulmonary arterial hypertension. *Journal of Clinical Investigation*. 2018;128(5):1720–1723.

11. Andruska A, Spiekerkoetter E. Consequences of BMPR2 Deficiency in the Pulmonary Vasculature and Beyond: Contributions to Pulmonary Arterial Hypertension. *International Journal of Molecular Sciences*. 2018;19(9):2499.

12. Klatsky AL. Alcohol and cardiovascular health ☆. 2010.

13. Biddinger KJ, Emdin CA, Haas ME, Wang M, Hindy G, Ellinor PT, Kathiresan S, Khera A V, Aragam KG. Association of Habitual Alcohol Intake With Risk of Cardiovascular Disease. *JAMA network open*. 2022;5(3):e223849.

14. El-Mas MM, Abdel-Rahman AA. Cardiovascular autonomic modulation by nitric oxide synthases accounts for the augmented enalapril-evoked hypotension in ethanol-fed female rats. *Alcohol*. 2013;47(4):339–346.

15. Di Federico S, Filippini T, Whelton PK, Cecchini M, Iamandii I, Boriani G, Vinceti M. Alcohol Intake and Blood Pressure Levels: A Dose-Response Meta-Analysis of Nonexperimental Cohort Studies. *Hypertension*. 2023.

16. Sidi A, Naik B, Muehlschlegel JD, Kirby DS, Lobato EB. Ethanol-induced acute pulmonary hypertension and right ventricular dysfunction in pigs. *British Journal of Anaesthesia*. 2008;100(4):568–569.

17. Nanji AA, Khwaja S, Khettry U, Hossein Sadrzadeh SM. Plasma endothelin levels in chronic ethanol fed rats: relationship to pathologic liver injury. *Life Sciences*. 1994;54(6):423–428.

18. Rodriguez DA, Moncada C, Núñez MT, Lavandero S, Ponnappa BC, Israel Y. Ethanol increases tumor necrosis factor-alpha receptor-1 (TNF-R1) levels in hepatic, intestinal, and cardiac cells. *Alcohol*. 2004;33:9–15.

19. Hong F, Kim WH, Tian Z, Jaruga B, Ishac E, Shen X, Gao B. Elevated interleukin-6 during ethanol consumption acts as a potential endogenous protective cytokine against ethanol-induced apoptosis in the liver: involvement of induction of Bcl-2 and Bcl-x(L) proteins. *Oncogene*. 2002;21(1):32–43.

20. Voelkel NF, Gomez-Arroyo J. The Role of Vascular Endothelial Growth Factor in Pulmonary Arterial Hypertension. The Angiogenesis Paradox. *American Journal of Respiratory Cell and Molecular Biology*. 2014;51(4):474–484.

21. Sakao S, Tatsumi K. The Effects of Antiangiogenic Compound SU5416 in a Rat Model of Pulmonary Arterial Hypertension. *Respiration*. 2011;81(3):253–261.

22. Sakao S, Tatsumi K. The Effects of Antiangiogenic Compound SU5416 in a Rat Model of Pulmonary Arterial Hypertension. *Respiration*. 2011;81(3):253–261.

23. Sitapara R, Sugarragchaa C, Zisman LS. SU5416 plus hypoxia but not selective VEGFR2 inhibition with cabozantinib plus hypoxia induces pulmonary hypertension in rats: potential role of BMPR2 signaling. *Pulmonary Circulation*. 2021;11(3):1–8.

24. GALIE N. The endothelin system in pulmonary arterial hypertension. *Cardiovascular Research*. 2004;61(2):227–237.

25. Nanji AA, Khwaja S, Khettry U, Hossein Sadrzadeh SM. Plasma endothelin levels in chronic ethanol fed rats: relationship to pathologic liver injury. *Life Sciences*. 1994;54(6):423–428.

26. Mazzuca MQ, Khalil RA. Vascular endothelin receptor type B: Structure, function and dysregulation in vascular disease. *Biochemical Pharmacology*. 2012;84(2):147–162.

27. Chester AH, Yacoub MH. The role of endothelin-1 in pulmonary arterial hypertension. *Global Cardiology Science and Practice*. 2014;2014(2):29.

28. Tirapelli CR, Legros E, Brochu I, Honoré J-C, Lanchote VL, Uyemura SA, De Oliveira AM, D'Orléans-Juste P. Chronic ethanol intake modulates vascular levels of endothelin-1 receptor and enhances the pressor response to endothelin-1 in anaesthetized rats. *British Journal of Pharmacology*. 2008;154(5):971–981.

29. Gonçalves FZ, Lizarte Neto FS, Novais PC, Gattas D, Lourenço LG, de Carvalho CAM, Tirapelli DPC, Molina CAF, Tirapelli LF, Tucci Jr S. Expression profile of endothelin receptors (ETA and ETB) and microRNAs-155 and -199 in the corpus cavernosum of rats submitted to chronic alcoholism and diabetes mellitus. *Brazilian Journal of Medical and Biological Research*. 2018;51(3).

30. Groth A, Vrugt B, Brock M, Speich R, Ulrich S, Huber LC. Inflammatory cytokines in pulmonary hypertension. *Respiratory Research*. 2014;15(1):47.

31. Browatzki M, Schmidt J, Kübler W, Kranzhöfer R. Endothelin-1 induces interleukin-6 release via acctivation of the transcription factor NF-κB in human vascular smooth muscle cells. *Basic Research in Cardiology*. 2000;95(2):98–105.

32. Steiner MK, Syrkina OL, Kolliputi N, Mark EJ, Hales CA, Waxman AB. Interleukin-6 Overexpression Induces Pulmonary Hypertension. *Circulation Research*. 2009;104(2):236–244.

33. Hashimoto-Kataoka T, Hosen N, Sonobe T, Arita Y, Yasui T, Masaki T, Minami M, Inagaki T, Miyagawa S, Sawa Y, Murakami M, Kumanogoh A, Yamauchi-Takihara K, Okumura M, Kishimoto T, et al. Interleukin-6/interleukin-21 signaling axis is critical in the pathogenesis of pulmonary arterial hypertension. *Proceedings of the National Academy of Sciences*. 2015;112(20).

34. Simplicio JA, Dourado TMH, Awata WMC, do Vale GT, Dias VR, Barros PR, de Martinis BS, Tostes RC, Tirapelli CR. Ethanol consumption favors pro-contractile phenotype of perivascular adipose tissue: A role for interleukin-6. *Life Sciences*. 2023;319:121526.

35. Browatzki M, Schmidt J, Kübler W, Kranzhöfer R. Endothelin-1 induces interleukin-6 release via acctivation of the transcription factor NF-κB in human vascular smooth muscle cells. *Basic Research in Cardiology*. 2000;95(2):98–105.

36. Mumby S, Perros F, Grynblat J, Manaud G, Papi A, Casolari P, Caramori G, Humbert M, John Wort S, Adcock IM. Differential responses of pulmonary vascular cells from PAH patients and controls to TNFα and the effect of the BET inhibitor JQ1. *Respiratory Research*. 2023;24(1):193.

37. Cooper IA, Beecher K, Chehrehasa F, Belmer A, Bartlett SE. Tumour Necrosis Factor in Neuroplasticity, Neurogenesis and Alcohol Use Disorder. *Brain Plasticity*. 2020;6:47–66.

38. Luedemann C, Bord E, Qin G, Zhu Y, Goukassian D, Losordo DW, Kishore R. Ethanol Modulation of TNF-alpha Biosynthesis and Signaling in Endothelial Cells: Synergistic Augmentation of TNF-alpha Mediated Endothelial Cell Dysfunctions by Chronic Ethanol. *Alcoholism: Clinical & Experimental Research*. 2005;29(6):930–938.

39. Sánchez-Duffhues G, García de Vinuesa A, van de Pol V, Geerts ME, de Vries MR, Janson SG, van Dam H, Lindeman JH, Goumans M, ten Dijke P. Inflammation induces endothelial-to-mesenchymal transition and promotes vascular calcification through downregulation of BMPR2. *The Journal of Pathology*. 2019;247(3):333–346.

40. Yang K, Wang J, Lu W. Bone morphogenetic protein signalling in pulmonary hypertension: advances and therapeutic implications. *Experimental Physiology*. 2017;102(9):1083–1089.

41. Maruyama H, Dewachter C, Belhaj A, Rondelet B, Remmelink M, Vachiéry J-L, Naeije R, Dewachter L. Endothelin-1 contributes to the downregulation of BMP/BMPR2 signaling induced by hypoxia. In: *4.3 Pulmonary Circulation and Pulmonary Vascular Disease*. European Respiratory Society; 2015:PA2429.

42. Hurst LA, Dunmore BJ, Long L, Crosby A, Al-Lamki R, Deighton J, Southwood M, Yang X, Nikolic MZ, Herrera B, Inman GJ, Bradley JR, Rana AA, Upton PD, Morrell NW. ARTICLE TNFa drives pulmonary arterial hypertension by suppressing the BMP type-II receptor and altering NOTCH signalling. 2017.

43. Brock M, Trenkmann M, Gay RE, Michel BA, Gay S, Fischler M, Ulrich S, Speich R, Huber LC. Interleukin-6 Modulates the Expression of the Bone Morphogenic Protein Receptor Type II Through a Novel STAT3–microRNA Cluster 17/92 Pathway. *Circulation Research*. 2009;104(10):1184–1191.

44. Steiner MK, Syrkina OL, Kolliputi N, Mark EJ, Hales CA, Waxman AB. Interleukin-6 Overexpression Induces Pulmonary Hypertension. *Circulation Research*. 2009;104(2):236–244.

45. Xu W-J, Wu Q, He W-N, Wang S, Zhao Y-L, Huang J-X, Yan X-S, Jiang R. Interleukin-6 and pulmonary hypertension: from physiopathology to therapy. *Frontiers in Immunology*. 2023;14.

46. Tanabe K, Matsushima-Nishiwaki R, Yamaguchi S, Iida H, Dohi S, Kozawa O. Mechanisms of tumor necrosis factor-α-induced interleukin-6 synthesis in glioma cells. *Journal of Neuroinflammation*. 2010;7(1):16.

47. Tian Q, Miyazaki R, Ichiki T, Imayama I, Inanaga K, Ohtsubo H, Yano K, Takeda K, Sunagawa K. Inhibition of Tumor Necrosis Factor-α–Induced Interleukin-6 Expression by Telmisartan Through Cross-Talk of Peroxisome Proliferator-Activated Receptor-γ With Nuclear Factor κB and CCAAT/Enhancer-Binding Protein-β. *Hypertension*. 2009;53(5):798–804.

48. Lan N, Massam B, Kulkarni S, Lang C. Pulmonary Arterial Hypertension: Pathophysiology and Treatment. *Diseases*. 2018;6(2):38.

49. Jernigan NL, Naik JS, Weise-Cross L, Detweiler ND, Herbert LM, Yellowhair TR, Resta TC. Contribution of reactive oxygen species to the pathogenesis of pulmonary arterial hypertension. *PLOS ONE*. 2017;12(6):e0180455.

50. Spyropoulos F, Vitali SH, Touma M, Rose CD, Petty CR, Levy P, Kourembanas S, Christou H. Echocardiographic markers of pulmonary hemodynamics and right ventricular hypertrophy in rat models of pulmonary hypertension. *Pulmonary Circulation*. 2020;10(2):1–10.

51. Shah M, Phillips MR, Quintana M, Stupp G, McLean SE. Echocardiography allows for analysis of pulmonary arterial flow in mice with congenital diaphragmatic hernia. *Journal of Surgical Research*. 2018;221:35–42.

52. Rosas PC, Neves LAA, Senese PB, Gralinski MR. Comprehensive Echocardiographic Assessment of Right Ventricle Function in a Rat Model of Pulmonary Arterial Hypertension. *Journal of Visualized Experiments*. 2023;(191).

53. Ibrahim BM, Fan M, Abdel-Rahman AA. Oxidative Stress and Autonomic Dysregulation Contribute to the Acute Time-Dependent Myocardial Depressant Effect of Ethanol in Conscious Female Rats. 2014.

54. Yao F, Abdel-Rahman AA. Estrogen receptor ERα plays a major role in ethanol-evoked myocardial oxidative stress and dysfunction in conscious female rats. *Alcohol*. 2016;50:27–35.

55. Yao F, Abdel-Rahman AA. Estrogen Receptors a and b Play Major Roles in Ethanol-Evoked Myocardial Oxidative Stress and Dysfunction in Conscious Ovariectomized Rats. 2016.

56. Katary M, Abdel-Rahman AA. Alcohol suppresses cardiovascular diurnal variations in male normotensive rats: Role of reduced PER2 expression and CYP2E1 hyperactivity in the heart. 2020.

57. Schwenke DO, Tokudome T, Shirai M, Hosoda H, Horio T, Kishimoto I, Kangawa K. Exogenous Ghrelin Attenuates the Progression of Chronic Hypoxia-Induced Pulmonary Hypertension in Conscious Rats. *Endocrinology*. 2008;149(1):237–244.

58. Henriques-Coelho T, Roncon-Albuquerque Júnior R, Lourenço AP, Baptista MJ, Oliveira SM, Brandão-Nogueira A, Correia-Pinto J, Leite-Moreira AF. Ghrelin reverses molecular, structural and hemodynamic alterations of the right ventricle in pulmonary hypertension. *Revista portuguesa de cardiologia : orgao oficial da Sociedade Portuguesa de Cardiologia = Portuguese journal of cardiology : an official journal of the Portuguese Society of Cardiology*. 2006;25(1):55–63.

59. Lippmann MR, Maron BA. The Right Ventricle: From Embryologic Development to RV Failure. *Current Heart Failure Reports*. 2022;1:3.

60. Forfia PR, Vaidya A, Wiegers SE. Pulmonary Heart Disease: The Heart-Lung Interaction and its Impact on Patient Phenotypes. *Pulmonary Circulation*. 2013;3(1):5–19.

61. Wijeratne DT, Lajkosz K, Brogly SB, Lougheed MD, Jiang L, Housin A, Barber D, Johnson A, Doliszny KM, Archer SL. Increasing Incidence and Prevalence of World Health Organization Groups 1 to 4 Pulmonary Hypertension. *Circulation: Cardiovascular Quality and Outcomes*. 2018;11(2).

62. Humbert M, Morrell NW, Archer SL, Stenmark KR, MacLean MR, Lang IM, Christman BW, Weir EK, Eickelberg O, Voelkel NF, Rabinovitch M. Cellular and molecular pathobiology of pulmonary arterial hypertension. *Journal of the American College of Cardiology*. 2004;43(12):S13–S24.

63. Sarah B, Ashrith G, Sandeep S. Evaluation, Diagnosis, and Classification of Pulmonary Hypertension. *Methodist DeBakey cardiovascular journal*. 2021;17(2):86–91.

64. Boucherat O, Agrawal V, Lawrie A, Bonnet S. The Latest in Animal Models of Pulmonary Hypertension and Right Ventricular Failure. *Circulation Research*. 2022;130(9):1466–1486.

65. Katary M, Abdel-Rahman AA. Alcohol suppresses cardiovascular diurnal variations in male normotensive rats: Role of reduced PER2 expression and CYP2E1 hyperactivity in the heart. 2020.

66. Dorfmuller P, Perros F, Balabanian K, Humbert M. Inflammation in pulmonary arterial hypertension. *European Respiratory Journal*. 2003;22(2):358–363.

67. Rubens C, Ewert R, Halank M, Wensel R, Orzechowski H-D, Schultheiss H-P, Hoeffken G. Big Endothelin-1 and Endothelin-1 Plasma Levels Are Correlated With the Severity of Primary Pulmonary Hypertension. *Chest*. 2001;120(5):1562–1569.

68. Soon E, Holmes AM, Treacy CM, Doughty NJ, Southgate L, Machado RD, Trembath RC, Jennings S, Barker L, Nicklin P, Walker C, Budd DC, Pepke-Zaba J, Morrell NW. Elevated Levels of Inflammatory Cytokines Predict Survival in Idiopathic and Familial Pulmonary Arterial Hypertension. *Circulation*. 2010;122(9):920–927.

69. Yuan S-M. Interleukin-6 in pulmonary artery hypertension. *Journal of Laboratory Medicine*. 2019;43(4):177–183.

70. Maruyama H, Dewachter C, Belhaj A, Rondelet B, Remmelink M, Vachiéry J-L, Naeije R, Dewachter L. Endothelin-1 contributes to the downregulation of BMP/BMPR2 signaling induced by hypoxia. In: *4.3 Pulmonary Circulation and Pulmonary Vascular Disease*. European Respiratory Society; 2015:PA2429.

71. Soon E, Crosby A, Southwood M, Yang P, Tajsic T, Toshner M, Appleby S, Shanahan CM, Bloch KD, Pepke-Zaba J, Upton P, Morrell NW. Bone Morphogenetic Protein Receptor Type II Deficiency and Increased Inflammatory Cytokine Production. A Gateway to Pulmonary Arterial Hypertension. *American Journal of Respiratory and Critical Care Medicine*. 2015;192(7):859–872.

72. Hurst LA, Dunmore BJ, Long L, Crosby A, Al-Lamki R, Deighton J, Southwood M, Yang X, Nikolic MZ, Herrera B, Inman GJ, Bradley JR, Rana AA, Upton PD, Morrell NW. TNFα drives pulmonary arterial hypertension by suppressing the BMP type-II receptor and altering NOTCH signalling. *Nature Communications*. 2017;8(1):14079.

73. Dasgupta A. Alcohol a double-edged sword. In: *Alcohol, Drugs, Genes and the Clinical Laboratory*. Elsevier; 2017:1–21.

74. Ryan JJ, Archer SL. The Right Ventricle in Pulmonary Arterial Hypertension. *Circulation Research*. 2014;115(1):176–188.

75. Zaky A, Zafar I, Masjoan-Juncos JX, Husain M, Mariappan N, Morgan CJ, Hamid T, Frölich MA, Ahmad S, Ahmad A. Echocardiographic, Biochemical, and Electrocardiographic Correlates Associated With Progressive Pulmonary Arterial Hypertension. *Frontiers in Cardiovascular Medicine*. 2021;8.

76. Ryan JJ, Huston J, Kutty S, Hatton ND, Bowman L, Tian L, Herr JE, Johri AM, Archer SL. Right Ventricular Adaptation and Failure in Pulmonary Arterial Hypertension. *Canadian Journal of Cardiology*. 2015;31(4):391–406.

77. Suen CM, Chaudhary KR, Deng Y, Jiang B, Stewart DJ. Fischer rats exhibit maladaptive structural and molecular right ventricular remodelling in severe pulmonary hypertension: a genetically prone model for right heart failure. *Cardiovascular Research*. 2019;115(4):788–799.

78. Rol N, Timmer EM, Faes TJC, Vonk Noordegraaf A, Grünberg K, Bogaard H-J, Westerhof N. Vascular narrowing in pulmonary arterial hypertension is heterogeneous: rethinking resistance. *Physiological Reports*. 2017;5(6):e13159.

79. Hirata Y, Emori T, Eguchi S, Kanno K, Imai T, Ohta K, Marumo F. Endothelin receptor subtype B mediates synthesis of nitric oxide by cultured bovine endothelial cells. *Journal of Clinical Investigation*. 1993;91(4):1367–1373.

80. El-Mas MM, Abdel-Rahman AA. Exacerbation of myocardial dysfunction and autonomic imbalance contributes to the estrogen-dependent chronic hypotensive effect of ethanol in female rats. *European Journal of Pharmacology*. 2012;679(1–3):95–100.

81. Umar S, Rabinovitch M, Eghbali M. Estrogen paradox in pulmonary hypertension: current controversies and future perspectives. *American journal of respiratory and critical care medicine*. 2012;186(2):125–31.

82. Strielkov I, Weissmann N. Role of the Aryl Hydrocarbon Receptor in Su5416/Hypoxia-induced Pulmonary Hypertension: A New Mechanism for an “Old” Model. *American Journal of Respiratory Cell and Molecular Biology*. 2018;58(3):279–281.

83. Wu X-H, Ma J-L, Ding D, Ma Y-J, Wei Y-P, Jing Z-C. Experimental animal models of pulmonary hypertension: Development and challenges. *Animal models and experimental medicine*. 2022;5(3):207–216.

84. Hilton LR, Ormiston ML. Legumain in Pulmonary Arterial Hypertension. *Arteriosclerosis, Thrombosis, and Vascular Biology*. 2019;39(4):536–537.

85. Peloquin GL, Johnston L, Damarla M, Damico RL, Hassoun PM, Kolb TM. SU5416 does not attenuate early RV angiogenesis in the murine chronic hypoxia PH model. *Respiratory Research*. 2019;20(1):123.

86. Mizuno S, Farkas L, Al Husseini A, Farkas D, Gomez-Arroyo J, Kraskauskas D, Nicolls MR, Cool CD, Bogaard HJ, Voelkel NF. Severe Pulmonary Arterial Hypertension Induced by SU5416 and Ovalbumin Immunization. *American Journal of Respiratory Cell and Molecular Biology*. 2012;47(5):679–687.

87. Star GP, Giovinazzo M, Lamoureux E, Langleben D. Effects of vascular endothelial growth factor on endothelin-1 production by human lung microvascular endothelial cells in vitro. *Life Sciences*. 2014;118(2):191–194.

88. Leite LN, Lacchini R, Carnio EC, Queiroz RH, Tanus-Santos JE, de Oliveira AM, Tirapelli CR. Ethanol Consumption Increases Endothelin-1 Expression and Reactivity in the Rat Cavernosal Smooth Muscle. *Alcohol and Alcoholism*. 2013;48(6):657–666.

89. Bogaard HJ, Legchenko E, Ackermann M, Kühnel MP, Jonigk DD, Chaudhary KR, Sun X, Stewart DJ, Hansmann G. The Adult Sprague-Dawley Sugen-Hypoxia Rat Is Still “the One:” A Model of Group

1 Pulmonary Hypertension: Reply to Le Cras and Abman. *American Journal of Respiratory and Critical Care Medicine*. 2020;201(5):621–624.

90. Spyropoulos F, Vitali SH, Touma M, Rose CD, Petty CR, Levy P, Kourembanas S, Christou H. Echocardiographic markers of pulmonary hemodynamics and right ventricular hypertrophy in rat models of pulmonary hypertension The first two authors contributed equally to this manuscript. *Pulmonary Circulation*. 2020;10(2).

91. Maron BA. Revised Definition of Pulmonary Hypertension and Approach to Management: A Clinical Primer. *Journal of the American Heart Association*. 2023;12(8).

92. Schimmel K, Ichimura K, Reddy S, Haddad F, Spiekerkoetter E. Cardiac Fibrosis in the Pressure Overloaded Left and Right Ventricle as a Therapeutic Target. *Frontiers in Cardiovascular Medicine*. 2022;9.

93. Ashikaga H, Covell JW, Omens JH. Diastolic dysfunction in volume-overload hypertrophy is associated with abnormal shearing of myolaminar sheets. *American Journal of Physiology-Heart and Circulatory Physiology*. 2005;288(6):H2603–H2610.

94. Yun M, Li S, Yan Y, Sun D, Guo Y, Fernandez C, Bazzano L, He J, Zhang T, Chen W. Blood Pressure and Left Ventricular Geometric Changes: A Directionality Analysis. *Hypertension*. 2021;78(5):1259–1266.

95. Chester AH, Yacoub MH. The role of endothelin-1 in pulmonary arterial hypertension. *Global Cardiology Science and Practice*. 2014;2014(2):29.

96. Humbert M, Lau EMT, Montani D, Jaïs X, Sitbon O, Simonneau G. Advances in Therapeutic Interventions for Patients With Pulmonary Arterial Hypertension. *Circulation*. 2014;130(24):2189–2208.

97. Hurst LA, Dunmore BJ, Long L, Crosby A, Al-Lamki R, Deighton J, Southwood M, Yang X, Nikolic MZ, Herrera B, Inman GJ, Bradley JR, Rana AA, Upton PD, Morrell NW. ARTICLE TNFa drives pulmonary arterial hypertension by suppressing the BMP type-II receptor and altering NOTCH signalling. 2017.

98. Ma L, Chung WK. The role of genetics in pulmonary arterial hypertension. *The Journal of Pathology*. 2017;241(2):273–280.

99. Vitali SH, Hansmann G, Rose C, Fernandez-Gonzalez A, Scheid A, Mitsialis SA, Kourembanas S. The Sugen 5416/Hypoxia Mouse Model of Pulmonary Hypertension Revisited: Long-Term Follow-Up. *Pulmonary Circulation*. 2014;4(4):619–629.

100. Donovan MK, Abdel-Rahman AA. Abstract P2026: Moderate Ethanol Consumption Causes Right Ventricular Hypertrophy And Pulmonary Hypertension Via The Pro-inflammatory Endothelin-interleukin Pathway. *Circulation Research*. 2023;133(Suppl_1).

101. Ryan JJ, Archer SL. The Right Ventricle in Pulmonary Arterial Hypertension. *Circulation Research*. 2014;115(1):176–188.

102. Simpson CE, Hassoun PM. Myocardial Fibrosis as a Potential Maladaptive Feature of Right Ventricle Remodeling in Pulmonary Hypertension. *American Journal of Respiratory and Critical Care Medicine*. 2019;200(6):662–663.

103. Guimaron S, Guihaire J, Amsallem M, Haddad F, Fadel E, Mercier O. Current Knowledge and Recent Advances of Right Ventricular Molecular Biology and Metabolism from Congenital Heart Disease to Chronic Pulmonary Hypertension. *BioMed Research International*. 2018;2018:1–10.

104. Trittmann JK, Almazroue H, Nelin LD, Shaffer TA, Celestine CR, Green HW, Malbrue RA. PATET ratio by Doppler echocardiography: noninvasive detection of pediatric pulmonary arterial hypertension. *Pediatric Research*. 2022;92(3):631–636.

105. Georgiopoulou V V., Kalogeropoulos AP, Borlaug BA, Gheorghiade M, Butler J. Left Ventricular Dysfunction With Pulmonary Hypertension. *Circulation: Heart Failure*. 2013;6(2):344–354.

106. Ryan JJ, Thenappan T, Luo N, Ha T, Patel AR, Rich S, Archer SL. The WHO Classification of Pulmonary Hypertension: A Case-Based Imaging Compendium. *Pulmonary Circulation*. 2012;2(1):107–121.

107. Hirt MN, Sörensen NA, Bartholdt LM, Boeddinghaus J, Schaaf S, Eder A, Vollert I, Stöhr A, Schulze T, Witten A, Stoll M, Hansen A, Eschenhagen T. Increased afterload induces pathological cardiac hypertrophy: a new in vitro model. *Basic research in cardiology*. 2012;107(6):307.

108. Husain K, Ansari RA, Ferder L. Alcohol-induced hypertension: Mechanism and prevention. *World journal of cardiology*. 2014;6(5):245–52.

109. Nagendran J, Sutendra G, Paterson I, Champion HC, Webster L, Chiu B, Haromy A, Rebeyka IM, Ross DB, Michelakis ED. Endothelin Axis Is Upregulated in Human and Rat Right Ventricular Hypertrophy. *Circulation Research*. 2013;112(2):347–354.

110. Yao X, Jing T, Wang T, Gu C, Chen X, Chen F, Feng H, Zhao H, Chen D, Ma W. Molecular Characterization and Elucidation of Pathways to Identify Novel Therapeutic Targets in Pulmonary Arterial Hypertension. *Frontiers in Physiology*. 2021;12.

111. Sánchez-Duffhues G, García de Vinuesa A, van de Pol V, Geerts ME, de Vries MR, Janson SG, van Dam H, Lindeman JH, Goumans M, ten Dijke P. Inflammation induces endothelial-to-mesenchymal transition and promotes vascular calcification through downregulation of BMPR2. *The Journal of Pathology*. 2019;247(3):333–346.

112. Levy PT, Patel MD, Groh G, Choudhry S, Murphy J, Holland MR, Hamvas A, Grady MR, Singh GK. Pulmonary Artery Acceleration Time Provides a Reliable Estimate of Invasive Pulmonary Hemodynamics in Children. *Journal of the American Society of Echocardiography*. 2016;29(11):1056–1065.

113. Zhu Z, Godana D, Li A, Rodriguez B, Gu C, Tang H, Minshall RD, Huang W, Chen J. Echocardiographic assessment of right ventricular function in experimental pulmonary hypertension. *Pulmonary Circulation*. 2019;9(2):1–9.

114. Kusner J, Krasuski RA. Echocardiographic Evaluation of the Right Heart in Pulmonary Hypertension. *Advances in Pulmonary Hypertension*. 2023;22(3):122–129.

115. Rodriguez-Arias JJ, García-Álvarez A. Sex Differences in Pulmonary Hypertension. *Frontiers in Aging*. 2021;2.

116. Mohamed M, Abdel-Rahman A. Effect of long-term ovariectomy and estrogen replacement on the expression of estrogen receptor gene in female rats. *European Journal of Endocrinology*. 2000:307–314.

117. Chaudhary KR, Deng Y, Yang A, Cober ND, Stewart DJ. Penetrance of Severe Pulmonary Arterial Hypertension in Response to Vascular Endothelial Growth Factor Receptor 2 Blockade in a Genetically Prone Rat Model Is Reduced by Female Sex. *Journal of the American Heart Association*. 2021;10(15).

118. Lippmann MR, Maron BA. The Right Ventricle: From Embryologic Development to RV Failure. *Current Heart Failure Reports*. 2022;19(5):325–333.

APPENDIX

Appendix A: AUP #W258a Amendment Approval Letter

Animal Care and Use Committee
003 Ed Warren Life Sciences Building | East Carolina University | Greenville NC 27834 - 4354
252-744-2436 office | 252-744-2355 fax

October 25, 2022

Abdel Abdel-Rahman, Ph.D.
Department of Pharmacology and Toxicology, ECU

Subject: Protocol W258a, original approval date 02/02/2022

Dear Dr. Abdel-Rahman:

The amendment#3 to your Animal Use Protocol entitled, "Sex/estrogen-dependent vulnerability to alcohol-evoked cardiotoxicity" (AUP#W258a) was reviewed by this institution's Animal Care and Use Committee on 10/25/2022. The following action was taken by the Committee:

"Approved as submitted"

Please contact Aaron Hinkle prior to any hazard use

A copy of the protocols is enclosed for your laboratory files. Please be reminded that all animal procedures must be conducted as described in the approved Animal Use Protocol. Modifications of these procedures cannot be performed without prior approval of the ACUC. The Animal Welfare Act and Public Health Service Guidelines require the ACUC to suspend activities not in accordance with approved procedures and report such activities to the responsible University Official (Vice Chancellor for Health Sciences or Vice Chancellor for Academic Affairs) and appropriate federal Agencies. Please ensure that all personnel associated with this protocol have access to this approved copy of the AUP/Amendment and are familiar with its contents.

Sincerely yours,

Susan McRae, Ph.D.
Chair, Animal Care and Use Committee

SM/GD

enclosure

Appendix B: AUP #W258a Amendment Approval Letter

ECU
Animal Care and Use Committee
003 Ed Warren Life Sciences Building | East Carolina University | Greenville NC 27834 - 4354
252-744-2436 office | 252-744-2355 fax

January 5, 2022

Abdel Abdel-Rahman, Ph.D.
Department of Pharmacology and Toxicology, ECU

Subject: Protocol W258, original approval date 03/15/2019

Dear Dr. Abdel-Rahman:

The amendment#4 to your Animal Use Protocol entitled, "Sex/Estrogen-dependent vulnerability to alcohol-evoked cardiotoxicity" (AUP#W258) was reviewed by this institution's Animal Care and Use Committee on 01/05/2022. The following action was taken by the Committee:

"Approved as submitted"

Please contact Aaron Hinkle prior to any hazard use

A copy of the protocols is enclosed for your laboratory files. Please be reminded that all animal procedures must be conducted as described in the approved Animal Use Protocol. Modifications of these procedures cannot be performed without prior approval of the ACUC. The Animal Welfare Act and Public Health Service Guidelines require the ACUC to suspend activities not in accordance with approved procedures and report such activities to the responsible University Official (Vice Chancellor for Health Sciences or Vice Chancellor for Academic Affairs) and appropriate federal Agencies. Please ensure that all personnel associated with this protocol have access to this approved copy of the AUP/Amendment and are familiar with its contents.

Sincerely yours,

Susan McRae, Ph.D.
Chair, Animal Care and Use Committee

SM/GD

enclosure